DEVELOPMENT OF A VIBRO-ULTRASOUND METHOD FOR MUSCLE STIFFNESS MEASUREMENT IN VIVO

Cong-zhi Wang

Ph.D.

The Hong Kong Polytechnic University
2011

The Hong Kong Polytechnic University
Department of Health Technology and Informatics

Development of a Vibro-ultrasound Method for Muscle Stiffness Measurement In Vivo

Cong-zhi Wang

A thesis submitted in partial fulfillment of the

requirements for the degree of Doctor of Philosophy

December 2010

CERTIFICATE OF ORIGINALITY

I hereby declare that this thesis is my own work and that, to the best of my knowledge and belief, it reproduces no material previously published or written, nor material that has been accepted for the award of any other degree or diploma, except where due acknowledgement has been made in the text.

_____ _____ (Signed)

Cong-zhi WANG (Name of student)

Abstract of thesis

"Development of a Vibro-ultrasound Method for Muscle Stiffness Measurement In Vivo"

Submitted by Cong-zhi Wang

for the Degree of Doctor of Philosophy

at The Hong Kong Polytechnic University

in December 2010

Stiffness has been proved to be a very important property of skeleton muscle and contribute significantly to muscle function. A number of methods have been developed to quantitatively assess muscle stiffness, such as indentation assessment, sonoelastography, transient elastography, supersonic shear imaging (SSI), shear-wave dispersion ultrasound vibrometry (SDUV) and magnetic resonance elastography (MRE). Each of them has unique features and limitations in *in vivo* studies. One major limitation of these methods is that the measurement ranges using these methods cannot exceed 50% of the maximum voluntary contraction (MVC) level. However, the information at high intensity contraction levels is more important for muscle functional assessment.

Previous studies have reported that skeleton muscle stiffness is positively correlated to the non-fatiguing muscle contraction level. However, due to the limitation mentioned above, this conclusion has not been verified in a full range of isometric muscle contraction, i.e. from 0% to 100% MVC level. Furthermore, the relationship between

muscle stiffness and isometric contraction level has seldom been studied systematically, with missing knowledge on how joint angle, gender and age may affect the relationship.

In this study, a novel vibro-ultrasound muscle stiffness assessment system based on the measurement of shear wave velocity in tissue was developed and its feasibility was evaluated on custom-made phantoms with different stiffness using traditional indentation method. Then it was used to assess the shear modulus of vastus intermedius (VI) muscle, one of the quadriceps femoris muscles, along the direction of muscle action. The relationship between the muscle stiffness and the step isometric contraction level was studied from 0% to 100% MVC under two different knee joint angles. The differences of muscle stiffness of the subjects with different gender and age ranges were also studied at different step isometric contraction levels. Furthermore, VI muscle shear modulus values were compared with the root mean square (RMS) values of the surface electromyography (EMG) signals collected from vastus lateralis (VL) muscle.

Forty healthy subjects volunteered to participate in the experiment and were divided into four groups: young males (n = 10, 29.4 ± 4.8 yr), young females (n = 10, 27.6 ± 5.0 yr), elder males (n = 10, 60.6 ± 7.6 yr) and elder females (n = 10, 56.7 ± 4.9 yr). The experiments were repeated at two different knee joint angles, 90º and 60º (0º for full extension). During the tests, MVC torque value was first determined as the highest torque of knee extensor achieved under voluntary contraction, which could be maintained for at least 5 seconds. Next, muscle stiffness measurements were performed under relaxed condition with 3 trials. Then the subjects were asked to maintain isometric contraction at different percentage of MVC levels, from 10% to 100%, for approximately 4 seconds. For each level, there were 3 trials and one-minute rest was allowed between any two measurements to avoid muscle fatigue.

The Pearson's correlation coefficient (CC) between the shear modulus values measured on the 10 pieces of silicone using indentation method and those measured using vibro-ultrasound method phantoms was 0.994. The Bland-Altman plot, in which the differences between the pairs of corresponding results against their mean were plotted, demonstrated that all the plots were in the range between mean ± 2sd and this indicated that the results of these two methods have a high agreement. These results proved the feasibility of our system. The results of in vivo test showed that the stiffness of VI muscle along the direction of muscle action was positively correlated to the step isometric contraction level in a full range for both knee joint angles (both $p < 0.001$). The relationship between them was close to a quadratic polynomial curve ($p < 0.001$). It was also found that under both relaxed condition and all step isometric contraction levels, the VI muscle shear modulus measured at 90º knee joint angle was larger than that measured at 60º knee joint angle (both $p < 0.001$). There was no significant difference in the relaxed muscle shear modulus between different genders ($p = 0.156$) and age ranges ($p = 0.221$). However, when performing step isometric contraction, the muscle shear modulus of the male subjects was larger than that of the females ($p < 0.001$), and the muscle shear modulus of the young subjects was larger than that of the elderly participants ($p < 0.001$) at the same contraction level and knee joint angle. A high correlation was found between the muscle shear modulus values of the VI muscle and the normalized RMS values of the surface EMG of the VL muscle.

In conclusion, we have successfully demonstrated that the newly developed vibro-ultrasound method can provide us a unique tool for muscle stiffness assessment in research and clinical practices. Muscle stiffness can provide complementary information of muscle mechanical properties in comparison with the traditional bioelectrical and

morphological information, such as EMG and sonomyography (SMG). For the first time, we measured the muscle shear modulus change over a full range of isometric contraction, i.e. from 0% to 100% MVC. We also investigated the relationships between the muscle stiffness and the isometric contraction levels, with the effects of gender, age, and joint angle considered. The newly developed vibro-ultrasound method together with these results can help us to better understand the muscle recruitment strategies under different isometric contractions levels. Future studies are needed to further improve the reliability and measurement range of the vibro-ultrasound method, to apply our new technology in more clinical practices, and to combine it with other measurement systems.

Keywords: Skeletal muscles stiffness, Ultrasound, Shear wave velocity, Shear modulus, Vibro-ultrasound method, Isometric contraction, Maximum voluntary contraction, MVC, Vastus intermedius, Electromyography, EMG, Sonomyography, SMG

PUBLICATIONS ARISING FROM THE THESIS

Journal Paper

1. **Wang CZ**, Zheng YP. Comparison between reflection-mode photoplethysmography and arterial diameter change detected by ultrasound at the region of radial artery, Blood Pressure Monitoring, Vol. 15 (4), pp. 213-219, 2010.

2. **Wang CZ**, Zheng YP. Newly developed vibro-ultrasound method for skeleton muscle stiffness assessment under higher step isometric contraction levels, IEEE Transactions on Biomedical Engineering, to be submitted.

3. **Wang CZ**, Zheng YP. Age and Gender dependences of the stiffness of vastus intermedius muscle under different step isometric contraction levels, Ultrasound in Medicine and Biology, to be submitted.

Conference Proceedings

1. Wang CZ, Guo JY and Zheng YP. Muscle Elasticity Measurement using ultrasound at isometric step contraction, 6th World Congress of Biomechanics (WCB 2010), Singapore, IFMBE Proceedings, Vol. 31, Part 3, pp. 965-968, August, 2010.

2. Wang CZ, Zheng YP. Skeleton muscle stiffness assessements at different muscle activity levels using an ultrasound based method, BME2010 Biomedical Engineering International Conference, Hong Kong, November, 2010.

3. Wang CZ, Zheng YP. Local arterial stiffness measurement using a high frame rate ultrasound system. 8th International Conference on the Ultrasonic Measurement and Imaging of Tissue Elasticity, Vlissingen Zeeland, the Netherlands, pp. 80, September, 2009.

4. Wang CZ, Zheng YP, Relationship between photoplethysmography (PPG) and arterial diameter change measured by ultrasound, WACBE World Congress on Bioengineering 2009, Hong Kong, China, July, 2009.

ACKNOWLEDGEMENTS

I would like to express my sincere appreciation to the people who have contributed their dedication and efforts in this study. Without their guidance and support, this thesis would not have been possible.

First and foremost, I would like to extend my utmost gratitude to my supervisor, Prof. Yong-ping Zheng, for giving me this opportunity to undertake this project and providing me with all the facilities needed to carry out my research. His rigorous scholarship, enterprising spirit and profound knowledge gave me a deep impression. His guidance, encouragement, concern and enthusiasm, have kept me motivated throughout these years. When I encountered difficulties in either the academic matters or my life, I could always get good suggestions and ideas from him. I also want to thank him for the helpful criticism and constructive comments during the writing of my thesis. Great thanks are also given to Ms. Sally Ding, Prof. Zheng's wife, for her kindly encouragement, great help in recruiting subjects for my study and in checking my thesis closely and carefully with regard to English style and grammar.

I would like to thank Dr. Phoebe Chan, Dr. Eric Tam, Dr. Michael Ying and Dr. Mo Yang for assessing my proposal and confirmation report, providing valuable comments and suggestions to my study. And I want to address my gratitude to Dr. Jing-yi Guo, for her kindly help on the tests for human subjects, which consumed her much time and many efforts on finding suitable subjects and collecting data. I also want to thank Mr. Man Mak Tak-man for his great help on discussion of the vibro-ultrasound method and in phantom fabrication.

I would also like to acknowledge all my colleagues and fellow students in our group, who have learned and worked along with me for these years, for their kindly help on my

daily life and research work. Sincere thanks are given to Dr. Xin Chen, Mr. James Cheung, Mr. William Chiu Man-wai, Mr. Jun-feng He, Dr. Qing-hua Huang, Mr. Yan-ping Huang, Mr. Zheng-ming Huang, Miss Wei-wei Jiang, Miss Yen Law Siu-yin, Mr. Louis Lee, Ms. Jia-wei Li, Miss Tian-jie Li, Dr. Carrie Ling, Mr. Wen-tao Liu, Dr. Ming-hua Lu, Mr. Tim Tang Pak-tim, Mr. Li-ke Wang, Ms. Shu-zhe Wang, Dr. Queeny Yuen, Dr. Yong-jin Zhou and Mr. Guang-quan Zhou.

I am also deeply thankful to my parents, Mr. Wang Wan-sheng and Mrs. Wang Hui-min, for their kindly care, enthusiastic encouragement and persistent supports over all these years when I could not stay with them as a filial son.

Finally, I would like to thank the volunteers who participated in my study. And I would like to acknowledge the financial support from The Hong Kong Polytechnic University (J-BB69) and Research Grant Council of Hong Kong (PolyU 5331/06E).

Thank you all from my heart!

TABLE OF CONTENTS

LIST OF ABBREVIATIONS

1D	One-dimensional
2D	Two-dimensional
3D	Three-dimensional
CC	Correlation coefficient
CCF	Cross-correlation function
CSA	Cross sectional area
CT	Computerized Tomography
EMG	Electromyography
ICC	Intraclass correlation coefficient
LG	Lateral gastrocnemius muscle
MG	Medial gastrocnemius muscle
MRE	Magnetic resonance elastography
MRI	Magnetic resonance imaging
MU	Motor unit
MUAP	Motor unit action potential
MVC	Maximal voluntary contraction
NRMSD	Normalized root mean squared deviation
RF	Rectus femoris
RMS	Root mean square
ROI	Region of interest
SDUV	Shear-wave dispersion ultrasound vibrometry
SL	Soleus muscle
SMG	Sonomyography
SNR	Signal-noise ratio
SSI	Supersonic shear imaging
STDEV	Standard deviations

TA	Tibialis anterior muscle
VI	Vastus intermedius muscle
VL	Vastus lateralis muscle
VM	Vastus medialis muscle

LIST OF FIGURES

LIST OF TABLES

CHAPTER 1 INTRODUCTION

1.1 Background and Significances

Ultrasonography has been used to evaluate the morphological changes in skeleton muscles as an effective method (Mannion et al., 2008; Nogueira et al., 2009; Okita et al., 2009; Springer and Gill, 2007). It has also been employed to characterize the muscular disfunction and diseases (Botteron et al., 2009; Chester et al., 2008; Sikdar et al., 2008). Moreover, ultrasound has been used along with electromyography (EMG) signal to provide more comprehensive information on the activities and properties of different muscles (Andrade et al., 2009; Ferreira et al., 2004; Ishikawa et al., 2006).

In a previous study, Zheng et al. (1999) used the tissue ultrasound palpation system (TUPS), an indentation method, to determine the soft tissue stiffness of lower limbs under different contraction conditions. In another study, sonomyography (SMG) was proposed to describe the real-time muscle thickness change detected by B-mode images during its contraction (Zheng et al., 2006). Recently, the relationship between SMG and wrist extension angle was investigated. It was claimed that SMG signal could successfully predict the wrist extension angle and this signal had potential for prosthetic control (Guo et al., 2009).

Stiffness is also a very important property of skeletal muscle. It may change in some physiological conditions, such as muscle voluntary contraction, and in some pathological conditions, such as spasm, cramps, oedema and delayed onset muscle soreness (Gennisson, 2005). The stiffness has also been shown to contribute

significantly to muscle efficiency (Wilson et al., 1994). Obviously, quantifying the muscle stiffness can help to improve the understanding of some muscular functional changes. Therefore, a number of methods have been developed for muscle stiffness assessment, such as indentation assessment method (Leonard et al., 2003; Murayama et al., 2000; Zheng and Mak, 1999; Zheng and Mak, 2000), sonoelastography (Levinson et al., 1995; Parker et al., 1990; Wu et al., 2006), transient elastography (Catheline et al., 1999; Gennisson et al., 2005; Nordez et al., 2009), supersonic shear imaging (SSI) (Nordez and Hug, 2010; Sandrin et al., 1999; Sandrin et al., 2002), shear-wave dispersion ultrasound vibrometry (SDUV) (Chen et al., 2008; Chen et al., 2009), and magnetic resonance elastography (MRE) (Bensamoun et al., 2008; Dresner et al., 2001; Muthupillai et al. 1995; Ringleb et al., 2007). Each of them has unique features and limitations in *in vivo* studies. The major limitation is that none of these studies exceeded 50% maximum voluntary contraction (MVC) level. However, it is well known that the information under high intensity contraction is more important for muscle function assessment.

Previous studies have reported that skeleton muscle stiffness is positively correlated to the non-fatiguing muscle contraction level. However, due to the limited measurement range of the available methods, this conclusion has not been verified in a full range of isometric contraction levels, i.e. from 0% to 100% MVC. Furthermore, the effects of joint angle, gender and age on the relationship between muscle stiffness and isometric contraction level have not been studied systematically. And little has been done on the relationship between the muscle stiffness and traditional surface EMG signal under different MVC levels.

Therefore, development of a new ultrasound based method which can measure the

muscle stiffness in a full range can provide us a unique tool for muscle assessment in research and clinical practices. If the muscle stiffness is proved to be positively correlated with isometric contraction level in a full range, it would have potential to be used to estimate the muscle activity level or muscle stress, which is important for muscle function assessment. Furthermore, studies on the joint angle, gender and age dependences of the muscle stiffness under different contraction levels can provide a new perspective to investigate the influence of these factors on the muscle structure, function and recruitment strategies, to understand better the reasons for the higher risk of anterior cruciate ligament (ACL) and cartilage injury among females, and to explore the process of muscle ageing and rehabilitation.

1.2 Objectives of This Study

The objectives of this study are:

1. To develop a new method for quantitative muscle stiffness assessment based on shear wave velocity measurement, with the capability of measuring muscle stiffness from 0% to 100% MVC.

2. To characterize the stiffness of vastus intermedius (VI) muscle, one of the quadriceps femoris muscles, along the direction of muscle action, and to determine the relationship between muscle stiffness and relative isometric contraction level, from 0% to 100% MVC. From another point of view, the relationship between muscle stiffness and absolute torque of knee extensor is also to be studied.

3. To study the influences of knee joint angle, gender and age, on the muscle stiffness

at relaxed condition and different step isometric contraction levels.

4. To determine the relationship between the muscle shear modulus and the root mean square (RMS) values of surface EMG signal.

1.3 Outline of the Dissertation

Following the introduction chapter, Chapter 2 presents a literature review on the fundamental physiology of skeletal muscle, the technology utilized for muscle assessment, and the gender and age dependences of muscle structure and functions.

In Chapter 3, the methods used in this study are introduced. The experimental protocols are presented in detail. The principle of vibro-ultrasound measurement system is described. It was evaluated using custom-made phantoms with different stiffness and applied to determine the shear modulus of skeletal muscle on forty subjects. In addition, the relationship between muscle stiffness and different isometric contraction levels was studied. The knee joint angle, gender and age dependences of muscle stiffness were investigated at different isometric contraction levels. Furthermore, muscle shear modulus was compared with the RMS values of surface EMG signal.

In Chapter 4, the results of the corresponding studies in Chapter 3 are reported, including the evaluation of the vibro-ultrasound system, the positive correlation and quadratic relationships between the muscle shear modulus and both the relative % MVC level and absolute torque, and the comparison between the muscle stiffness measured from different groups of subjects with different genders or age ranges. Finally, the positive correlation and the quadratic relationship between the muscle shear modulus

and the RMS values of surface EMG signal are presented.

Chapter 5 presents discussion on the new method, the experiment protocols and the results. Discussion on the vibro-ultrasound method and the experiments described in Chapters 3 and 4 is divided into several parts according to their purposes. The results of our study are compared with the results of related previous studies. And the explanations for our findings are also given in this chapter.

Chapter 6 summarizes the findings of this study and the potential applications of the vibro-ultrasound method in research, clinical practices and sports training. Limitations of the system and suggestions on future research directions are also given.

CHAPTER 2 LITERATURE REVIEW

This chapter presents a review of the literature on skeletal muscle physiology, its assessment methods including EMG, mechanomyography (MMG) and methods for muscle stiffness assessment, and the age and gender dependences of skeletal muscle properties. There are three major parts. The first part (Section 2.1) addresses the anatomy of skeletal muscle, motor units and muscle fiber types. The second part (Section 2.2) presents the techniques used for skeletal muscle assessment. The last part (Section 2.3) describes the currently available knowledge on age and gender dependences of skeletal muscle structure, properties and function.

2.1 Skeletal Muscle Physiology

2.1.1 Anatomy of Skeletal Muscle

Skeletal muscle represents the majority of muscular tissue in the body. It is the classic biological example of a structure-function relationship. At both the macroscopic and microscopic levels, the structure of skeletal muscle is exquisitely tailored for its primary functions, force generation and movements (Jones et al., 2004; Lieber, 2009). As shown in Fig. 2.1, skeletal muscle is surrounded by a connective tissue sheath called epimysium and is bound into compartments called fasciculus. Each fasciculus is contained in a layer of connective tissue called perimysium and is formed by grouping bundles of muscle fibers, which is also surrounded by connective tissue called endomysium. Each muscle fiber is a multinucleated single cylindrical muscle cell which is made up of an array of stacked myofibrils. Muscle fibers cross the entire muscle lengthwise and attach to the bone through a tendon, which is a tough band of fibrous connective tissue and is designed to withstand the tension. A rich network of blood vessels and nerves weaves

between and within the muscle fibers. On the lowest level, myofibrils are bundles of myofilaments (actin and myosin) and divided into segments known as sarcomeres. Sarcomeres are the basic units of contraction. Each sarcomere will shorten during contraction, thus shortening the entire cell and the entire muscle (Macintosh et al., 2005; Lieber, 2009).

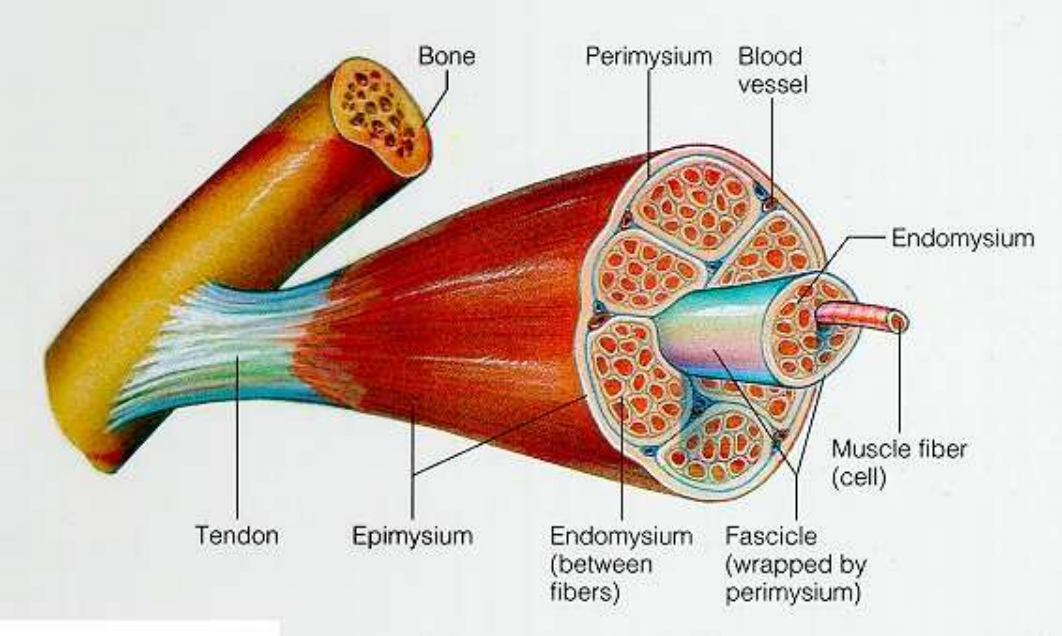

Fig. 2.1 Structure of a skeletal muscle (from http://www.tarleton.edu/).

2.1.2 Motor Units

Although the functional unit of force generation is sarcomere, the functional unit of movement is motor unit (MU). It is defined as a single motoneuron plus the muscle fibers it innervates (Fig. 2.2). One muscle has a certain number of motor units, groups of which often work together to coordinate the contractions. In addition, larger motor units have stronger twitch tensions.

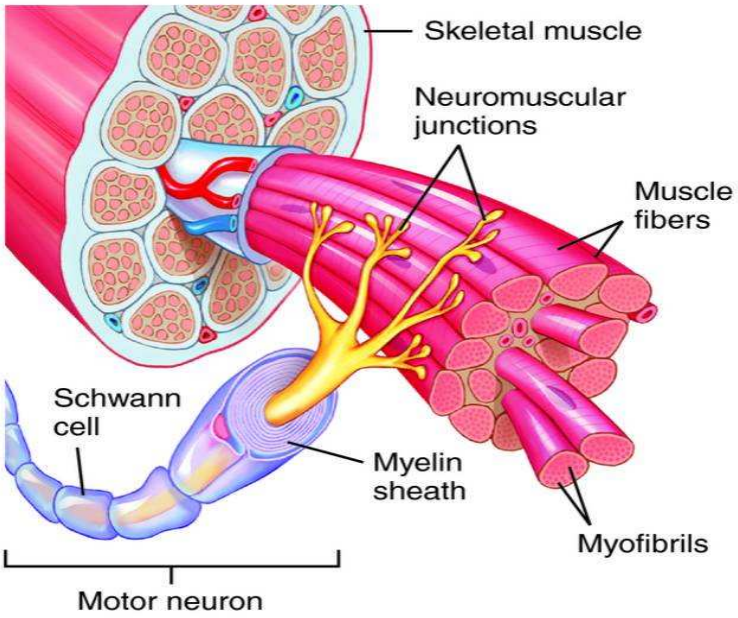

Fig. 2.2 Structure of motor unit (from http://www.thefreedictionary.com/).

When an impulse initiated in the motoneuron passes down the axonal branches, all the muscle fibers are activated by a synchronous action potential, depolarize as the signal propagates along their surface and generate a twitch of force. The size and speed of the twitch depends on the number of muscle fibers in the motor unit and their contractile properties. Surface electrodes located near the muscle can detect the electric field induced by the depolarization. The combination of muscle fiber action potentials from all the muscle fibers is the motor unit action potential (MUAP) and the sum of electrical activity generated by each active motor unit is the EMG signal (De Luca et al., 1982).

2.1.3 Skeletal Muscle Fiber Type

The skeletal muscle fibers can be categorized into type I and type II according to their type of myosin (fast or slow twitch in contraction). Fast twitch fibers can be further classified into type IIa, type IIx and type IIb fibers. Type I fibers appear red and suited for endurance. Type II fibers are white and efficient for short bursts of speed. The

distribution of fiber types varies in different skeletal muscles. For example, both types of fibers are almost evenly distributed in biceps brachii muscle while there are more type II fibers in rectus femoris (RF) muscle (Johnson et al., 1973). Table 2.1 describes the most obvious differences among muscle fiber types.

Table 2.1 List of the properties of type I and type II muscle fibers. (http://en.wikipedia.org/wiki/Skeletal_muscle).

Fiber Type	*Type I fibers*	*Type IIa fibers*	*Type IIx fibers*	*Type IIb fibers*
Contraction time	Slow	Moderately Fast	Fast	Very fast
Size of motor neuron	Small	Medium	Large	Very large
Resistance to fatigue	High	Fairly high	Intermediate	Low
Activity Used for	Aerobic	Long-term anaerobic	Short-term anaerobic	Short-term anaerobic
Maximum duration of use	Hours	<30 minutes	<5 minutes	<1 minute
Power produced	Low	Medium	High	Very high

2.1.4 Muscle Motor Control Strategies: Size Principle

The force output during a voluntary contraction can be increased either by increasing the firing frequency or the number of active motor units. According to the size principle, at lower force levels, motor units with small axons are first recruited, and as force increases, larger axons are increasingly recruited. Generally, small axons innervate slow motor units and larger axons innervate fast motor units (Henneman, 1981). It is the anatomical basis for the orderly recruitment of motor units to produce a smooth contraction. Motor units from different regions of the same muscle may be also separately involved in different movement patterns (Cope and Pinter, 1995).

As an indicator of the firing frequency of recruited motor units and an index of muscle force or torque (Orizio, 1993; Orizio et al., 2003; Jaskolska et al., 2006), the frequency and amplitude of EMG and mechanomyography (MMG) signals, of which the later one is the oscillation generated by the muscle during its contraction, have been examined to identify the motor control strategies during ramp or step isometric contraction, in which the force or torque is linearly increased or steadily maintained (Akasaka et al., 1996; Akasaka et al., 1997; Akataki et al., 2001; Beck et al., 2004, 2005; Bilodeau et al., 1997; Ryan et al., 2008a; Ryan et al., 2008b). For example, EMG has been used to study the difference between various muscle contraction protocols (Bilodeau et al., 1991; Lariviere et al., 2001; Nadeau et al., 1993; Sanchez et al., 1993).

2.1.5 Muscle Contraction Pattern

Voluntary muscle contractions can be classified according to either the length change or the force level, such as isometric, isokinetic, isotonic, concentric and eccentric contractions (Lieber, 2009). In isometric contraction, the muscle remains the same length. The MVC value was defined as the highest value of force or torque recorded during the isometric contraction (Hakkinen and Hakkinen, 1991). Two common isometric contraction types are ramp and step. In the ramp increasing and decreasing contractions, the subject is required to linearly increase the force or torque from 0 to MVC (or a sub-maximal MVC value) and then decrease back to zero. While in the step contraction, the subject is required to maintain the force or torque at a stable sub-maximal MVC value for a predefined length of time. In isokinetic contraction, the muscle contraction velocity remains unchanged. True isokinetic contractions are rare in daily life and are primarily an analysis method which is used in experiments on isolated muscles dissected out of the organism. In isotonic contraction, the tension remains

constant with the changes of muscle length. It means the maximum force or torque generated by the muscle exceeds the total load on it. The contraction with the shortening of muscle length is referred to as a concentric contraction. When the muscle is forced to lengthen due to the generated force is insufficient to overcome the external load, the contractions is referred to as an eccentric contraction (MacIntosh et al., 2005).

2.1.6 Muscle Stiffness

Skeletal muscle is composed of contractile (myosin) and passive elastic (actin and connective tissues) components (Shorten, 1987). Stiffness, which is observed in both active and passive muscle behaviors (Fung, 1993), has been shown to contribute significantly to muscle efficiency (Wilson et al., 1994). Passive stiffness of muscle is important for the control of movement because it determines the muscle resistance to the external perturbations. On the other hand, active muscle stiffness plays a key role in both the force generation and the body movements procedures. In addition, the stiffness of fast fibers (type II) was found to be lower than that of slow fibers (type I) (Goubel and Marini, 1987). And it was also found that different muscles exhibited different muscle stiffness at relaxed condition. This may be caused by the different muscle fiber orientation, e.g. biceps brachii, which is a bipennate muscle, exhibited a higher muscle stiffness than the unipennate muscles, such as vastus lateralis (VL) and vastus medialis (VM) (Bensamoun et al., 2006). The stiffness of skeletal muscle will be altered due to pathology or injury. It is well-known from palpation that muscle stiffness changes in some physiological conditions, such as voluntary contraction, and in some pathological conditions, such as spasm, cramps, oedema and delayed onset muscle soreness (Gennisson, 2005). Quantifying the muscle stiffness can help to improve the understanding of several kinds of muscular functional changes. Therefore, the *in vivo*

assessment of muscle stiffness is a valuable complement to muscle diagnosis and therapy monitoring, and several methods have been developed to meet this requirement.

2.1.7 Quadriceps Femoris Muscles

Quadriceps femoris muscles were selected as the target of this study. Quadriceps femoris is a large muscle group which includes four prevailing muscles on the front of the thigh. One of them, rectus femoris (RF), occupies the middle of the thigh, covering most of the other three quadriceps muscles. Vastus lateralis (VL) is on the lateral side of the femur (i.e. on the outer side of the thigh). Vastus medialis (VM) is on the medial side of the femur (i.e. on the inner part thigh). Vastus intermedius (VI) lies between VL and VM, right under the RF in the front of the femur. The anatomy of the four portions of quadriceps femoris is shown in Fig. 2.3. It forms a large fleshy mass which covers the front and sides of the femur and all four component muscles are powerful extensors of the knee joint. They are the strongest and leanest muscle in the human body and are crucial in walking, running, jumping and squatting (Abernethy et al., 2005). Therefore, studying the mechanical properties of quadriceps femoris muscles and assessing their functions are important when making a diagnosis, therapy or muscle strength training (Bensamoun et al., 2006; Karamanidis and Arampatzi, 2006; Kubo et al., 2001; Kubo et al., 2006).

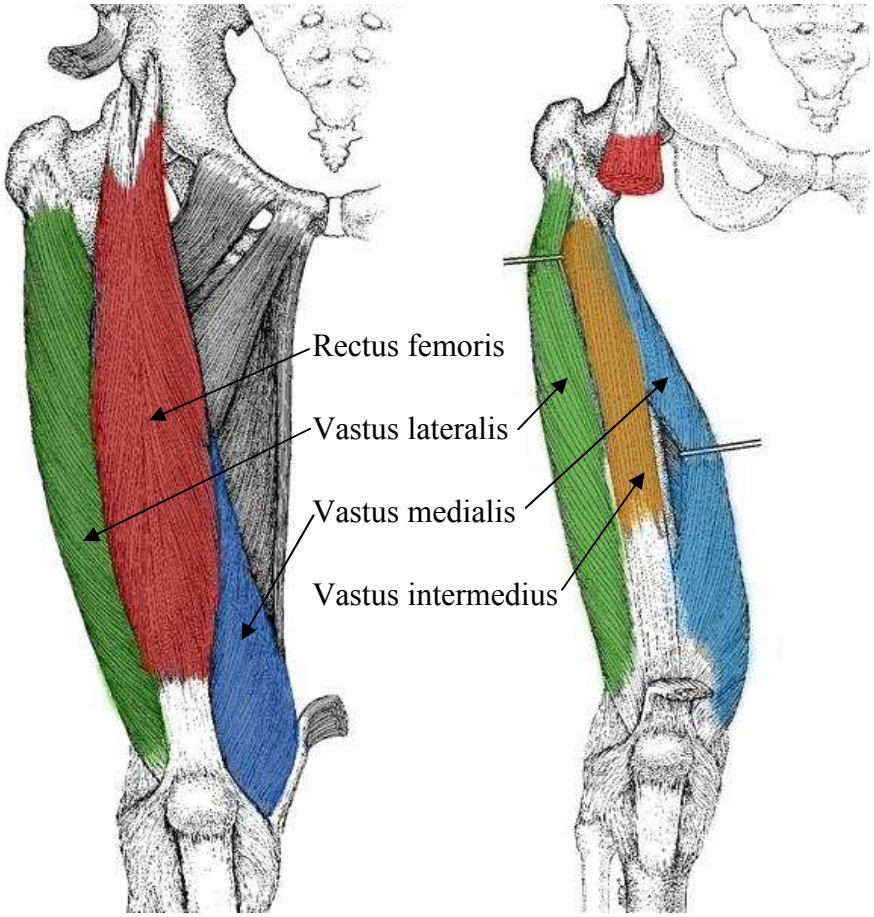

Fig. 2.3 Anatomy of quadriceps femoris muscle group (rectus femoris, vastus lateralis, vastus medialis and vastus intermedius). (from http://anatomy.askthetrainer.com/)

Various studies have been performed to investigate the structure, function and characteristics of quadriceps femoris muscles. Surface EMG, fine wire EMG and MMG have been used to study the activity level of the four muscles of quadriceps femoris during isometric knee extension and some other complex actions (Ebersole et al., 1999; Kimura et al., 2008; Pincivero et al., 2006). Muscle thickness, fascicle angle and fascicle length at multiple regions of the quadriceps muscles have been measured using ultrasound and other imaging methods (Arts et al., 2010; Karamanidis and Arampatzi, 2006; Rutherford and Jones, 1992; Willan et al., 1992; Willan et al., 2002). In addition, the gender difference between adult men and women (Blazevich et al. 2006), the age difference between adults and children (O'Brien et al., 2010), and between young and

elderly adults (Karamanidis and Arampatzi, 2006) of these morphological parameters have also been compared. Furthermore, the isometric MVC torque of knee extensor was compared with the volumes, pennation angles of quadriceps femoris muscles and knee joint angles (Narici et al., 1992). Using biopsy method, fiber type composition of VL and VM of young men and women was also studied (Staron et al., 2000).

2.2 Techniques for Muscle Assessment

2.2.1 Electromyography

Electromyography (EMG), the electrical signal collected by the electrodes during muscle contractions, reveals the electrical activity of a skeletal muscle and demonstrates the physiological process for muscle contraction. There are two types of EMG: fine wire EMG and surface EMG. Fine wire EMG is collected from two fine-wire electrodes which are inserted into the muscle. It is used to reflect the MUAP of certain muscle fibers and therefore can be used to detect the neuromuscular disorders and diseases (http://en.wikipedia.org/wiki/Electromyography). Otherwise, surface EMG signal is collected from the electrodes attached to the skin surface. It is the summation of individual MUAPs generated during the muscle activation. Compared with the fine wire EMG, it provides the information of overall muscle function rather than certain muscle fibers. In addition, surface EMG is non-invasive and non-painful to the patient. Therefore, surface EMG is widely used in both the clinical diagnosis and research. However, sometimes the electrical cross-talk from the adjacent muscles reduces its validity on studying a single muscle. In situations where this issue is of concern, it is advisable to reduce the size of the electrodes (De Luca, 1997; De Luca, 2002).

EMG is a direct reflection of muscle activity and various analyses have been carried out to investigate the relationship between the features of EMG patterns and muscle forces (Liu et al., 1999), joint angles (Sepulveda et al., 1993), joint moments (Wang and Buchanan, 2002), and joint torques and trajectory (Hahn, 2007; Koike and Kawato, 1995). Moreover, it has been widely used for the evaluation of muscle function in biomechanics and kinesiology (Benoit and Dowling, 2006; Paavolainen et al., 2006), muscle pathology (Labarre, 2006), muscle fatigue (Masuda et al., 1999; MacIsaac et al., 2006), and prosthetic device control (Kermani et al., 1995; Kuiken et al., 2004). During the past decade, lots of different algorithms have been developed to process EMG signals, such as time-frequency representation (Engelhart et al., 1999; Karlsson and Gerdle, 2001), wavelet analysis (Al-Assaf 2006; Englehart et al., 1999), fractal method (Talebinejad et al., 2009), and support vector machine (SVM) algorithm which has been applied to EMG-related neuromuscular disease diagnosis (Xie et al., 2003). All these efforts aim to extract efficient features of the EMG signal to represent the skeletal muscle physiological characteristics.

2.2.2 Mechanomyography

Mechanomyography (MMG) is the oscillation generated by the muscle during its contraction (Orizio et al., 2003). As the mechanical consequence of the motor unit electrical activity, MMG was detected from the body surface overlaying the muscle with, for example, accelerometers (Beck et al., 2004). It has been advised that the lateral oscillations detected by MMG could be decomposed into three parts: (1) a gross lateral movement at the beginning of a muscle contraction (2) smaller subsequent lateral oscillations produced at the resonant frequency of the muscle, (3) dimensional changes of the muscle fiber (Beck et al., 2004; Orizio, 1993).

The features of MMG have been reported to examine the kinematic and physiological characters during postural control (Kouzaki and Fukunaga, 2008), concentric muscle contractions (Ebersole et al., 1999), cycle ergometry (Housh et al., 2000; Perry et al., 2001), and to detect various muscular disorders, including cerebral palsy (Akataki et al., 1996), myotonic dystrophy (Orizio et al., 1997), low back pain (Yoshitake et al., 2001), and muscle fatigue (Mamaghani et al., 2002). MMG signal can also be used for monitoring the muscle activity level and has the potential for prosthetic control (Xie et al., 2009b). Furthermore, EMG and MMG have been acquired simultaneously to investigate the skeletal muscle characteristics, for example, to study the difference of agonist and antagonist muscles between elderly and young women (Jaskolska et al., 2003), and to estimate the reason of elbow flexor torque changes at different joint angles (Jaskolska et al., 2004). Additionally, EMG and MMG have been thoroughly compared during isometric, concentric and eccentric contractions at different MVC (Madeleine et al., 2002).

2.2.3 Morphological Parameters Measured by Imaging Methods

2.2.3.1 Morphological Parameters

Besides EMG and MMG, some morphological parameters of muscles, such as muscle thickness, pennation angle, fascicle length and cross-sectional area, can be estimated *in vivo* from the images collected by ultrasonography, computerized tomography (CT), or magnetic resonance imaging (MRI). In some muscles, the fibers insert into a sheet of membrane named aponeurosis, which thickens to become the tendon at the ends of a skeletal muscle. Pennation angle is defined as the angle at which the fascicles run into the aponeurosis. The force acting along the muscle axis is the product of the muscle

fiber force and the cosine of the pennation angle. Fascicle length is another important morphological parameter. In many cases, when investigators refer to muscle fiber length, they are actually referring to fascicle length. The propagation velocity of action potentials is correlated with the fascicle length (Arendt-Nielsen et al., 1992). Fig. 2.4 shows an example of muscle morphological parameters measurement, where Ito et al. (1998) used ultrasound images to detect the pennation angle and fascicle length of human tibialis anterior muscle.

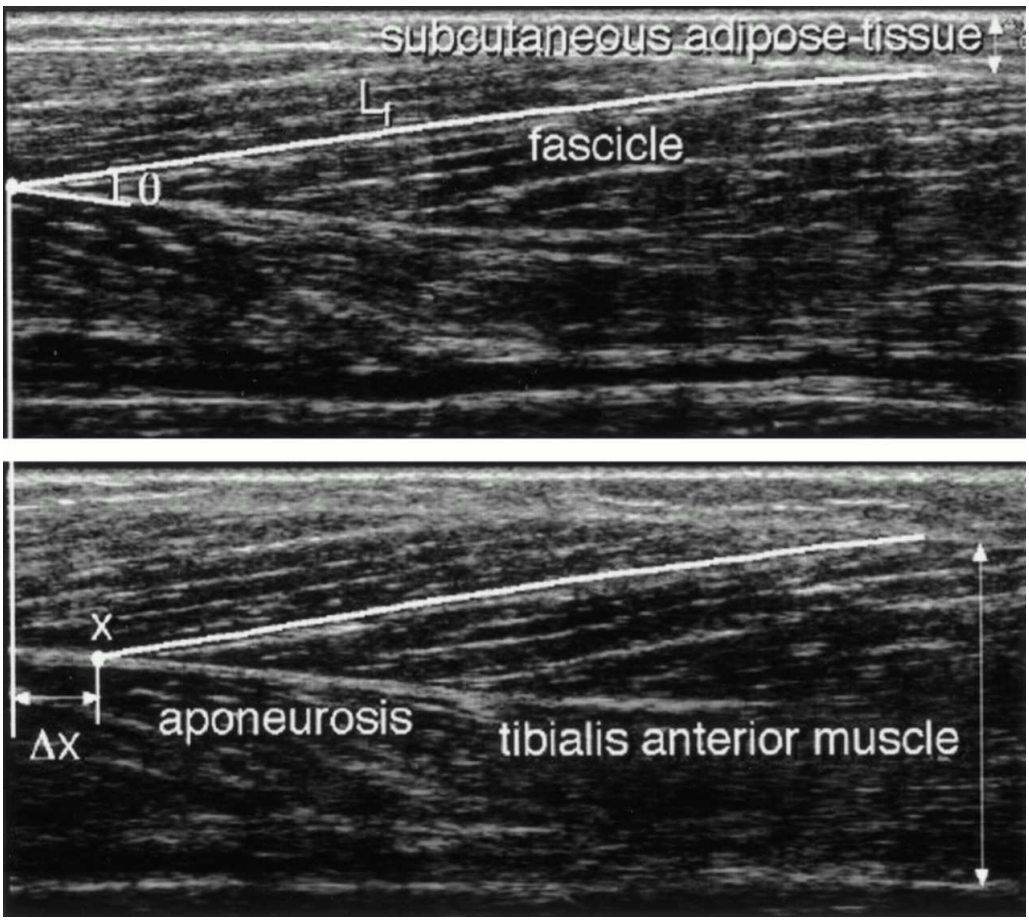

Fig. 2.4 Pennation angle and fascicle length of tibialis anterior muscle (Ito et al., 1998).

A cross-sectional image of leg at the mid-thigh level produced by CT scanning was shown for muscles' physiological cross-sectional area (CSA) calculation (Fig. 2.5). The isometric force of a muscle is closely correlated with its CSA and is not dependent

on its length (Ikai et al., 1970; Morris, 1948). In addition, a significant positive correlation between the CSA of knee extensor muscles and the MVC force was also reported (Maughan et al. 1983).

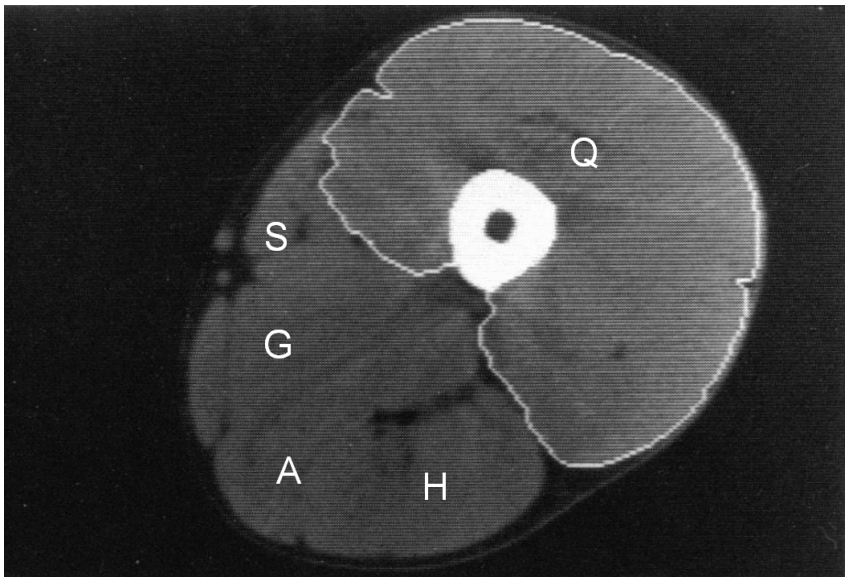

Fig. 2.5 CT scan obtained from an untrained healthy subject. The knee extensor muscles: A: adductors, G: gracilis, H: hamsstrings, Q: quadriceps, S: sartorius (Maughan et al., 1983).

2.2.3.2 Ultrasonography

Ultrasonography is widely used in the measurement of morphology changes of skeletal muscles due to its advantages, such as being stable, easy to use, cheap and able to record instantaneous activities from the deeper muscles without cross-talk from adjacent ones (Hodges et al., 2003). It has been used to detect the changes of muscle thickness or displacement (Bojsen-Moller et al., 2003; Farella et al., 2003; Mannion et al., 2008; Matsubayashi et al., 2008; Muller et al., 2000; Nogueira et al., 2009; Sallinen et al., 2008; Springer and Gill, 2007; Suzana et al., 2008), pennation angle (Ichinose et al., 1997; Mahlfeld et al., 2004), cross-sectional areas (Kanehisa et al., 1995; Narici et al., 1996; Reeves et al., 2004), and muscle fascicle length (Fukunaga et al., 2001; Griffiths, 1987; Ichinose et al., 1997). These ultrasound parameters have also been suggested to

characterize muscular pain, injuries and dysfunction (Bernathova et al., 2008; Botteron et al., 2009; Chester et al., 2008; Diaz et al., 2008; Sikdar et al., 2008). However, most of these measurements were in static and quasi-static conditions.

Since skeletal muscle architecture is closely correlated with its function (Lieber and Friden, 2000), ultrasound has been used together with EMG to provide more comprehensive information about the muscle activities and properties (Andrade et al., 2009; Ferreira et al., 2004; Hides et al., 1994; Hodges et al., 2003; Ishikawa et al., 2006; Whittaker et al., 2007). It has been reported that the relationship between EMG and muscle morphological parameters is almost linear only in lower range of forces, but not in higher range of forces for tibialis anterior (TA) (Hodges et al., 2003), biceps brachii (Hodges et al., 2003; Shi et al., 2008), transversus abdominis (Hodges et al., 2003; McMeeken et al., 2004) and masseter muscle (Georgiakaki et al., 2007).

In a previous study, Zheng et al. (2006) used sonomyography (SMG) to describe the real-time muscle thickness change detected using B-mode ultrasound images during its dynamic contraction. A system was developed to record and analyze ultrasound images, force, joint angle and surface EMG simultaneously. The system has been successfully used for the analysis of muscle fatigue and it was found that the muscle thickness increased during the fatigue process (Shi et al., 2007). The correlation between EMG and SMG of muscles during isometric contraction has also been investigated (Shi et al., 2008). It has been proposed to use the real-time muscle morphological change detected by ultrasound, i.e., SMG, for the prosthetic control (Guo et al., 2009; Zheng et al., 2006), assessment of isometric muscle contraction (Shi et al., 2007, 2008; Zhou et al., 2008) and isotonic contraction (Xie et al., 2009a).

2.2.4 Muscle Stiffness Measurement

Skeleton muscle stiffness *in vivo* may differ strongly from the stiffness of excised muscle due to variations in hydrostatic pressure and biomechanical mechanisms such as muscle tension (Fung, 1993). Experimental techniques, such as quick release and sinusoidal perturbations, are classically used to study the mechanical behavior of muscle *in vivo* (Brown et al. 2009; Feit et al., 1985; Ochala et al. 2004; Robinson et al., 1994). They can only assess global mechanical properties of the musculotendinous and musculoarticular complexes without differentiation of the various structures in them (i.e., muscle, tendon, joint) and the different muscles involved in the task. Recently, more localized techniques have been implemented to quantify the muscle mechanical properties, such as shear stiffness and viscosity.

2.2.4.1 Indentation Methods

Palpation is widely used clinically to detect abnormal regions of increased stiffness as an indicator of pathological conditions. However, it is only a qualitative method. For quantitative estimation of muscle stiffness, some indentation assessment devices have been developed to obtain force-deformation relationship, which can be used to extract intrinsic material parameter based on the mathematical model of elastic indentation problem, e.g., the Hayes model (Hayes et al., 1972). A portable device called myotonometer was developed by applying external pressure on the skin surface with a small rod and analyzing the amount of deformation that occurs within a muscle. It has been used to assess the human elbow flexor muscles after eccentric exercise (Leonard et al., 2003; Murayama et al., 2000). Another device is the Tissue Ultrasound Palpation System (TUPS) (Zheng et al., 1997). It is comprised of a hand-held indentation probe with an ultrasound transducer, which can measure the tissue deformation and

simultaneously provide the muscle thickness, and a strain gauge load cell connected in series, which can measure the force exerted on it. The Young's modulus of the tissue then can be determined by the load-deformation relationship (Zheng and Mak, 1999; Zheng and Mak, 2000). Although these devices have acceptable reliability, the stiffness of muscle and other subcutaneous tissues, such as fat, is still difficult to be differentiated. And it is also not suitable for the assessment of deep muscles, of which the conditions are much different with the hypothesis defined by the commonly used mathematical models. Furthermore, indentation technique cannot provide stiffness measurement along the muscle action direction.

2.2.4.2 Methods Based on Shear Wave Velocity Measurement

A number of methods have also been proposed to assess the elasticity of soft tissue based on ultrasound imaging. Static elastography applies a quasi-static compression to the tissue and forms a 2-D image which provides a relative mapping of the estimated tissues strain (Ophir et al., 1991). Although this method is useful in detecting abnormal lesions, it is inadequate for assessing diffuse disease, where abnormality is not confined to a local region and there is no normal background tissue to provide contrast. Such circumstances require quantitative methods, where the tissue elastic parameters, such as Young's modulus or shear modulus, can be measured.

Based on the wave theory, for linear elastic, locally homogeneous, isotropic and incompressible material, the shear wave velocity c_s, by which the wave propagates in the material, is related to the shear modulus μ_1, which is one of several quantities for measuring stiffness of material, via the following well-known equation:

$$\mu_1 = \rho c_s^{\,2} \tag{2.1}$$

where ρ is the mass density of the material. Thus the estimation of shear wave velocity propagating in the muscle can yield an estimation of the muscle shear modulus. The velocity can be calculated from the time delay between the waveforms collected from two positions along the wave propagation path, or from the wave length measured from the 2-D strain images. Biological tissues always exhibit elasticity and viscosity simultaneously. For a more complicated model, they were assumed as a Voigt body, which consists of a linear elastic spring in parallel with a viscous dashpot (Fig. 2.6). Theoretically, for a homogeneous medium, the shear wave propagation velocity c_s for the Voigt model is related to the vibration frequency f_s (Oestreicher, 1951):

$$c_s = \sqrt{\frac{2(\mu_1^2 + f_s^2\mu_2^2)}{\rho(\mu_1 + \sqrt{\mu_1^2 + f_s^2\mu_2^2})}} \tag{2.2}$$

where μ_1 denotes the shear modulus, μ_2 denotes the shear viscosity and ρ is the mass density of the material. Note that in the absence of tissue viscosity (i.e., $\mu_2 = 0$), Eq. 2.2 will be simplified to the expression described by Eq. 2.1. In these models, the reconstruction assumption of a homogeneous and isotropic material is not valid for skeletal muscle, but these assumptions are generally assumed to yield an acceptable estimation of the tissue stiffness and viscosity. These models has been shown to be a promising technique for estimating the shear modulus and also the shear viscosity of various tissues including the skeletal muscle (Catheline et al., 1999; Gennisson et al., 2005; Kruse et al., 2000; Madsen et al., 1983; Muthupillai et al. 1995; Muthupillai et al. 1996). In addition, they have also been proved to be better than the other models, e.g. Maxwell model, for the agar-gelatin phantom and bovine muscle (Catheline S et al., 2004).

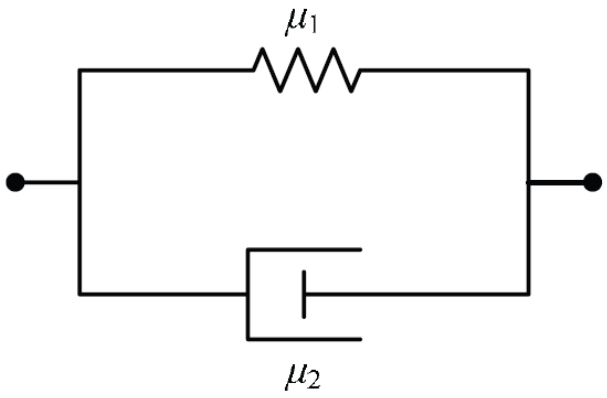

Fig. 2.6 Voigt viscoelastic model where μ1 and μ2 are the coefficients of elasticity and viscosity. (Hoyt et al., 2008)

Sonoelastography consists of steps of stimulating the tissue with a low-frequency monochromatic mechanical vibration (10 to 1000 Hz) and measuring the relative tissue displacement with a Doppler instrument. From the Doppler images, the shear wave velocity could be determined, and then the shear modulus can be calculated (Gao et al., 1996; Parker et al., 1990). Applied on human quadriceps muscles, this technique showed that the muscle shear modulus was highly correlated to the different weight of muscle active load (Levinson et al., 1995). Recently, crawling wave sonoelastography was developed by Wu et al. (2004). With this modality, slowly moving shear wave interference patterns (termed crawling waves) were generated using a pair of mechanical sources and imaged using sonoelastography, as shown in Fig. 2.7. The main advantage to this technique is that crawling wave wavelength can reflect local tissue stiffness (Wu et al., 2006; Hoyt et al., 2008). However, since sonoelastography requires long acquisition time, it is not desirable for studying the muscle at any significant fraction of MVC force or torque since the muscle will soon fatigue.

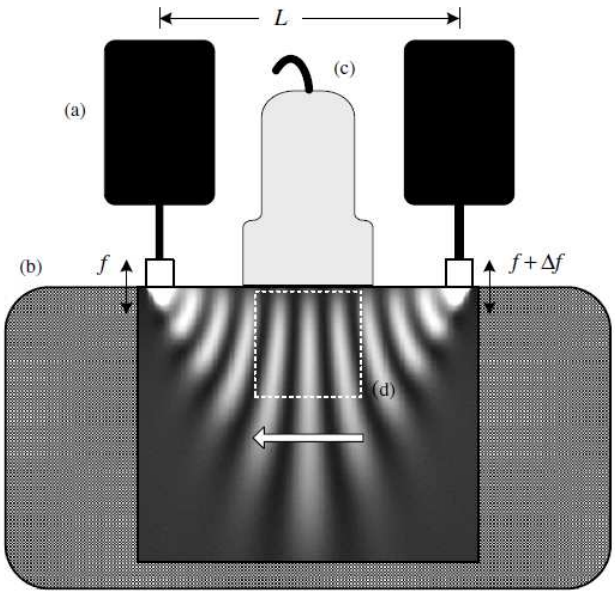

Fig. 2.7 Illustration of the crawling wave sonoelastography. Two mechanical sources (a) separated by distance L vibrate at slightly offset frequencies (double arrows) and coupled normal to the imaging material (b). Slowly moving shear wave displacement fields are imaged using an ultrasound probe (c) for a given region-of-interest (d) as these crawling wave propagate through the medium (large arrow). (Hoyt et al., 2008)

In contrast, transient elastography provides instantaneous measurement and can be used to track the muscle stiffness changes in the contraction process. In transient elastography, an ultrasound transducer is used also as a piston-like vibrator to apply a pulsed excitation on the tissue, and the direction of the studied shear wave propagation is perpendicular to the muscle action direction (Catheline et al., 1999; Sandrin et al., 2002). The displacements induced by the transient shear wave are estimated using a speckle tracking method (Ophir et al., 1991). The M-mode displacement field image of transient elastography is shown in Fig. 2.8. This method has been used to assess the stiffness of biceps brachii muscle and the gastrocnemius medius muscle (Gennisson et al., 2005; Nordez et al., 2009; Sandrin et al., 2002), and it has been shown that the transverse shear modulus of muscles is related to their activity level (Gennisson et al., 2005) and their passive tension (Nordez et al., 2008). However, the coefficients of determination reported by Gennisson et al. ($R^2 = 0.55$) and the repeatability reported by

Nordez et al. were both lower than desired levels. This indicated the limitations of this 1D technique to accurately estimate muscle activity from the elastic modulus. Since the skeletal muscle is an anisotropic tissue, the shear modulus along the direction of muscle action is desired to be more related to the muscle activity level than the transverse shear modulus, and thus more desirable in research and clinical studies. Recently，the transient elastography has been extended to investigate the 2D shear wave propagation, which is termed as supersonic shear imaging (SSI) (Sandrin et al., 1999; Sandrin et al., 2002). In SSI, besides the shear modulus, the dispersion phenomenon of shear wave propagation, in which the shear wave velocity varies depending on its frequency, was used to estimate the shear viscosity of soft tissues based on the Voigt model. SSI has been reported to study the stiffness of biceps brachii muscle (Nordez and Hug, 2010) and muscles in the lower leg (Shinohara et al., 2010). The results confirmed that the use of SSI can improve the calculated correlation coefficients between muscle shear modulus and EMG expressing muscle activity levels. This also showed that SSI has potential to be used to indirectly estimate muscle stress. However, this technique requires super fast imaging speed to achieve a very high frame rate, which is not compatible with current commercial ultrasound scanners. The frame rate limitation also made the stiffness measurements of SSI saturates at 100 kPa. In Nordez and Hug's recent study (2010), the incremental isometric ramp tasks were analyzed on the biceps brachii muscle only under $28 \pm 7\%$ of maximum EMG activity level due to this saturation issue. In Shinohara et al.'s study (2010), the contraction level of the lower leg muscles they studied was 30% MVC and all the shear modulus values they reported also did not exceed 100 kPa.

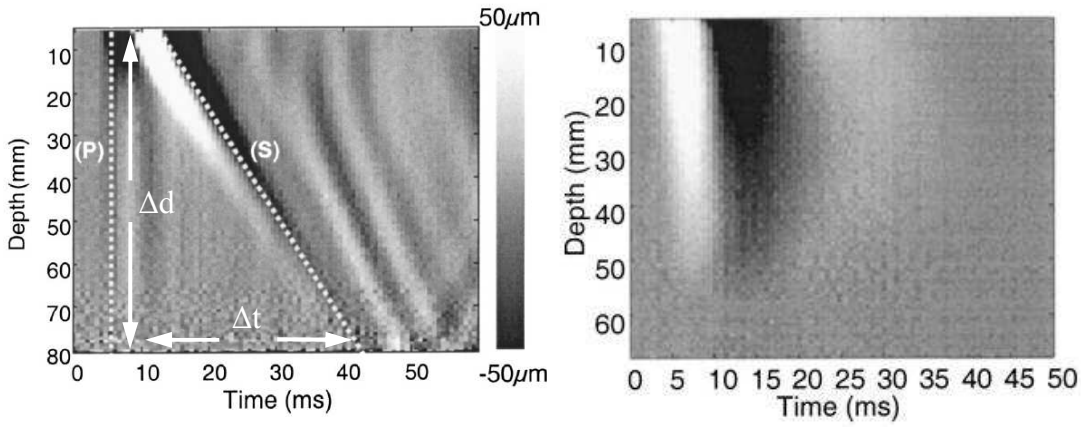

Fig. 2.8 Two typical displacement fields obtained for a pulse (100 Hz disturbance) in the transient elastography method. The displacements of a compressional wave (P) and of a shear wave (S) in an Agar-gelatin based phantom can be observed in the left one. The shear wave velocity can be obtained by divided depth Δd with time Δt. The experimental displacement field along depth versus time on a beef muscle is shown in the right one (Gennisson et al., 2003).

Another instantaneous measurement technique which is called shearwave dispersion ultrasound vibrometry (SDUV) focused on the measurement of tissue elasticity along the same direction of shear wave propagation (Chen et al., 2009). A harmonic shear wave is produced by the acoustic force generated by a focused ultrasound beam, and its propagation is monitored by a pulse echo ultrasound beams at one side of the vibration source. The shear wave velocity is calculated from the time delay and distance between the two positions, as shown in Fig. 2.9. Besides the shear modulus, it can also solve the shear viscosity of the soft tissues using the frequency-velocity dispersion curve. The technique has been verified using two separated ultrasound transducers, one for pushing and the other one for detection. However, penetration depth of SDUV is limited by whether enough ultrasound intensity can be delivered to the depth of measurement to generate sufficient tissue vibration. It is not very successful when using the single commercial linear array transducer to generate both the acoustic force and the detection beam, since the acoustic force cannot generate decent shear waves at enough depth of the deep muscle (Chen et al., 2008). This technique has been evaluated on the porcine muscle (Urban et al., 2009) and bovine muscle (Chen et al., 2008), but has not been

reported to be used for the assessment of human muscle stiffness *in vivo*.

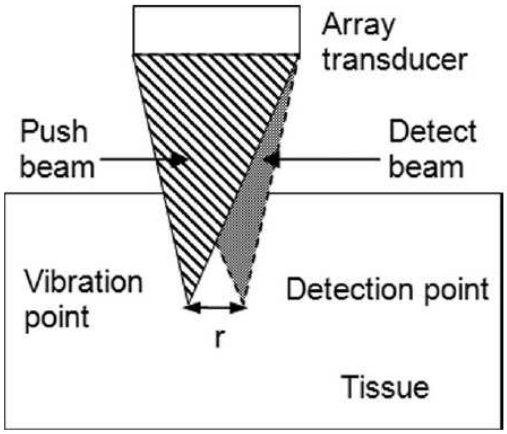

Fig. 2.9 Illustration of the principle of shearwave dispersion ultrasound vibrometry (SDUV). The pushing and detecting beams are focused at two different locations separated by distance r. The shear wave velocity can be calculated by divided the distance r with the time delay Δt. (Chen et al., 2009)

Magnetic resonance elastography (MRE) is a novel non-invasive phase-contrast MR technique which is capable of visualizing small amplitude wave propagation excited by an external vibrator (Muthupillai et al. 1995; Muthupillai et al. 1996). The wavelength λ of shear wave can be measured from the MR images and used to calculate shear wave velocity c_s with the following equation:

$$c_s = \lambda f_s \tag{3}$$

where f_s is the vibration frequency. An elastogram of the spatial elasticity distribution then can be produced throughout the tissue. Fig. 2.10 shows the MR modulus image and corresponding wave image of a human's calf. In contrast to ultrasound, MRE has no limitations in penetration depth and can provide images with a high resolution. Many studies have been reported about the assessment of muscle stiffness using MRE method (Bensamoun et al., 2006; Bensamoun et al., 2008; Dresner et al., 2001; Ringleb et al., 2007; Sack et al., 2002; Uffmann et al., 2004). However, it is expensive and requires very long acquisition time (about 1-3 minutes for one acquisition). This greatly limits its

application, particularly when under high intensity muscle contraction. It was also observed that the SNR of the MRE wave images decreased with the increase of contraction levels after 20% MVC (Bensamoun et al., 2008).

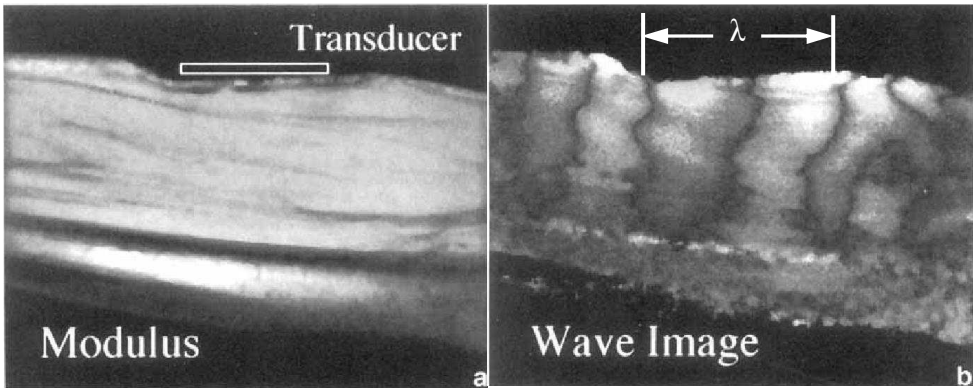

Fig. 2.10 Shear waves were applied to the calf of a human volunteer at the location illustrated in the modulus image (a). The corresponding wave image (b) was acquired using magnetic resonance elastography (MRE) with two cycles of motion-sensitizing gradients and clearly depicts propagating waves in vivo. (Muthupillai et al. 1996)

2.2.4.3 Shear Wave Generation and Propagation Pattern in Skeleton Muscle

There are two methods often to be used to generate shear waves in soft tissue. One is to generate mechanical shear waves at the skin surface using an electromagnetic vibrator and the waves will propagate into the tissue, as used in the transient elastography and MRE. The other one is using the focused ultrasound beam to generate acoustic force at a given depth and the shear waves will propagate from this starting point to the surrounding tissue, as used in the SSI and SDUV. The former method can generate much larger amplitude waves than the later one, so the displacement of the tissue can be easily tracked. In addition, the generated shear waves can be monochromatic and so the tracking results can be easily filtered to remove noise. However, the external mechanical vibration is difficult to standardize for *in vivo* experiments. In the process of the propagation from the skin surface to the inside tissue, refraction and reflection will

occur at the interfaces between two tissue layers with different mechanical properties, especially when there is complex bone-muscle geometry (Heers et al., 2003). This will change the wave patterns and make the wavelength or time delay hardly to be measured accurately. The later method can reduce the interference from wave reverberation phenomenon and make the system more compact. However, due to the power limitation caused by safety consideration, it can only generate very small amplitude vibrations at a limited depth. This shortage limits its usage on the deep muscles and makes the tissue displacement tracking much harder.

Shear wave propagation patterns in the soft tissue has demonstrated several wave phenomena. The wave front undergoes refraction and reflection at the interface between the stiff and soft medium, such as an aponeurosis or a bone. Attenuation of the shear wave as it propagates through the tissue is also evident. All of these phenomena will affect the wave patterns in the skeleton muscle and the measured shear wave velocity (Muthupillai et al., 1996). How to avoid the negative influences of these wave phenomena must be thoroughly considered when designing the experiment. Skeleton muscle is known to be anisotropic. Muscle filaments can slide along each other and the coupling between them may be the reason that muscle demonstrates lower stiffness in the direction across the muscle fibers than in the direction along the fibers, which is approximately the muscle action direction. So for the mechanical vibration method, the short push-bar mounted on the rod of the vibrator must be kept in a consistent orientation to generate shear wave propagation parallel to the muscle fibers to minimize the anisotropic effects (Chen et al., 2009; Gennisson et al., 2005; Hoyt et al., 2008; Kruse et al., 2000). When the external excitation is applied on different positions, the shear wave patterns in the muscle will also be different (Sack et al., 2002). V-shaped

waves were observed when excitation was applied on the tendon, since the shear wave propagation in a central band of stiff fascicles was about twice as fast as that in surrounding soft tissues. However, when excitation was applied on the muscle belly surface using a short push-bar, the shear wave patterns were planar as all muscle fibers were simultaneously excited.

The influence of viscosity on shear wave velocity measurements in muscle has been previously studied (Catheline et al., 2004; Deffieux et al., 2009). Using SSI, Deffieux et al. (2009) found that in the direction along the muscle action direction, the shear wave propagation was practically non-dispersive, whereas in the direction perpendicular to the muscle action, the propagation was highly dispersive. In addition, at several different isometric contraction levels, the shear wave velocity along the direction of muscle action still remained quasi-constant when the exciting frequency increased. Their results are also in accordance with those reported by Catheline et al. (2004) using transient elastography method on bovine muscles. Therefore, the shear wave velocity is almost independent of the exciting frequency and the viscous effects can be neglected when the muscle shear modulus along the muscle action direction is measured.

2.3 Muscle Variations with Age, Gender and Other Factors

2.3.1 Muscle Ageing

Sarcopenia is a term referring to the degenerative loss of skeletal muscle mass and strength in elderly humans. It starts as early as 30 years elderly and becoming significant around the age of 60 years (Jones and Haan et al., 2004; Lieber, 2009). With the age increasing, these degenerations will be associated with increased susceptibility

to fall and a decreasing mobility. Some studies have been reported about the relationship between the age-related muscle weakness of elderly adults and their ability of dynamic stability control (Arampatzis et al., 2008; Grabiner et al., 2005; Karamanidis et al. 2008). Since the aged population is the fastest growing subgroup in the world, muscle ageing presents a serious problem for the health and social services.

2.3.1.1 Strength Changes with Ageing

Comparisons of the isometric MVC force or torque in young and elderly subjects have been performed for several different muscle groups, such as the ankle plantarflexors, the knee extensors, the handgrips and the elbow extensors. It has been demonstrated by these studies that the loss of muscle strength occurs in all the muscle groups tested and it affects men and women equally (MacIntosh et al., 2005). The decline in the muscle strength of elderly adults comparing to the young ones is in a range from about 20% to larger than 60%. Likewise, the maximum velocity of contraction also decreases in the elderly subjects (Abernethy et al., 2005; MacIntosh et al., 2005).

2.3.1.2 Muscle Fibers Changes with Ageing

Corresponding to the loss of muscle strength, the muscle size estimated from the muscle CSA has also been proved to be about 20% smaller in elderly adults compared to young adults (Klein et al. 2001; Narici et al. 2003). The decrease in muscle volume could be due to fiber atrophy and decreased numbers of fibers. Lexell et al. (1983) found that the VL muscle of elderly men contain about 25% fewer fibers than the corresponding muscles of young men. In addition, ageing also leads to marked alterations in muscle architecture that potentially contribute to the strength loss. Muscle fascicle lengths and pennation angles in elderly individuals were reported to be significantly smaller than

those in young adults (Morse et al., 2005; Narici et al., 2003; Narici et al., 2008). Moreover, according to the studies on the fiber types, an increase in the relative percentage of type I fibers was found, and the fiber atrophy with ageing is most pronounced for type II fibers (Larsson et al., 1978). The dominant loss of the fast fibers also explained the slowing of the contractile properties of the ageing muscle (MacIntosh et al., 2005).

2.3.1.3 Antagonist Muscle Coactivation with Ageing

Muscle coactivation is the concurrent activity of agonist and antagonist muscles surrounding a joint. The conventional interpretation of coactivation is that it serves to increase joint stiffness to absorb the energy of impact (Hortobagyi et al., 2000). As a prerequisite for studying the muscle coactivation, it has been observed that both young and elderly subjects could fully activate their muscles (Phillips et al., 1992). However, the level of coactivation has been observed increasing slowly with age (Klein et al., 2001). In a recent study, coactivation in elderly adults was reported to be increasing with age independent of the different muscle or the type of muscle contraction (Hortobagyi et al., 2009). These changes of skeleton muscles can increase the joint stability and safety to compensate the reduction of muscle strength in the elderly adults (Ochala et al., 2004).

2.3.2 Gender Differences of Muscle

Anterior cruciate ligament (ACL) is a major ligament of human knee and important for proper movement. ACL injury is the most common knee ligament injury in athletes (http://en.wikipedia.org/wiki/Anterior_cruciate_ligament). Tears in the ACL often take place when the knee receives a direct impact from the front while the leg is in a stable

position, or when the knee is forced to make sharp changes in movement. The risk of ACL injury in female athletes is more than twice higher compared to equivalently trained males. Research has failed to identify a sole factor responsible for this gender discrepancy and this has been attributed to the multi-factorial effects of the gender differences in anatomy, muscular strength, reaction time of muscle contraction and training techniques (Aune et al., 1996; Eiling et al., 2007; Padua et al., 2005; Park et al., 2008; Withrow et al., 2006; Zhang et al., 1997). The best way to prevent an ACL injury is to implement warm up drills before training or match. These drills will increase neuromuscular control and conditioning. In turn, muscular reactions will improve thus decreasing the risk of an ACL injury.

Previous researches indicated that the muscle mass and cross-sectional area are greater in males than in females (Miller et al., 1993; Staron et al., 2000). Muscle architecture is also different between genders. Females were found to have longer muscle fiber length and males have thicker muscles and larger pennation angles (Chow et al., 2000). Although many studies have found gender differences related to fiber size, conflicting reports have been published regarding the gender differences in fiber type distribution. Inconsistent results have been reported with a higher percentage of slow fibers in women, in men, or no difference between men and women (Blackburn et al., 2009; Staron et al., 2000). As a global mechanical property of the knee joint including muscle, tendon, bone and cartilage, the knee flexor stiffness of males was greater than that of females. However, no gender difference in knee flexor stiffness was found after normalizing to the anthropometric characteristics (Blackburn et al., 2004; Granata et al., 2002). When focusing on an individual muscle, the elastic modulus of hamstring was found to have no gender difference (Blackburn et al., 2009). But at a different muscle,

triceps surae, the elastic modulus was significantly greater in males than females (Blackburn et al., 2006).

2.4 Summary

This chapter has mainly reviewed the previous studies for the methods of skeletal muscle stiffness assessment, and the age and gender differences of skeletal muscle properties. The method based on shear wave velocity measurement can provide quantitative estimation of muscle stiffness, i.e. shear modulus, and is becoming a promising technique in this field. Many previous studies have been reported about the correlation between muscle stiffness and muscle activity level during non-fatiguing contraction. Some of them used different weight loads to represent the different muscle activity levels at step isometric contraction, such as from 1kg to 10 kg (Dresner et al., 2001; Sandrin et al., 2002). But for individuals with different muscle strength, especially when the age and gender dependences of muscle stiffness are to be considered, the same weight load does not mean the same relative muscle activity level compared with the maximum contraction capability of the individuals their own. The more reasonable method is to use the percentage of MVC as an indicator, such as dividing the range from 0% MVC to 100% MVC into different levels, to describe the different muscle activity levels. However, all current muscle stiffness assessment methods mentioned above are not suitable for this kind of study due to the limitation of the measurement range. MRE has been used under different percentage of MVC levels, but acceptable quantitative results can be only achieved under up to 20% MVC level (Bensamoun et al., 2008). At higher percent levels, the SNR of the MRE images was significantly reduced due to the long acquisition time. In contrast, ultrasound methods

can provide instantaneous measurement and thus overcome the fatigue issue. SSI has been applied to study the muscle stiffness at different contraction levels (Nordez and Hug, 2010; Shinohara et al., 2010). However, the small imaging region and the limited frame rate made the measured shear modulus saturate at 100 kPa. The isometric contraction tasks were analyzed only under up to 30% MVC level due to this saturation issue. On the other hand, quadriceps femoris muscles are extensors of the knee joint. They are the strongest and leanest muscle in the human body and play an important role in normal actions and movements. Although many studies have been performed on this muscle group using traditional assessment methods, such as EMG, MMG and morphology measurement, the stiffness of its four separate portions was rarely studied (Bensamoun et al., 2006; Bensamoun et al., 2008), especially the deeper one, VI muscle. In addition, very little has been done on the age and gender dependences of muscle stiffness under different muscle contraction levels. To fix these gaps, the main objectives of this study are 1) to develop a new vibro-ultrasound method to characterize the stiffness of VI along the muscle action direction in a full muscle contraction range, i.e. from 0% to 100% MVC levels of step isometric contraction; 2) to determine the relationship between the measured muscle stiffness and the incremental step isometric contraction levels of knee extensor; 3) to compare the results of above assessments obtained from four divided groups of subjects with different age ranges and genders; 4) to correlate the muscle stiffness with the EMG expressing muscle activity level.

CHAPTER 3 METHODS

3.1 Skeletal Muscle Stiffness Measurement System

3.1.1 System Setup

The measurement system consisted of a programmable ultrasound scanner, a custom-made program for ultrasound data acquisition and a mechanical vibrator. An electromagnetic vibrator (minishaker type 4810, Brüel & Kjær, Nærum, Denmark), which was driven by a power amplifier and controlled by a conventional function generator, was used to induce shear waves in the muscle. The reason for selecting mechanical vibrator but not acoustic force method was that it can generate shear waves with enough large amplitude in the deep muscle, such as VI, and hence increase the SNR of the tracking results of tissue displacements. Moreover, for VI muscle and the RF muscle above it, their sizes are large, shapes are plane and their muscle fibers are almost aligned on the same axis to form a simple structure. Therefore, the refraction and reflection phenomenon along the direction of muscle action, i.e. the wave propagation direction we studied, can be greatly reduced and almost neglected. The vibrator impacted the muscle with monochromatic low-frequency sinusoidal pulses (100 Hz, 10 cycles for a train in this study). As mentioned in Section 2.2.4.3, the shear wave velocity is almost independent of the exciting frequency and the viscous effects can be neglected when measuring the muscle shear modulus along the muscle action direction. For soft tissue like skeleton muscle, low-frequency mechanical vibration must be used because of the power limitation of mechanical actuator and the rapid attenuation of propagating shear wave with a high frequency. In general, the vibration frequency of 90 to 150 Hz are typically used in MRE for the skeletal muscle assessment (Bensamoun et

al., 2008; Brauck et al., 2007; Domire et al., 2009; Ringleb et al., 2007; Suga et al., 2001). For a more reasonable comparison with the results of previous studies using MRE, which include almost all the studies of muscle shear modulus assessment at step isometric contraction, 100 Hz frequency was also selected to be used in this study. For the consideration of safety issue, the maximum force of the vibrator was 10 N and the maximum peak-to-peak displacement of the piston was 6 mm, thus the generated vibrations were very safe for the human subjects.

The shear wave velocity measurement system was developed based on a commercial ultrasound scanner SonixRP (Ultrasonix Medical Corp. Vancouver, Canada) with a 5-14 MHz (driven by the central frequency, 9.5 MHz) linear array probe and its software developing kits programmed by Visual C++ (Microsoft Corporation, USA). As demonstrated in Fig. 3.1, shear wave generated by the external vibrator propagated along the muscle action direction. The long axis of the linear array probe was placed along this direction. At the proximal and distal positions, the tissue displacements were monitored by two focused ultrasound beams. The distance between these two scan lines was Δr and the time delay between the two detected waveforms was Δt. The wave velocity c could then be calculated by

$$c = \Delta r / \Delta t \tag{3.1}$$

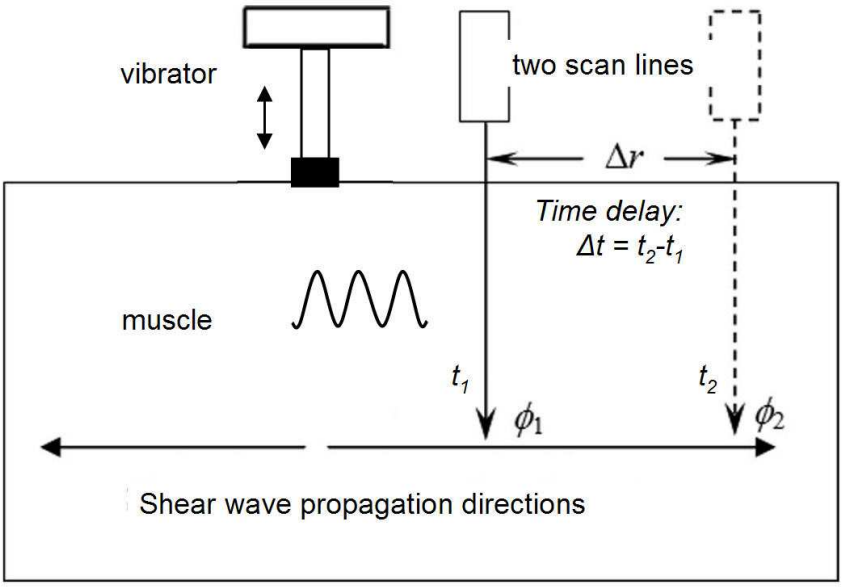

Fig. 3.1 Diagram of shear wave velocity measurement method using two scan lines.

A custom-designed ultrasound transmission and reception sequence was developed by programming the beamformer of the system. After the sequence started running, B-mode images were first acquired with 256 scan lines (corresponding to a width of 38 mm) and a predefined penetration depth (65 mm for the measurements on VI muscle) for helping position the probe on the expected place with a right orientation, where RF and VI could be clearly distinguished with aponeurosis and the transducer surface was parallel to the muscle action direction, as shown in Fig. 3.2. The short bar of the vibrator was also oriented under ultrasound guidance to guarantee the direction of shear wave propagation was parallel to the direction of muscle action and hence the anisotropic effects was minimized (Gennisson et al., 2005; Hoyt et al., 2008; Kruse et al., 2000).

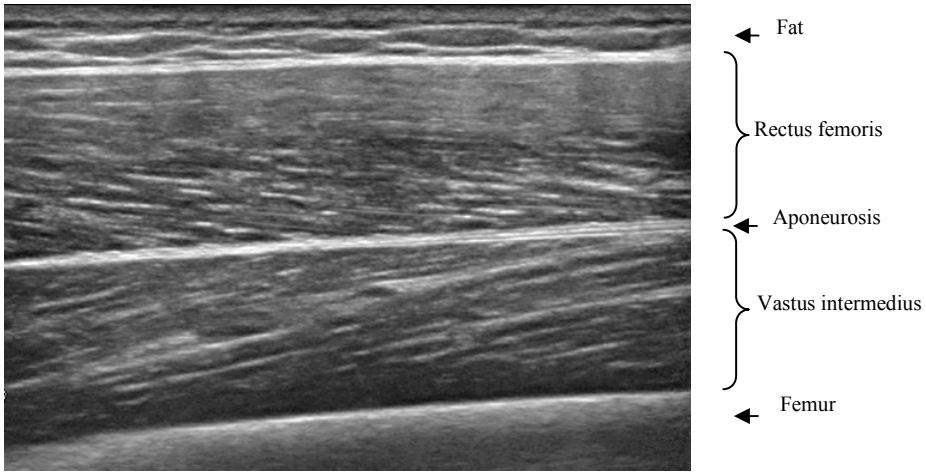

Fig. 3.2 A typical B-mode image of thigh muscles along the muscle action direction.

Then with an external trigger which was also used to control the vibrator, two scan lines with a predefined distance (in this study, a distance of 15 mm was used) were selected to measure the propagation of the shear wave. A very high frame rate could be achieved for the two scan lines. The exact frame rate depended on the predefined penetration depth, since the acquisition time for each frame increased with the penetration depth. The deeper was the depth, the longer the acquisition time, and thus the lower the frame rate. However, the exactly frame rate value would be different for different ultrasound scanner devices since the variations on hardware and software. Besides the frame rate, the distance between the two scan lines was another parameter which could affect the upper limit of shear wave velocity measurement. The larger the distance, the larger the time delay, hence when the frame rate was the same, the higher the velocity upper limit could be achieved. However, if the distance was too large, the amplitude of the shear wave detected at the distal point would be too small to be tracked. The 15 mm distance used in this study was the result of a compromise between the two factors mentioned above. The frame rate finally achieved in this study was up to 4.6 kHz at a 65 mm penetration depth, and theoretically the upper limit of velocity measurement was 69 m/s, assuming the minimally detectable time delay was 1 frame. This value

corresponded to a shear modulus of more than 4000 kPa, which could well satisfy the requirement of muscle stiffness measurement at even 100% MVC isometric contraction level. The sampling frequency of the received radio-frequency ultrasound signal was 40 MHz. The vibrator and the ultrasound scanner were synchronized using an external trigger signal to guarantee the vibration occurred in the ultrasound data acquisition period. The data acquisition was instantaneous and therefore the subject only needed to maintain the selected contraction level for a very short duration. For each measurement, 10000 frames radio-frequency data (equivalent to approximately 2s) were stored on the hard disk of SonixRP and then transferred to a computer for further analysis. As illustrated in Fig. 3.3, the whole experimental setup for human subjects also included a dynamometer and a system for surface EMG acquisition. The isometric torque production of knee extensor was assessed using a HUMAC NORM rehabilitation system (Computer Sports Medicine, Inc., Stoughton, MA, USA), which included a specially designed chair and a fixed dynamometer. The machine was set to the knee joint isolated movement pattern and isometric resistance mode. The knee joint angle of isometric contraction was also set using the machine. The surface EMG signal was captured using EMG bipolar Ag-AgCl electrodes (Noraxon U.S.A. Inc., USA) and pre-amplified with a gain of 100 using a circuit located near the electrodes. The signal was further amplified with another factor of 10 by the custom-designed EMG amplifier and filtered by a 10 to 400 Hz band-pass filter. The surface EMG was then digitized by a 12 bits data acquisition card (NI-DAQ 6024E, National Instruments Corporation, Austin, TX, USA) with a sampling rate of 4 kHz. Its sampling was also synchronized using the external trigger signal as mentioned above.

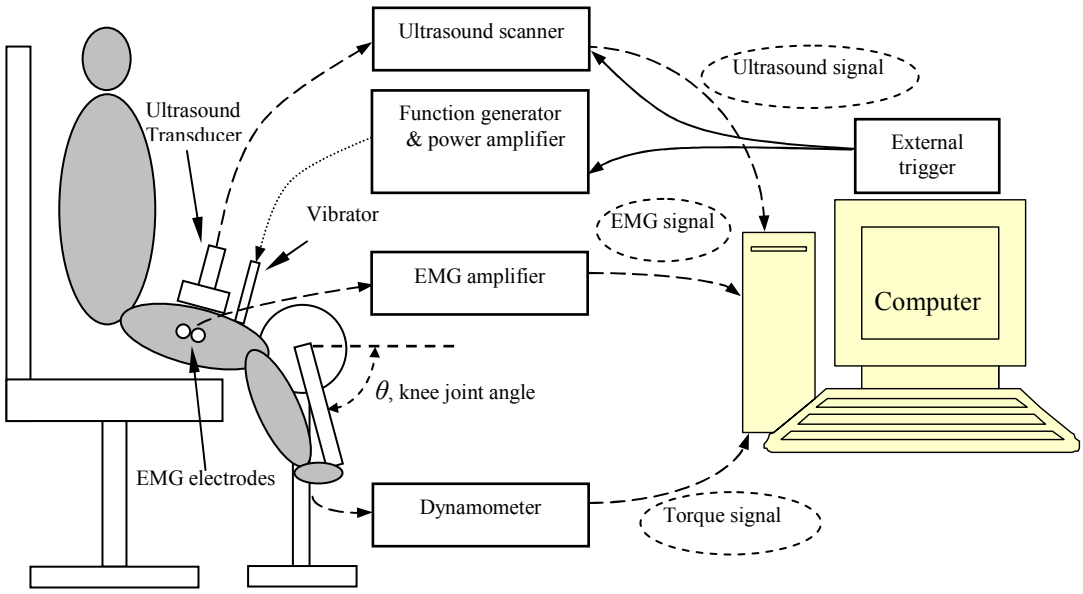

Fig. 3.3 Illustration of the data collection system used in this study.

3.1.2 Data Processing

3.1.2.1 Tissue Displacements Tracking

All signals were processed off-line using a custom-made program of Matlab (Version R2008, MathWorks, Inc., MA, USA). The tissue displacements induced by the vibrator at different depths were determined using the radio-frequency ultrasound signals by a modified cross-correlation algorithm, which is also called echo-tracking method (Cespedes et al., 1995; Ophir et al., 1991; Wang and Zheng, 2010). The function of Matlab *c=xcorr(x,y)* returns the cross-correlation sequence in a length *2*N-1* vector, where *x* and *y* are length *N* vectors (*N>1*). If *x* and *y* are not the same length, the shorter vector is zero-padded to the length of the longer vector. The equation used to calculate the one-dimensional cross-correlation is as follow:

$$R_{xy}(m) = \begin{cases} \sum_{n=0}^{N-m-1} x_{n+m} y_n^* & (m \geq 0) \\ R_{yx}^*(-m) & (m < 0) \end{cases} \quad (3\text{-}2)$$

The output vector *c* has elements given by:

$$c(m) = R_{xy}(m - N), \qquad m = 1, \ldots, 2N - 1 \quad (3\text{-}3)$$

It requires a reference signal segment from the initial frame of data and searches for the most similar segments to the reference one in the subsequent frames. Then the relative tissue movement in the vertical direction is estimated. Since tissue movement between two neighboring frame is generally not integral multiples of the sampling period, the location of the largest sample of the cross-correlation function (CCF) is an inexact estimator of the location of the peak. Therefore, we must interpolate between the samples of the CCF to improve the estimation precision. The maximum likelihood approach to interpolation is the application of a reconstruction filter to the discrete CCF. However, this method can only be approximated in practice and can be computationally intensive. For these reasons, a simple method has been widely used in the previous studies to fit a parabola to the samples of CCF in the neighborhood of its peak, as shown in Fig. 3.4 (Cespedes et al., 1995). In this study, the highest 3 points of the peak of CCF were linked with a fitted parabola and 200 points were interpolated in this range, then the location of the largest interpolated point was treated as the result.

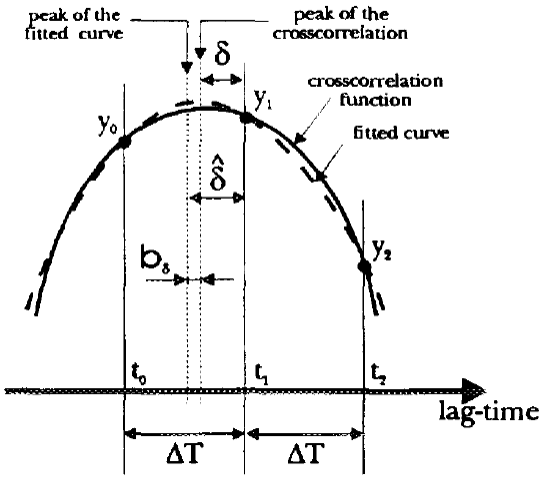

Fig. 3.4 Diagram of the cross-correlation function peak (solid line), its samples, and a fitted curve (dashed line) (Cespedes et al., 1995).

According to its size, the first frame of radio-frequency ultrasound signals was divided into 20 - 40 parts with equal length and 50% overlap (the number of segments depended on the selected penetration depth of ultrasound scanner). Each part was then treated as a reference signal segment and its movement was tracked and estimated using the cross-correlation algorithm frame by frame automatically. The tissue movements at different depths were then plotted with time along the x-axis and depth along the y-axis similar to an M-mode ultrasound image. Due to the high frame rate, the plotted waveforms could be very smooth, as demonstrated in Fig. 3.5. The shear wave velocity was estimated based on the two waveforms recorded by the two scan lines.

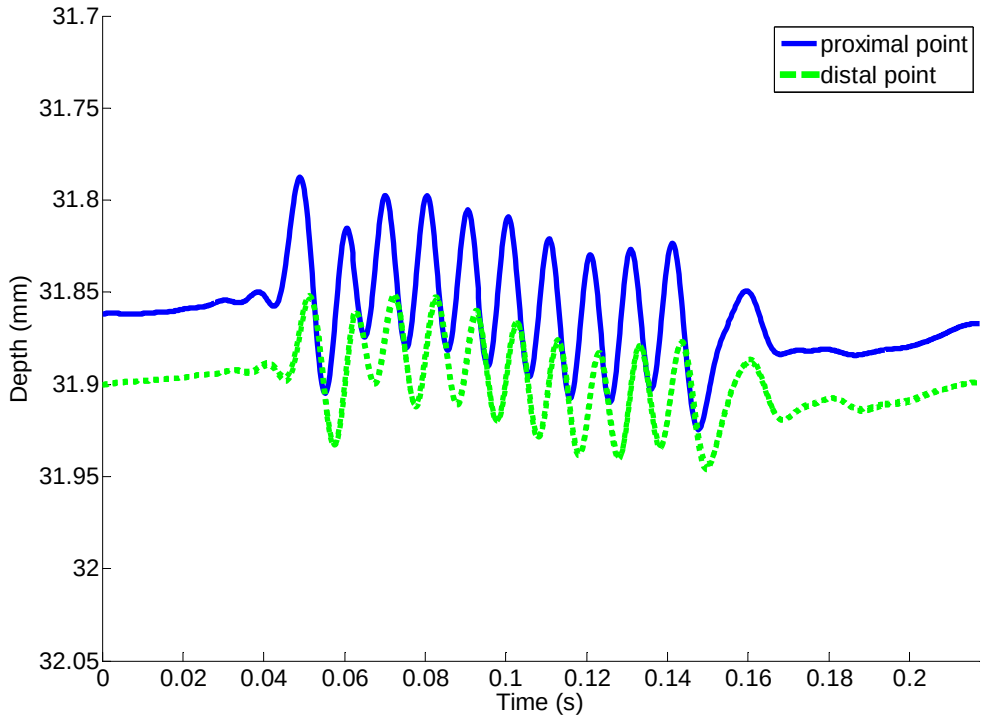

Fig. 3.5 Tracking result of the tissue movements at about 32 mm depth of a young male human subject's thigh muscle. The solid deep color line was the movement detected at the proximal point. The dashed light color line was the one detected at the distal point.

3.1.2.2 Shear Wave Velocity Estimation

The data interpolation method described in the last section was also used to improve the temporal resolution of the waveforms shown in Fig. 3.5, since the detected waveforms were sinusoidal and the interpolation could determine the peaks of the waves more accurately. With 200 points interpolation among three adjacent frames at the wave peaks, the equivalent frame rate was up to 460 kHz, with a time resolution of approximately 2μs. The time delays of the wave propagation detected at a selected depth were calculated for the shear wave velocity estimation. Fig. 3.6 shows an interim result on a young male subject. Fig. 3.6 (a) is the B-mode image of thigh muscles. The two vertical lines mark out the position of two scan lines and the distance between them is Δr. The rectangle drawn on the VI muscle marks the region of interest (ROI) with a

width of 15 mm (the distance between the two scan lines) and a depth of about 1/3 thickness of the VI muscle, where the shear modulus would be estimated. In this study, the part of VI muscle right under the RF muscle was selected as ROI. Fig. 3.6 (b) is the tracking result of tissue movements, without showing the continuous sinusoidal waveforms of the shear wave propagating in the muscle, only the peaks of every cycle of the two sinusoidal waveforms were plotted to easily determine the time delay between them. Fig. 3.6 (c) is an enlarged part of (b) at the depth of ROI including four wave cycles. The points marked by stars (*) indicate the peaks of sinusoidal waveforms collected from the proximal position to the vibration source. Correspondingly, the points marked by circles (o) show the peaks collected from the distal position. Obviously time delay values Δt can be calculated from these points. In order to minimize the variability of estimated shear modulus in ROI, all the time delay values calculated from these successive tracked wave cycles were averaged and used in Eq. 3.1 for the estimation of the shear wave velocity.

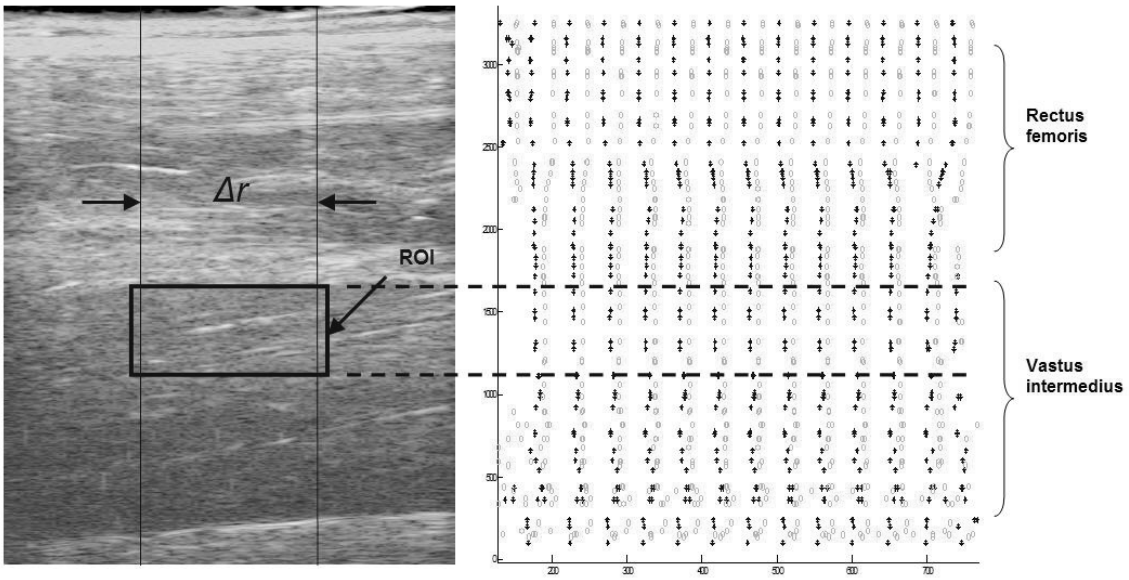

(a) (b)

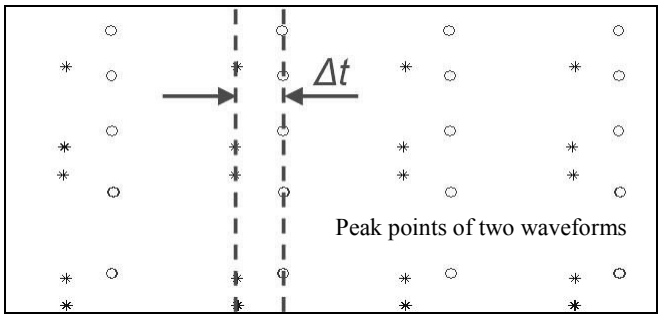

(c)

Fig. 3.6 The procedure of shear wave velocity calculation. (a) A B-mode image of thigh muscles of a young male subject with marks of scan lines and ROI; (b) Tracking results of tissue movements obtained from the corresponding data of (a) with time on the x-axis and depth on the y-axis; (c) An enlarged part of (b) which indicates the peaks of sinusoidal waveforms gotten from the proximal and distal positions.

In wave theory, shear wave is a kind of transverse wave, which means it is a moving wave that consists of oscillations occurring perpendicular to the direction of wave propagation. From Fig. 3.6 (c), the points of sinusoidal wave peaks collected at the ROI depth could be seen to form a wave front, of which the shape was straight line vertical to the time axis. Each pair of these lines gotten from two scan lines was also

approximately parallel. Hence the shear wave at this depth had the same pattern as a planar wave, of which the propagation direction was parallel to the direction of muscle action and vertical to the ultrasound scan lines. This was the reason why the shear wave velocity could be directly estimated from the distance between the two scan lines and the time delay consumed by the wave propagation. As mentioned in Section 2.2.4.3, the shear wave velocity was almost independent of the exciting frequency and the viscous effects could be neglected when the shear modulus along the direction of muscle action was measured. Therefore Eq. 2.1 could be directly used to estimate the shear modulus, using the reported muscle density of 1000 kg/m^3 (Gennisson et al., 2005). The planar wave patterns in the ROI of VI muscle were further verified by the results of the experiment described in Section 3.3.

3.2 System Evaluation Using Silicone Phantom

3.2.1 Objective

To evaluate the reliability of our newly developed vibro-ultrasound method, shear modulus values of several custom-made silicone phantoms with different stiffness were assessed. Their stiffness was also evaluated using the conventional indentation method, and comparison was made between the results by the two methods.

3.2.2 Phantom Fabrication

Ten pieces of tissue-mimicking phantoms with a size of 100 mm × 80 mm × 20 mm were prepared for the experiment. The phantoms were made of addition-curing RTV-2 silicone rubbers (M4600 A/B, Wacker Chemicals Hong Kong Ltd., Hong Kong, China). They were cured by mixing the two components A and B in the prescribed ratio by

weight (A: B = 10:1 for M4600). In addition, their stiffness was varied by adding the AK-35 silicone oil (Wacker Chemicals Hong Kong Ltd., Hong Kong, China), which can change the rubber compound softness in proportion to the amount added. The weight ratio between M4600A and AK-35 was selected as 1:0, 1:0.25, 1:0.5, 1:0.75 and 1:1, with a decreasing stiffness of corresponding phantoms. Because the components were mixed in air, a certain amount of air would be unavoidably introduced into the rubber mix. To obtain phantoms without any air bubbles, the mixtures were then deaerated in a vacuum cabinet until no more bubbles were formed by the reduced pressure. At last, the phantoms were heated at 60℃ for several hours to increase the speed of curing. A total of ten phantoms were made (two pieces for each concentration level). Different from the skeleton muscles, these phantoms were homogeneous and isotropy. However, since the VI muscle we measured has a large size, planar shape and its muscle fibers are almost aligned parallel around the same axis, it can be assumed to be locally homogenous and quasi-isotropy along the muscle action direction. Thus the results obtained from these phantoms could be used to verify the reliability of the new method.

3.2.3 Experimental Protocol

The shear modulus values of these phantoms were first assessed using indentation tests with a material testing machine (Instron ASTM Method Set, Braintree, MA, USA). The diameter a of the indenter we used is 10 mm. Phantoms were compressed for 2 mm with a velocity of 0.5 mm/sec and then relaxed at the same speed. During three cycles of compression-relaxation, the compression load P (N) and the deformation W (mm) values were sampled and saved to determine the load-deformation relationship. Then the effective Young's modulus E was calculated using the Eq. 3.4, which is based on the

Hayes model for the elastic indentation problem of a thin elastic layer bonded to a rigid half-space with a rigid, frictionless cylindrical plane-ended indenter (Hayes et al., 1972).

$$E = \frac{(1-\nu^2)}{2a\kappa(\nu, a/h)}\frac{P}{W} \tag{3.4}$$

where h is the phantom thickness, and κ is a scaling factor, which provides a theoretical correction for the finite thickness of the measured phantom and it depends on both the ratio a/h and the Poisson's ratio v. The Poisson's ratio v was defined as 0.5 in this study with an assumption that the silicone is nearly an incompressible material. Then the shear modulus μ of the phantoms could be calculated by the following equation:

$$\mu = \frac{E}{2(1+\nu)} = \frac{1}{3}E \tag{3.5}$$

where v is the Poisson's ratio, with a defined value of 0.5. The indentation tests were performed for 3 times on each piece of the phantoms. Then the stiffness of each phantom was assessed using our vibro-ultrasound method, also for 3 times. To reduce the reflection effects from upper and lower boundaries, the measured phantom was placed between two pieces of elastic silicone layers. And to avoid the reflection effects in the horizontal direction caused by the relatively smaller size of phantom comparing to the VI muscle, the vibration train included only 3 cycles comparing to the 10 cycles in the human tests. All the measurements were performed at room temperature (25 ± 1 ℃).

3.2.4 Data Analysis

The shear modulus values measured on the 10 pieces of phantoms by the indentation method were compared with those values measured by the vibro-ultrasound method.

The results of the 3 times of measurements were averaged. Then the Pearson's correlation coefficient (CC) between the results of two methods was calculated. A scatter figure of the corresponding pairs of shear modulus values and the line of equality were plotted. In addition, the differences between the pairs of results against their mean (Bland-Altman plot) were also plotted, which was used to illustrate the agreement of two different methods measuring the same characteristic. All the data were analyzed using SPSS Statistics (SPSS Inc. Chicago, IL, USA). Statistical significance was set at the 5% probability level.

3.3 System Evaluation for Different Distance between Vibration Source and Ultrasound Scan Lines

3.3.1 Objective

According to wave theory and literatures, the shear wave propagation velocity along the direction of muscle action is nearly independent of wave amplitude and frequency. However, whether the distance between vibration source and ultrasound scan lines (vibrator-beam distance) would influence the measured shear wave velocity was rarely studied. Actually, this is a deductive problem caused by the shear wave pattern in the muscle. If the wave pattern is planar, the vibrator-beam distance will not affect the measured shear wave velocity. Therefore, an experiment was designed to evaluate the effects of different vibrator-beam distances on the measurement results.

3.3.2 Subjects Selection

Ten healthy young subjects (8 males and 2 females, age: 30.7 ± 4.1 yr, height: 170.2 ±

10.7 cm, weight: 68.0 ± 14.4 kg) were recruited for the experiment. The human subject ethical approval was obtained from the human ethics committee of The Hong Kong Polytechnic University and informed consent was obtained from the subject prior to the experiment.

3.3.3 Experimental Protocol

The subjects were asked to sit on the chair with several straps restraining the waist and shoulders. A cuff was fastened around the right lower leg and fixed to the lever of the dynamometer. The axis of the lever was aligned with the supposed rotation axis of the right knee joint. The ultrasound probe and the vibrator were hung over the thigh and touched the skin surface on the middle part of the RF muscle belly with a predefined distance (if this distance was 10 mm, the distance between the vibrator and first scan line, i.e. the vibrator-beam distance, was about 20 mm), as shown in Fig. 3.7. Ultrasound gel was applied between the ultrasound probe and the skin to propagate ultrasound signal. With the help of the short bar connected to the piston of the vibrator and the selected position where the vibration occurs, planar pattern waves would be generated at the expected depth and propagate along the direction of muscle action. The experiments were performed at a 90º knee joint angle (0º = full extension). First, the MVC torque was assessed as the highest torque value produced from three successive isometric contractions for 5 seconds with about 30 seconds interval for rest. Next, muscle stiffness assessments were performed at relaxed condition and at 20% MVC level, and with three different vibrator-beam distances, i.e. 15 mm, 20 mm and 25 mm for comparison. For each measurement, the subject was asked to maintain the isometric contraction for approximately 4 seconds. The measurement was repeated for three times under the same condition with a 1 minute interval for rest.

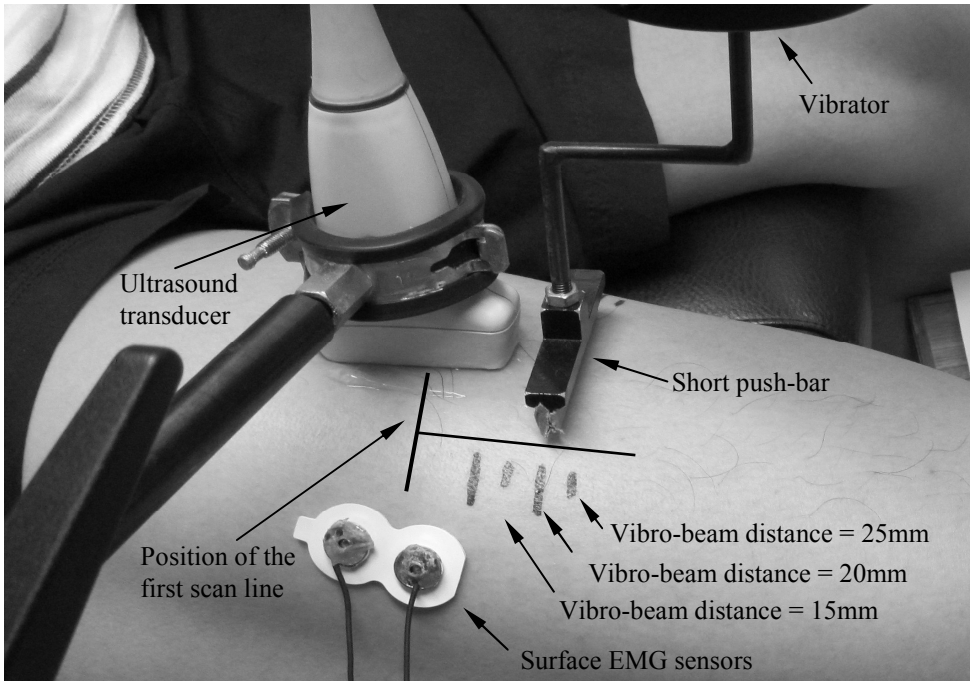

Fig. 3.7 The position of the ultrasound probe and the vibrator during the experiment. They were hung over the thigh touching the skin surface on the middle part of the RF muscle belly with a predefined distance. The surface EMG sensors were attached on the VL muscle belly. The three positions of the vibrator used for the different vibro-beam distance tests were also indicated.

3.3.4 Data Analysis

A total of 18 (2 [contraction levels: 0% and 20% MVC]×3 [vibrator-beam distances]× 3 [three times]) shear modulus assessments were performed by the same investigator. The intra-class correlation (ICC) based on two-way mixed model was performed to evaluate the intra-observer repeatability of measurements. The shear modulus was represented by the mean value of the results of the three repeated measurements. Then the shear modulus of the ten subjects measured at different vibrator-beam distances were plotted as scatter figures (one figure for the results between 15 mm and 20 mm vibrator-beam distance, the other one for the results between 25 mm and 20 mm distance) and the lines of equality were plotted. The shear modulus values were also analyzed using two-way repeated measure analyses of variance (ANOVA) (% MVC [0% and 20%, 2 levels]×vibrator-beam distances [15mm, 20 mm and 25 mm]) method

to evaluate their differences. The normalized root mean squared deviation (NRMSD) between the shear modulus measured at 15 mm and at 20 mm vibrator-beam distance, and the NRMSD value between the results measured at 25 mm and 20 mm distance, were calculated and expressed as a percentage. All the data were analyzed using SPSS Statistics (SPSS Inc. Chicago, IL, USA). Statistical significance was set at the 5% probability level.

3.4 Skeleton Muscle Stiffness Measurement at Rest and at Different Isometric Contraction Levels

3.4.1 Subjects Selection

Forty healthy subjects volunteered to participate in the experiment and were divided into four groups: young males, young females, elder males and elder females (Table 3.1). They were asked not to participate in any strength or flexibility training one day before the experiment, and subjects with recent injury were excluded. All subjects were explained with the experimental protocol and asked to sign on the informed consent prior to the experiment for their participation which had been approved by the human ethics committee of The Hong Kong Polytechnic University.

Table 3.1 Demographic information of the subjects presented with mean (SD)

	Age (yr)	*Height (cm)*	*Mass (kg)*
Young males (n = 10)	29.4 (4.8)	174.7 (8.1)	73.3 (13.0)
Young females (n = 10)	27.6 (5.0)	164.3 (4.4)	55.3 (4.0)
Elderly males (n = 10)	60.6 (7.6)	166.7 (5.8)	66.1 (11.9)
Elderly females (n = 10)	56.7 (4.9)	156.9 (5.6)	58.9 (8.4)

3.4.2 Experimental Protocol

The experimental setup was similar with that described in Section 3.3.3. The ultrasound probe was placed on the middle part of the RF muscle belly right above the VI and femur with the guidance of B-mode images. The positioning of the vibrator and transducer was manually controlled. The distance between the vibrator and the transducer was set to be about 10 mm (i.e. the vibrator-beam distance was about 20 mm). The MVC torque was assessed first as the highest torque value of the subject produced from three successive isometric contractions. Next, the muscle stiffness was measured for three times at relaxed condition. Then the subject was asked to maintain isometric contraction at different MVC levels, from 10% to 100%, with an increase of 10% for each step. The reason for selecting the step type of isometric contraction but not the ramp type was to reduce the effects of motion noises and improve the accuracy of shear modulus estimation. In the step type isometric contraction, muscle fibers were in a quasi-static situation when the measurement was performed. However, in the ramp type isometric contraction, muscle fibers would keep moving under skin in the direction of shear wave propagation. It would seriously affect the tracking results of radio-frequency signal and the accuracy of shear wave velocity estimation. At each MVC level, assessments were performed for three times with about 1 minute interval for rest. And for each trial, the subject was asked to maintain the isometric contraction for approximately 4 seconds. The experiments were performed at two different knee joint angles, 90º and 60º (0º = full extension). The surface EMG signal was simultaneously captured from the VL muscle during the tests for each contraction level.

3.4.3 Data Analysis

A total of 2640 (4 [groups: young males, young females, elder males and elder females] ×10 [subjects per group] ×11 [contraction levels: 0%-100%]×2 [knee joint angles] ×3 [three times]) shear modulus assessments were performed by the same investigator. The intra-class correlation (ICC) based on two-way mixed model was performed to evaluate the intra-observer repeatability.

To study the influences of the factors, including knee joint angle, gender and age, on the muscle stiffness at relaxed condition and different isometric contraction levels, four-way repeated measure analyses of variance (ANOVA) (gender [male vs. female] ×age [young vs. elder] × % MVC [0% -100%, 11 levels] ×knee joint angles [90º vs. 60º]) were used to analyze the shear modulus values of the VI muscle. Specially, the comparison of the muscle shear modulus measured at relaxed condition (0% MVC) was first performed separately using three-way ANOVA method.

Two methods were generally used to exhibit the different contraction intensities, one was to use the relative muscle contraction level (% MVC), and the other one was to use the absolute torque value of the joint extensor or flexor. These two methods focused on different features. Using the former method, the muscle stiffness was studied at the relative percentage levels of maximum muscle contraction capability for each person, considering the individual muscle strength difference. However, using the later method, the muscle stiffness was generally evaluated corresponding to the absolute torque values and this was meaningful among the whole population. Both methods could help us to further understand the muscle function and recruitment strategies from different perspectives.

To determine the relationship between the muscle stiffness and the relative isometric contraction levels (% MVC), polynomial regression analyses by linear, quadratic and cubic models were performed for each individual, and the coefficients of determination (R^2) values of these models were compared using one-way ANOVA to find the best one. The mean shear modulus values across the ten subjects in each group then were fitted with the relative isometric contraction levels (% MVC) using a quadratic regression model.

From another perspective, to study the relationship between the muscle shear modulus and the corresponding absolute torque values, quadratic regression was also performed for each individual subject at a given joint angle and the 10 sets of polynomial coefficients in each group were averaged to represent the trend of the relationship. The achieved quadratic curves were plotted within a range from 0 Nm to the mean value of MVC torques in each group and were compared to investigate the differences of their trends.

The correlation between the muscle shear modulus and the surface EMG magnitude was also studied. During each step isometric contraction, a 1-s epoch of EMG data was selected from the middle of the whole 4-s muscle contraction duration. The RMS values of the EMG signals were calculated for each epoch, and then expressed as a percentage of the maximum RMS value for each subject. Relationship between the mean shear modulus values and the RMS values of surface EMG signals was plotted as a scatter figure for each group and also evaluated by the correlation coefficients (CC).

All the data were analyzed using SPSS (SPSS Inc. Chicago, IL, USA). Statistical significance was set at the 5% probability level.

CHAPTER 4 RESULTS

In this chapter, the main findings are represented, including the comparison between the result by our vibro-ultrasound method and that by the traditional indentation method on silicone phantom, effect of different vibrator-beam distances on the measured shear modulus results, the positive correlation between the muscle shear modulus and the isometric contraction level, and the age and gender dependences of muscle shear modulus with different relative contraction levels (% MVC) and absolute contraction torque values (Nm). Finally, the correlation coefficients (CC) between the mean shear modulus values of VI muscle and the RMS values of surface EMG signals gotten from VL muscle in each group are also shown.

4.1 System Evaluation using Silicone Phantom

The Pearson's correlation coefficient (CC) between the results of indentation method and those of vibro-ultrasound method on the 10 pieces of silicone phantoms is 0.994. A scatter figure of the corresponding pairs of measured shear modulus values and the line of equality were plotted in Fig. 4.1 (a). The coefficient of determination (R^2) value was 0.989. The differences between the pairs of corresponding results against their mean (Bland-Altman plot) were plotted in Fig. 4.1 (b). The mean value of the differences was 0.9 kPa, and the standard deviation (SD) was 12.7 kPa. It was demonstrated that all plots were between the two dashed lines of mean ± 2SD, indicating that the results of these two methods had a high agreement, and the accuracy of the vibro-ultrasound method was comparable to that of the traditional indentation method for the stiffness assessment on the silicone phantoms.

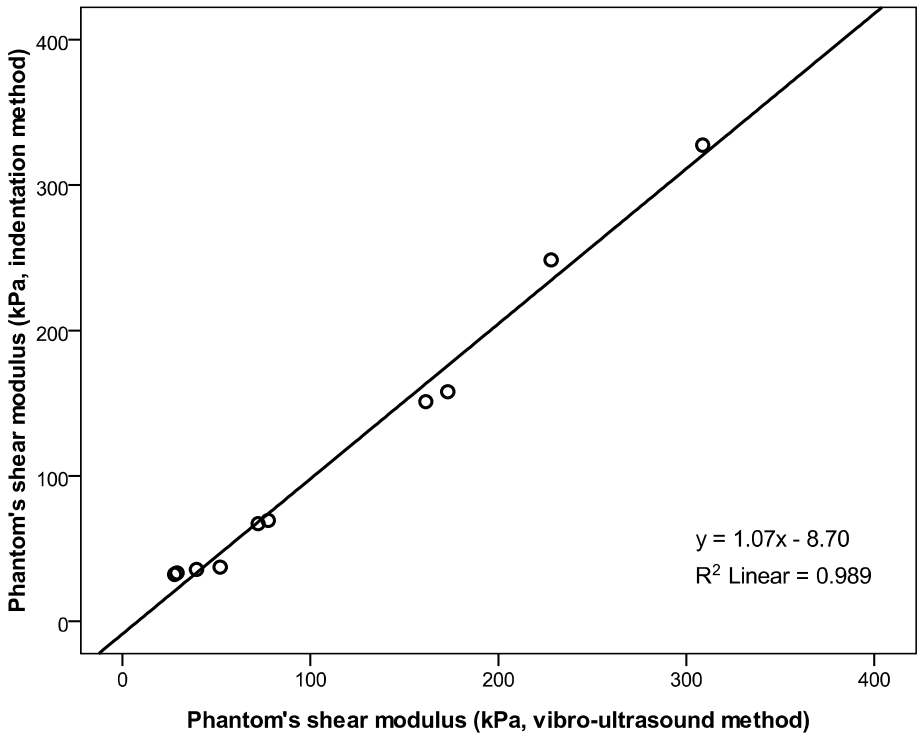

(a)

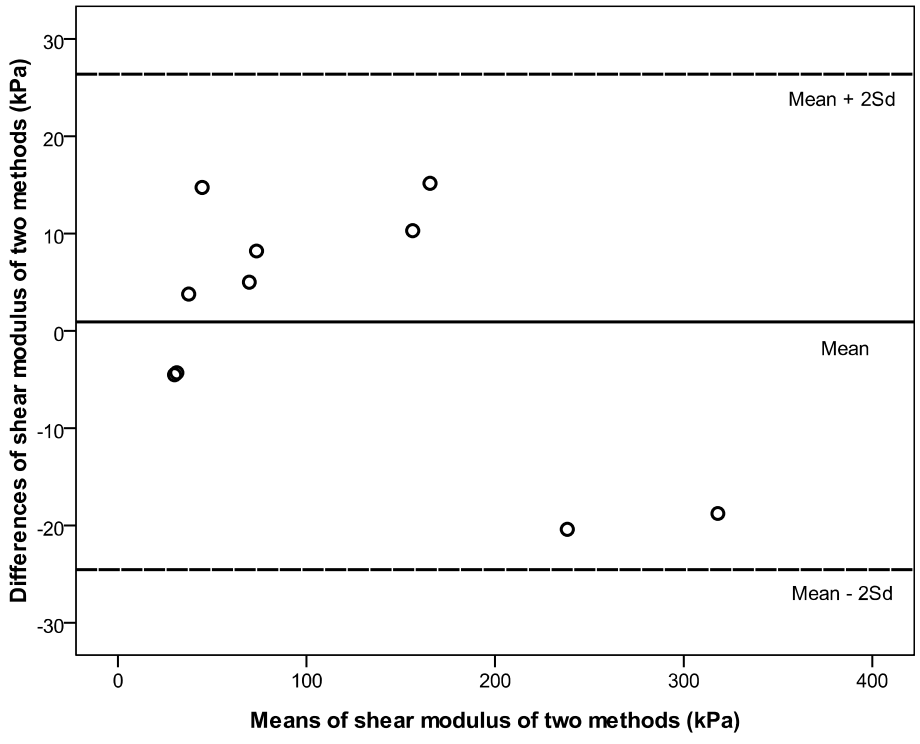

(b)

Fig. 4.1 (a) Correlation between the shear modulus values assessed by the indentation method and the corresponding values measured by vibro-ultrasound method. (b) The differences between the pairs of shear modulus values measured by the two methods against their mean (Bland-Altman plot).

In Fig. 4.1 (a), the shear modulus of one of the two hardest phantoms (228.1 kPa measured by indentation method, and 248.5 kPa by vibro-ultrasound method) was smaller than the other one (308.7 kPa and 327.5 kPa by indentation and vibro-ultrasound method, respectively). The reason was that the deaeration process of this piece of phantom was not fully successful (several very tiny bubbles could be seen on its surface). This may influence the completion of the curing process and thus reduce the final stiffness of the phantom. However, this inconsistent stiffness of the two phantoms would not affect the evaluation of the measurement system.

4.2 System Evaluation for Different Distances between Vibration Source and Ultrasound Scan Lines

The ICC for the measured shear modulus using two-way mixed model, type consistency and averaged measures was 0.982 (95% CI lower bound: 0.968; 95% CI upper bound: 0.991), which indicated a high degree of reliability in this experiment. Fig. 4.2 shows the scatter figures plotted by the shear modulus of the ten subjects measured at different vibrator-beam distances. Fig. 4.2 (a) is the figure between the results measured at 15 mm and 20 mm vibrator-beam distance. Fig. 4.2 (b) is the figure between the results of 25 mm and 20 mm distance. The coefficients of determination (R^2) values are 0.978 and 0.955, respectively. There was no significant effect for the two-way interactions between the isometric contraction levels and the vibrator-beam distance ($p = 0.860$) and the individual effect of vibrator-beam distance ($p = 0.818$), but the individual effect of isometric contraction levels was significant ($p < 0.001$). The NRMSD value between the shear modulus measured at 15 mm and at 20 mm vibrator-beam distance was 5.6%, and the NRMSD value between the results measured at 25 mm and 20 mm distance was

6.5%. These results proved that, although the vibrator-beam distance was set to be approximately 20 mm and not strictly controlled in the subsequent experiments, the measured muscle shear modulus would not be influenced by the variation of this parameter. It also provided another evidence for the inference that the shear wave patterns propagating in the ROI of VI muscle were close to planar waveforms.

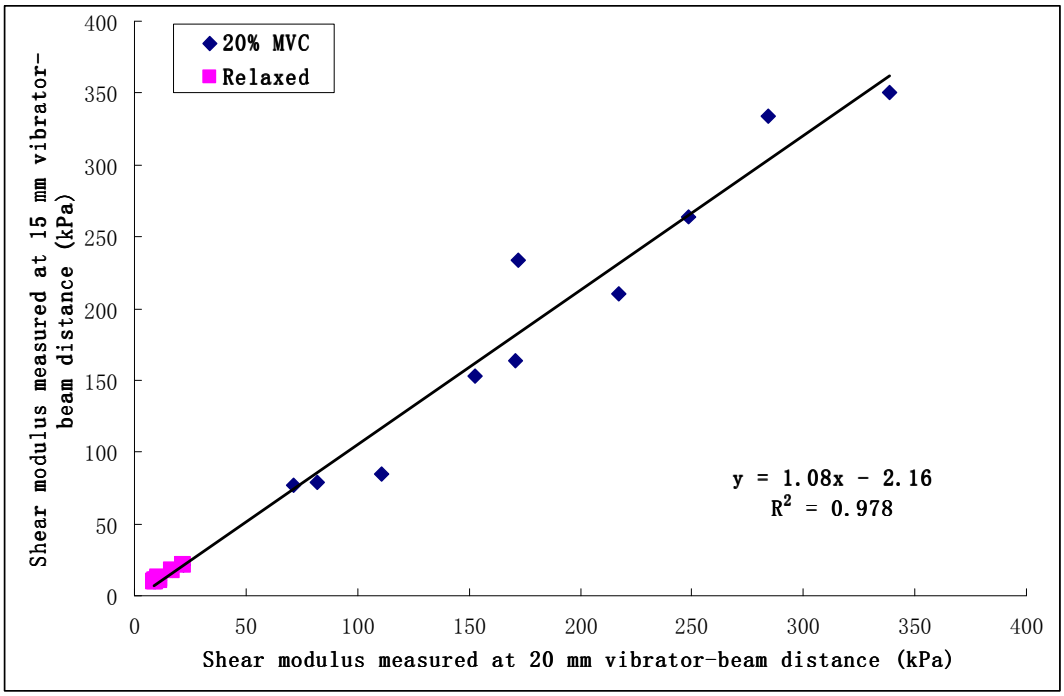

(a)

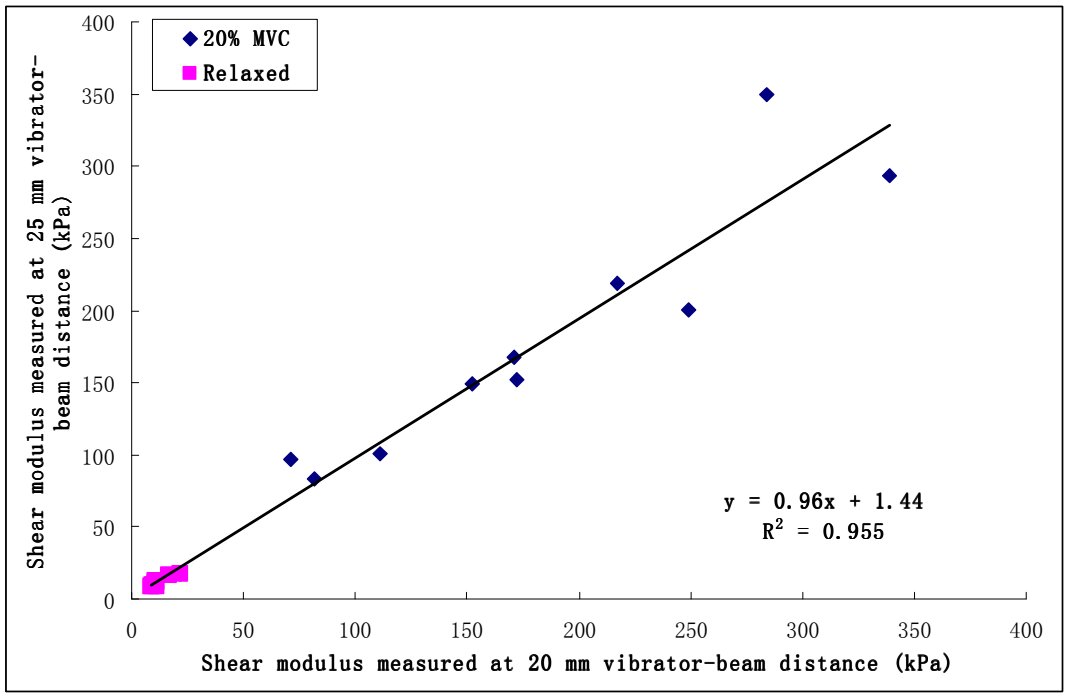

(b)

Fig. 4.2 The scatter figures plotted by the shear modulus of the ten subjects measured (a) at 15 mm and 20 mm vibrator-beam distance and (b) at 25 mm and 20 mm distance.

4.3 Skeleton Muscle Stiffness Measurement at Rest and at Different Isometric Contraction Levels

4.3.1 Results Using ICC and Multi-way ANOVA Analysis

First of all, the mean MVC torque values in each subject group and different knee joint angles are listed in Table 4.1. The results of three-way ANOVA showed that the main effects of age ($p = 0.01$), gender ($p < 0.001$) and knee joint angle ($p = 0.001$) factors were all significant for the MVC torque values. However, all the two-way interaction effects were not significant (All $p > 0.1$). According to the estimated marginal mean values provided by the ANOVA method (the marginal means for one factor are the means for that factor averaged across all levels of the other factors), the conclusion was that the MVC torque values of males were larger then females; the values from young subjects were larger than those from elderly subjects; the values measured at 90º knee joint angle were larger than those at 60º.

Table 4.1 The mean MVC torque values (Nm) of each group at 90º and 60º knee joint angles.

	Young male	Young female	Elderly male	Elderly female
90º knee joint angle	83±16.4	63±17.0	73±14.9	51±15.2
60º knee joint angle	68±9.2	51±16.0	65±14.3	42±9.2

The overall ICC for the measured shear modulus using two-way mixed model, type consistency and averaged measures was 0.994 (upper bound: 0.993; lower bound: 0.994), suggesting a high degree of reliability in this experiment. To estimate the

reliability under different isometric contraction levels, ICC under different percentages of MVC were also calculated, as shown in Table 4.2. It was found that, ICCs under higher percentage of MVC levels seemed to be a little smaller than those under lower levels. However, the differences was very small and all ICCs were larger than 0.980 which indicates a high degree of intra-observer repeatability

Table 4.2 The intra-class correlation coefficients (ICC) for the shear modulus of VI under different % MVC levels from three repeated measurements conducted by one operator.

% MVC	ICC	95% CI lower	95% CI upper
0	0.993	0.990	0.995
10	0.992	0.988	0.995
20	0.992	0.988	0.995
30	0.994	0.992	0.996
40	0.992	0.988	0.995
50	0.990	0.985	0.993
60	0.988	0.982	0.992
70	0.992	0.988	0.994
80	0.989	0.984	0.993
90	0.986	0.979	0.990
100	0.984	0.977	0.989

Comparison of the muscle shear modulus at relaxed condition (0% MVC) was performed first. The mean values of each group are shown in Table 4.3. Results of multi-way ANOVA showed that, there was no significant main effect for gender ($p = 0.156$) and age ($p = 0.221$) factors and interactive effect between each two factors (all $p > 0.05$) on the muscle shear modulus measured at relaxed condition. However, there was a significant main effect for knee joint angle factor ($p = 0.001$) on the muscle shear modulus measured at relaxed condition. The estimated marginal mean value of the

muscle shear modulus measured at relaxed condition and 90º knee joint angle (16.2 ± 8.1 kPa) was larger than the mean value at 60º knee joint angle (11.1 ± 4.4 kPa).

Table 4.3 The mean muscle shear modulus values (kPa) of each group at relaxed condition (0% MVC), shown separately for 90º and 60º knee joint angles.

Knee joint angle	Young male	Young female	Elderly male	Elderly female
90º	14.5 ± 6.3	19.0 ± 10.2	13.8 ± 7.4	17.2 ± 8.4
60º	11.6 ± 3.5	12.8 ± 5.4	10.3 ± 5.0	9.5 ± 3.3

There were no significant four- or three-way interaction effects among the four factors (gender × age × % MVC × knee joint angles, all $p > 0.05$). All the main effects of single factor on the muscle shear modulus were significant. The estimated marginal mean value of males was larger than the value of females ($p < 0.001$). The mean value of young subjects was also larger than that of elderly participants ($p < 0.001$). And the value measured at 90º knee joint angle was larger than the value measured at 60º ($p < 0.001$). The results of post-hoc Bonferroni test for the muscle shear modulus measured at different percentage of MVC levels are shown in Table 4.4. Furthermore, all the two-way interactions including gender factor were not significant (all $p > 0.1$) and all other two-way interaction effects, i.e., age vs. % MVC, joint angles vs. % MVC and age vs. joint angles, were significant (all $p < 0.001$). For age vs. % MVC interaction, with the increase of % MVC, differences between the muscle shear modulus of young subjects and that of elderly subjects increased. A similar relationship was also found for joint angles vs. % MVC, with the increase of % MVC, differences between the muscle shear modulus measured at 90º knee joint angle and that measured at 60º increased. For

age vs. joint angles, the difference between the muscle shear modulus of young subjects and elderly subjects was larger at 90º knee joint angle than the difference at 60º. The detailed relationships are shown in Fig. 4.3 by plotting the estimated marginal means of muscle shear modulus.

Table 4.4 Multi-way ANOVA showed significant main effects of percentage MVC levels on muscle shear modulus. The post hoc Bonferroni comparisons results showed the details of the relationships among these levels.

Percentage of MVC	Post hoc comparisons results
0%	< 30% - 100%, $p < 0.05$
10%	< 40% - 100%, $p < 0.005$
20%	< 50% - 100%, $p < 0.001$
30%	> 0%, $p < 0.05$; < 50% - 100%, $p < 0.05$
40%	> 0% - 10%, $p < 0.005$; < 60% - 100%, $p < 0.001$
50%	> 0% - 30%, $p < 0.05$; < 70% - 100%, $p < 0.001$
60%	> 0% - 40%, $p < 0.001$; < 80% - 100%, $p < 0.001$
70%	> 0% - 50%, $p < 0.001$; < 80% - 100%, $p < 0.05$
80%	> 0% - 70%, $p < 0.05$; < 90% - 100%, $p < 0.005$
90%	> 0% - 80%, $p < 0.005$; < 100%, $p < 0.001$
100%	> 0% - 90%, $p < 0.001$

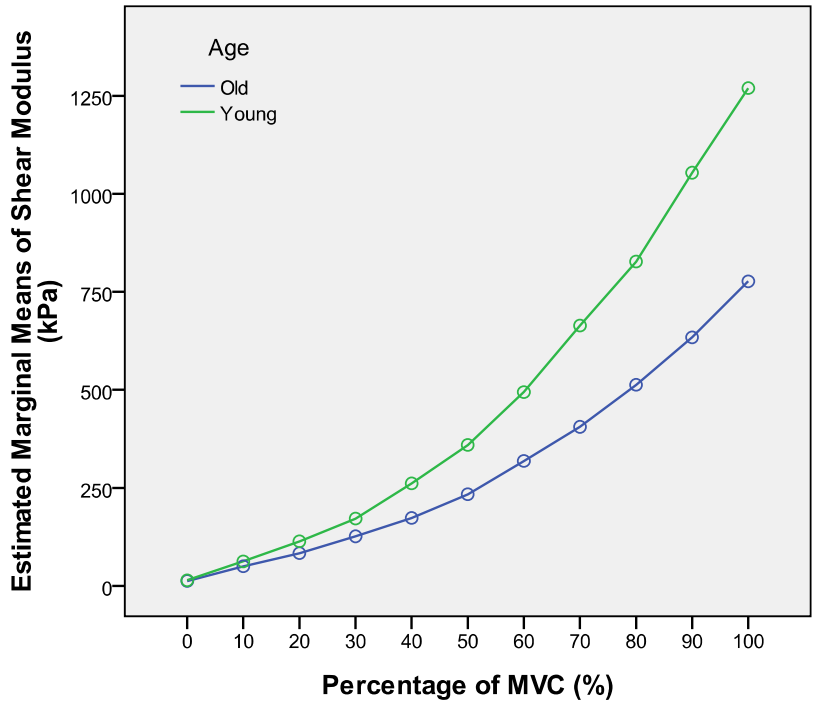
Age
Old
Young
Estimated Marginal Means of Shear Modulus (kPa)
1250
1000
750
500
250
0
0
10
20
30
40
50
60
70
80
90
100
Percentage of MVC (%)

(a)

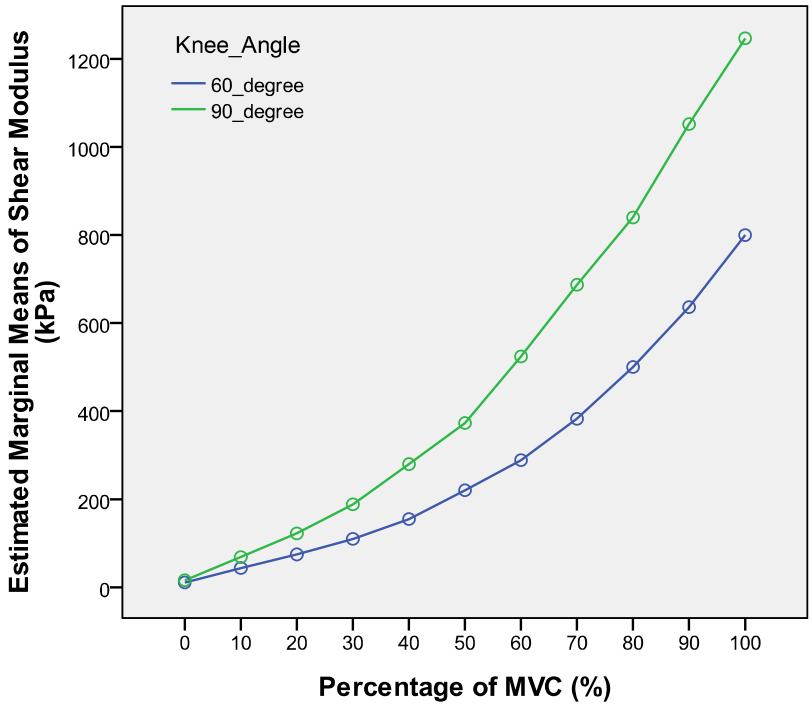
Knee_Angle
60_degree
90_degree
Estimated Marginal Means of Shear Modulus (kPa)
1200
1000
800
600
400
200
0
0
10
20
30
40
50
60
70
80
90
100
Percentage of MVC (%)

(b)

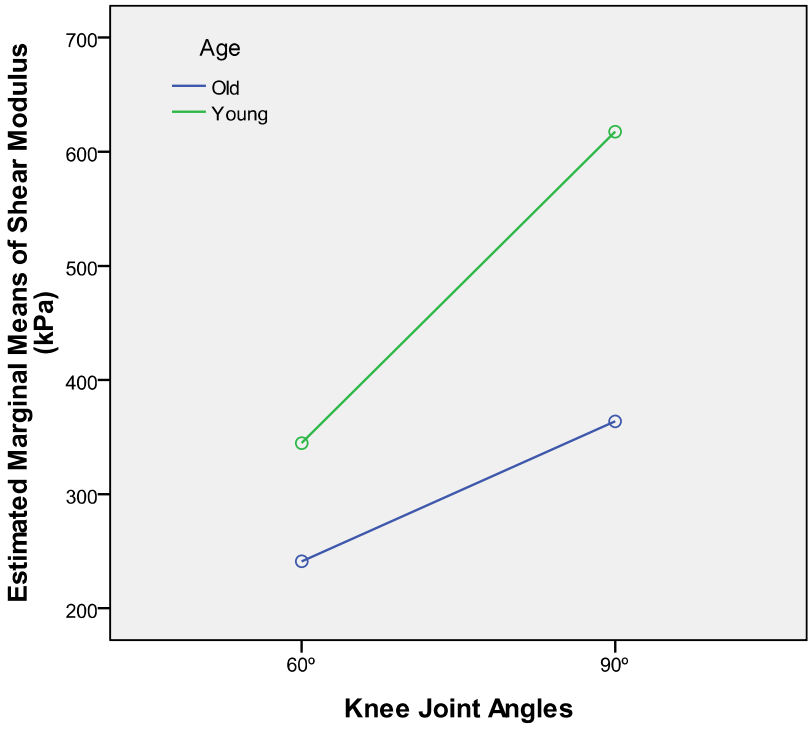

(c)

Fig. 4.3 Estimated marginal means of muscle shear modulus plotted for the significant two-way interaction effects. (a) For age vs. % MVC, with the increase of % MVC, shear modulus differences between young and elderly subjects increased. (b) For angles vs. % MVC, with the increase of % MVC, differences between the results measured at 90º knee joint angle and measured at 60º increased. (c) For age vs. angles, difference between the results of young and elderly subjects was larger at 90º knee joint angle than at 60º.

4.3.2 Analysis Based on Relative Isometric Contraction Level (% MVC)

Polynomial regression analyses by linear, quadratic and cubic models were performed on the relationship between shear modulus vs. % MVC levels for each individual and the mean R^2 values of three models were 0.937 ± 0.034 (linear), 0.992 ± 0.007 (quadratic) and 0.995 ± 0.004 (cubic), respectively. The results of one-way ANOVA indicated that there was no significant difference between the R^2 values of quadratic model and cubic model ($p = 0.390$). However, significant differences were found between the R^2 values of linear model and the other two models (all $p < 0.001$). Thus the quadratic model was selected to examine the relationship of muscle shear modulus vs. relative isometric contraction levels (% MVC). The mean shear modulus values

across the ten subjects in each group at the same knee joint angle were fitted using a quadratic regression model with the relative isometric contraction levels (% MVC), as shown in Fig. 4.4. The Pearson's correlation coefficients (CC) between the muscle shear modulus and the % MVC level in each group and knee joint angle are listed in Table 4.5, and were all larger than 0.96. This indicated that the stiffness of VI muscle along the direction of muscle action was positively correlated to the relative muscle activity level of the knee extensor in a full range of step isometric contraction. The plots also indicated that the muscle shear modulus measured at 90º knee joint angle was larger than the corresponding value measured at 60º knee joint angle at almost each % MVC level in each group of subjects, which was in agreement with the result of multi-ways ANOVA analysis.

Table 4.5 The Pearson's correlation coefficients between the mean shear modulus values of VI muscle and the relative isometric contraction levels in each group and at different knee joint angles.

Knee joint angle	Young male	Young female	Elderly male	Elderly female
90º	0.977	0.974	0.980	0.975
60º	0.971	0.968	0.975	0.979

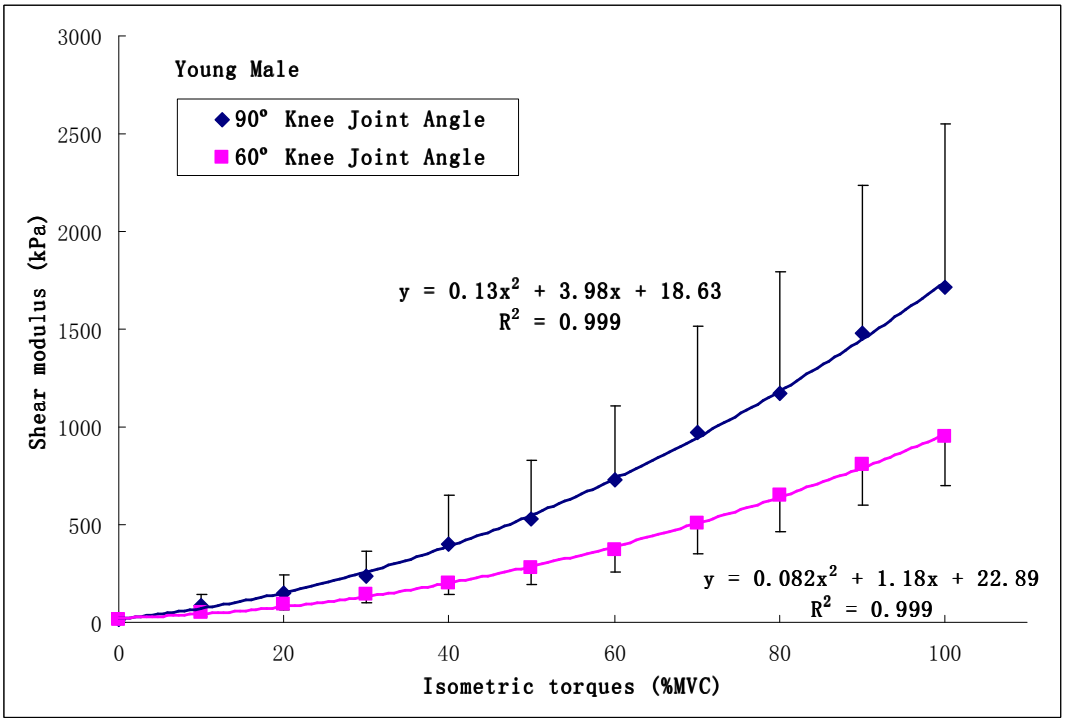
Young Male
90° Knee Joint Angle
60° Knee Joint Angle
y = 0.13x² + 3.98x + 18.63
R² = 0.999
y = 0.082x² + 1.18x + 22.89
R² = 0.999
Shear modulus (kPa)
Isometric torques (%MVC)
0
500
1000
1500
2000
2500
3000
0
20
40
60
80
100

(a)

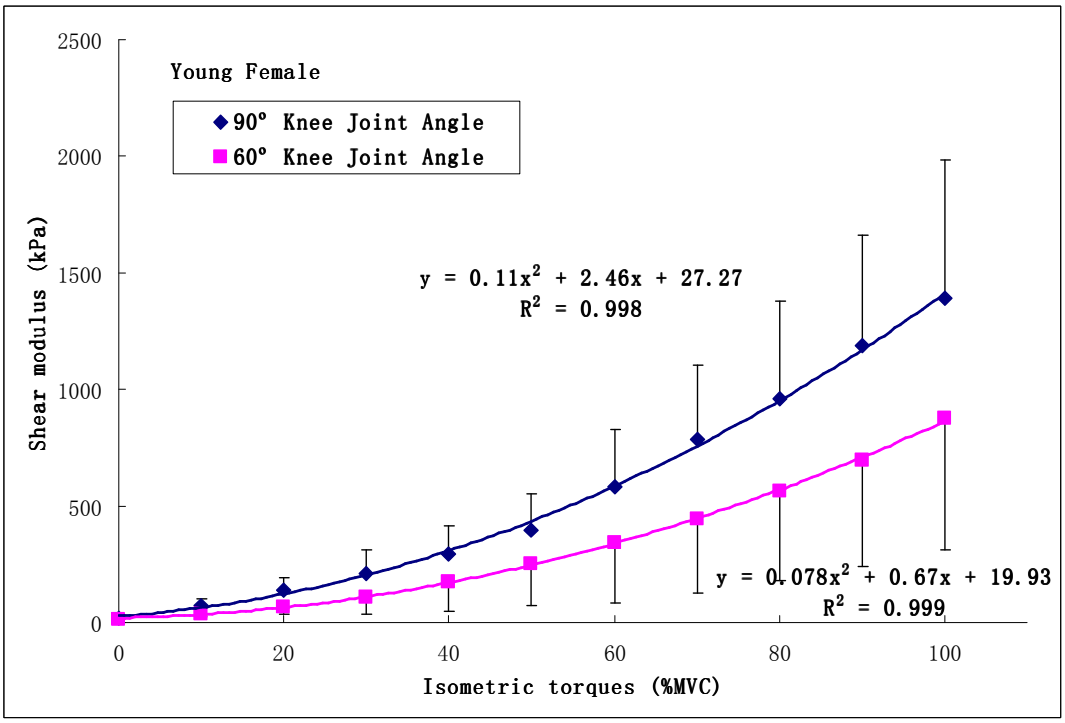
Young Female
90° Knee Joint Angle
60° Knee Joint Angle
y = 0.11x² + 2.46x + 27.27
R² = 0.998
y = 0.078x² + 0.67x + 19.93
R² = 0.999
Shear modulus (kPa)
Isometric torques (%MVC)
0
500
1000
1500
2000
2500
0
20
40
60
80
100

(b)

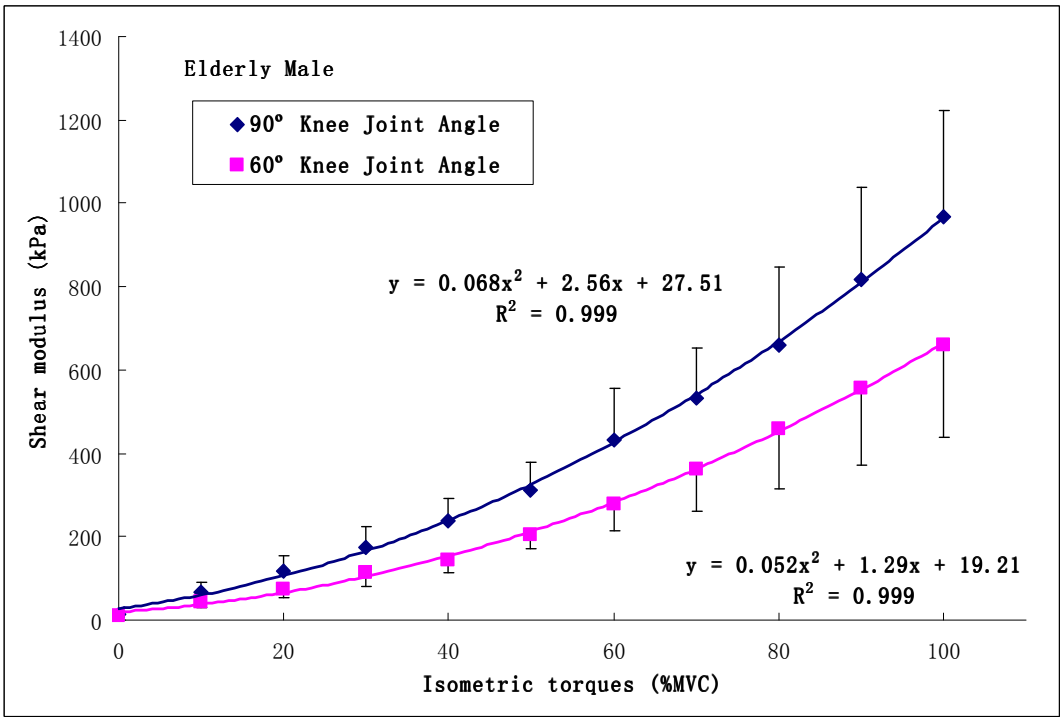

(c)

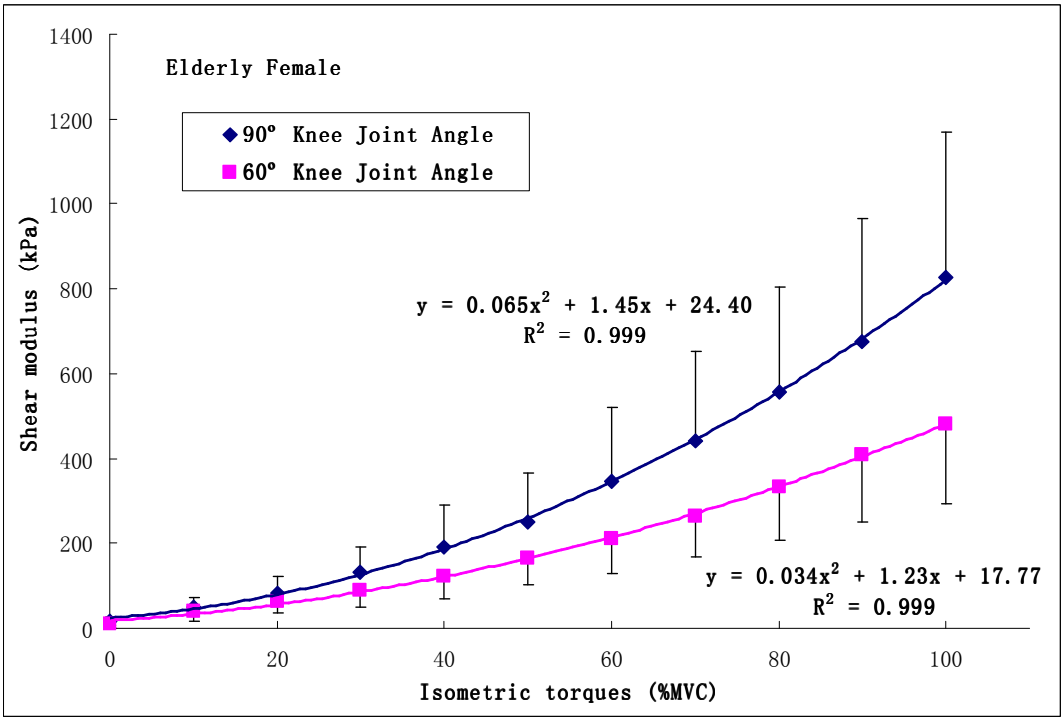

(d)

Fig. 4.4 The mean shear modulus values at different relative isometric contraction levels (% MVC) and different knee joint angles (90º and 60º) with the corresponding quadratic regression fitting curves for (a) young male subjects; (b) young female subjects; (c) elderly male subjects and (d) elderly female subjects.

The results between the young and elderly groups with the same gender at a given knee joint angle were compared, as shown in Fig. 4.5. It was observed that for both joint angles and genders, the shear modulus values of the young subjects were larger than those of the elderly participants, especially at the relatively higher % MVC levels. The results were in agreement with the previous ones obtained using multi-ways ANOVA with the main effect of age factor being significant.

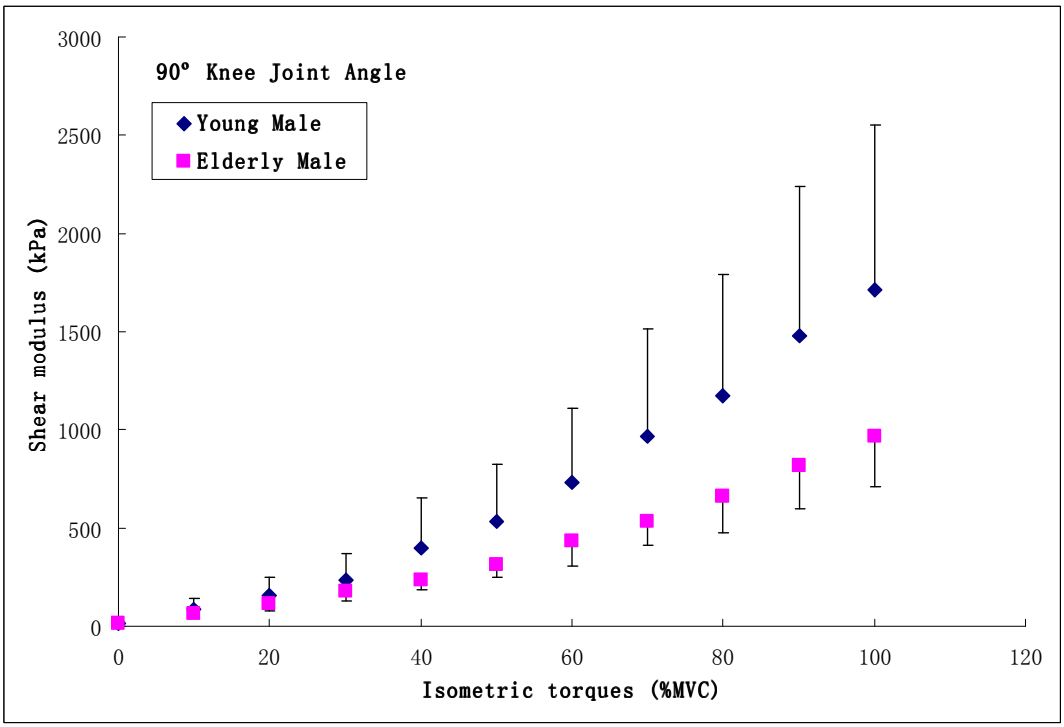

(a)

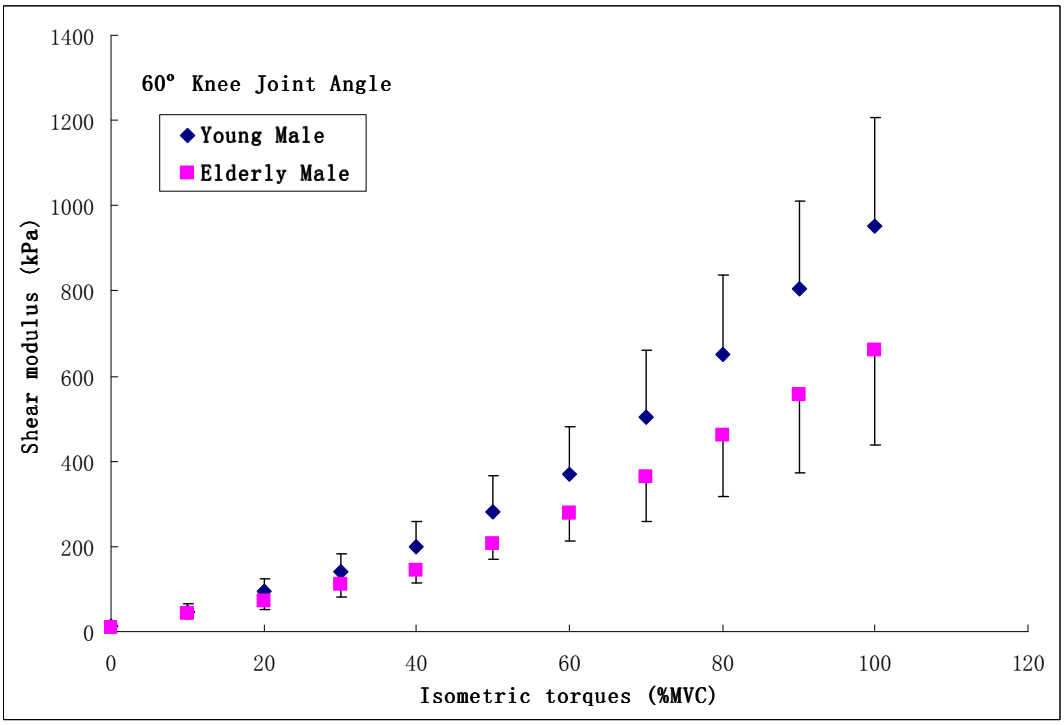
60° Knee Joint Angle
Young Male
Elderly Male
Shear modulus (kPa)
Isometric torques (%MVC)
0
200
400
600
800
1000
1200
1400
0
20
40
60
80
100
120

(b)

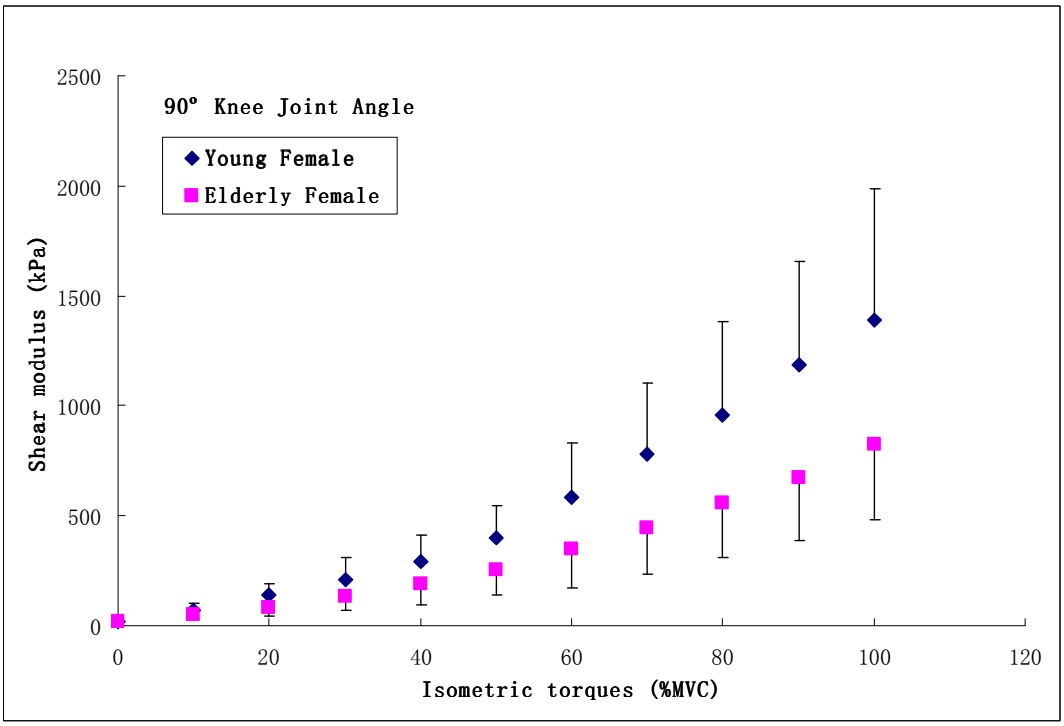
90° Knee Joint Angle
Young Female
Elderly Female
Shear modulus (kPa)
Isometric torques (%MVC)
0
500
1000
1500
2000
2500
0
20
40
60
80
100
120

(c)

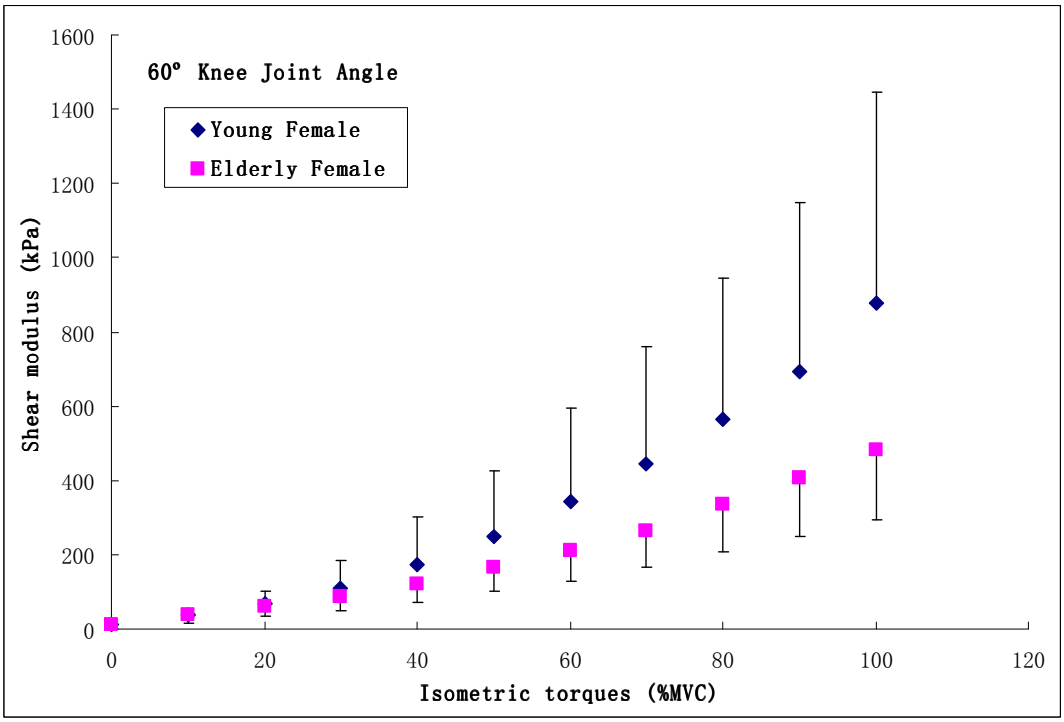

(d)

Fig. 4.5 The age differences of mean shear modulus values at different relative isometric contraction levels (% MVC) between the subjects with the same gender. Comparisons were made between young and elderly male subjects at (a) 90º and (b) 60º knee joint angles, and between young and elderly female subjects at (c) 90º and (d) 60º knee joint angles.

The results were also compared between the genders with similar age range at a given knee joint angle, as shown in Fig. 4.6. The comparison showed that for both age ranges and joint angles, the shear modulus values of males were larger than those of females, especially at the relatively higher % MVC level. However, at the corresponding relative muscle contraction level, the gender difference seemed to be smaller than the age difference. These results were also in agreement with those obtained using multi-ways ANOVA, that the main effect of gender factor was significant.

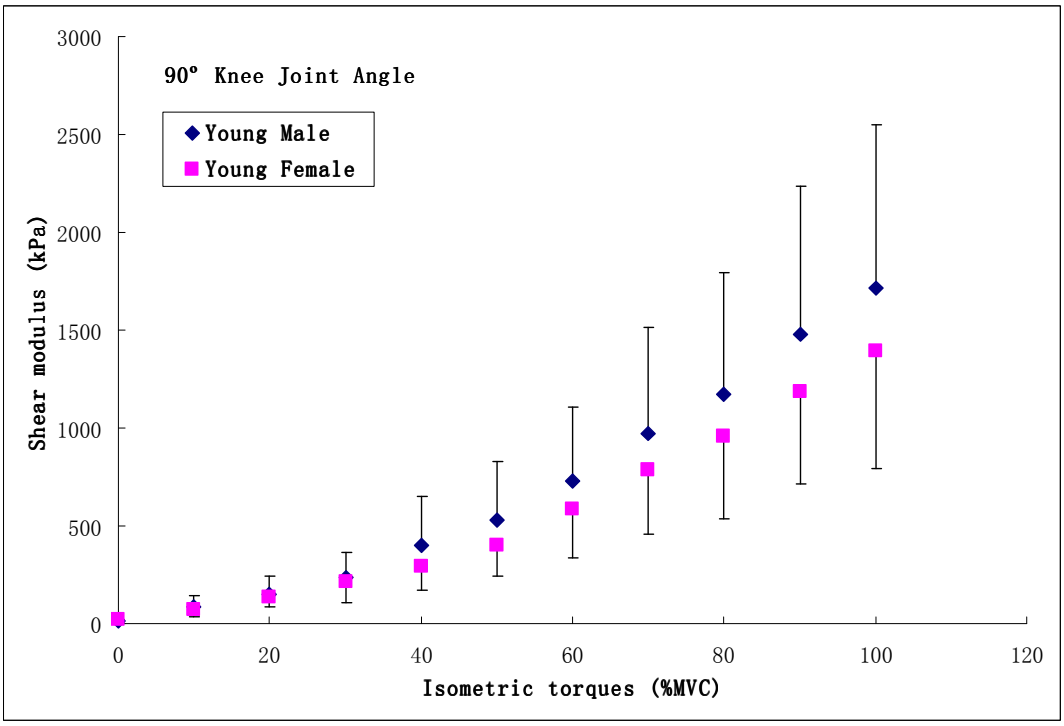
90° Knee Joint Angle
Young Male
Young Female
Shear modulus (kPa)
Isometric torques (%MVC)
0
500
1000
1500
2000
2500
3000
0
20
40
60
80
100
120

(a)

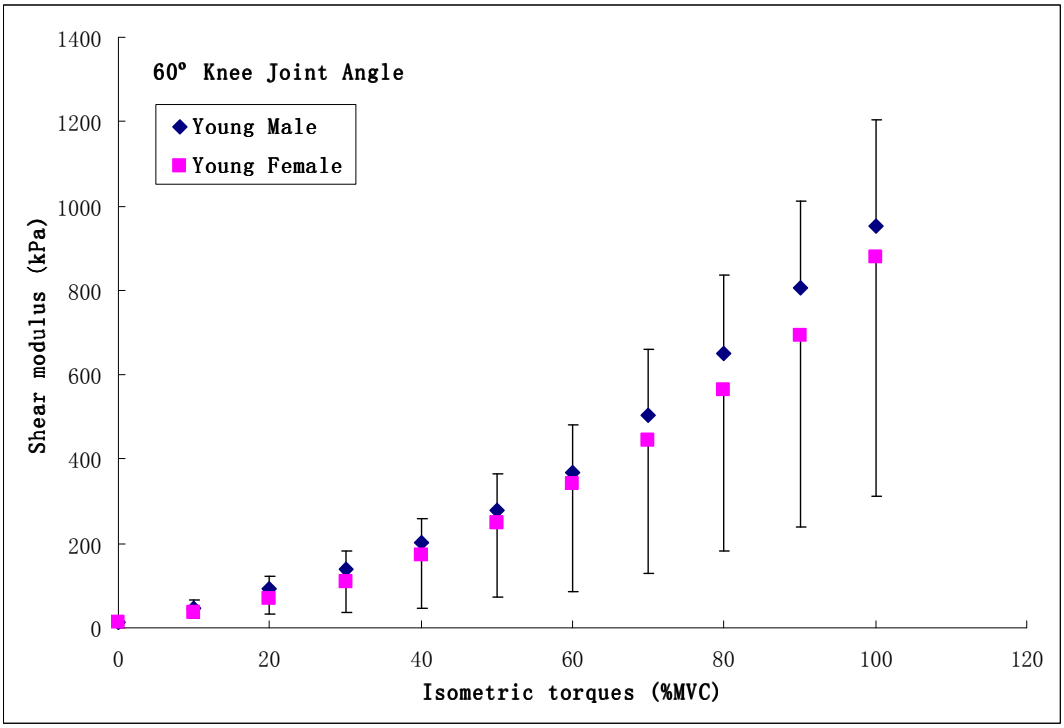
60° Knee Joint Angle
Young Male
Young Female
Shear modulus (kPa)
Isometric torques (%MVC)
0
200
400
600
800
1000
1200
1400
0
20
40
60
80
100
120

(b)

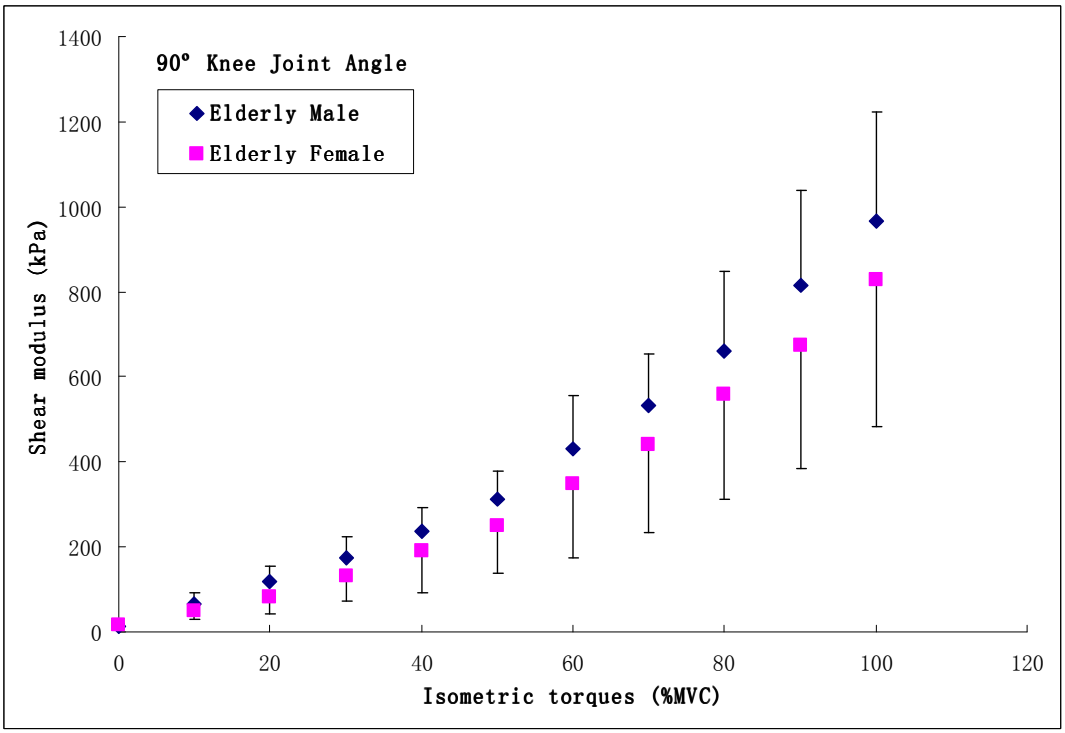

(c)

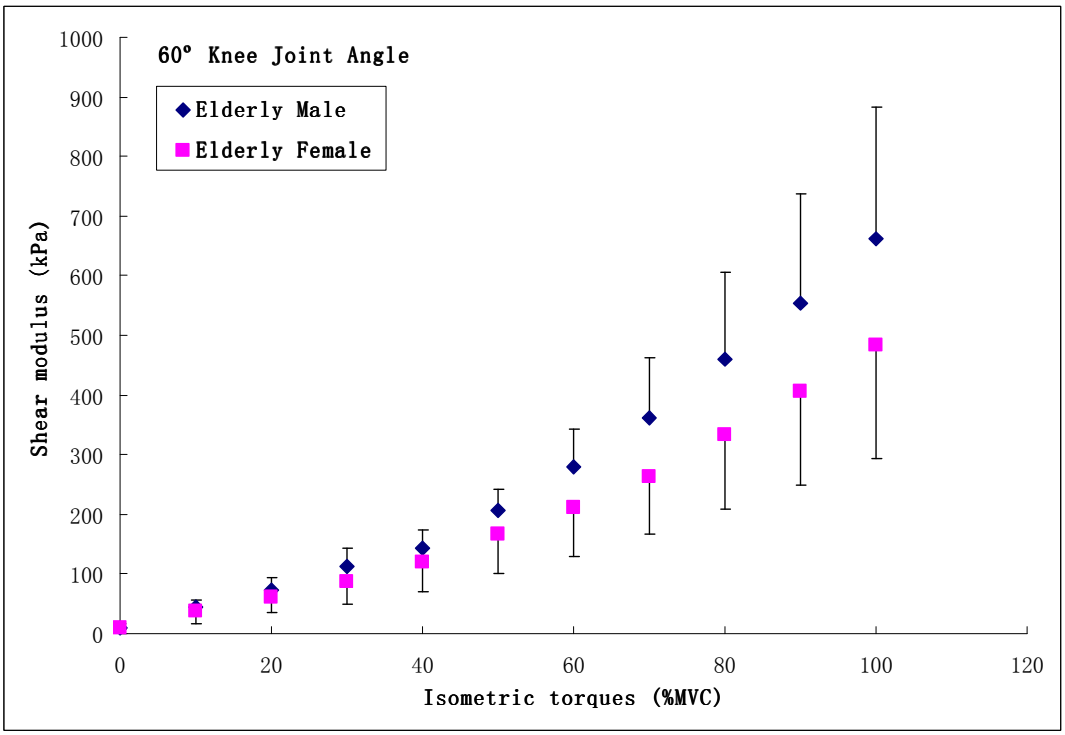

(d)

Fig. 4.6 The gender differences of mean shear modulus values at different relative isometric contraction levels (% MVC) between subjects with similar age range. Comparisons were made between young male and female subjects at (a) 90º and (b) 60º knee joint angles, and between elderly male and female subjects at (c) 90º and (d) 60º knee joint angles.

4.3.3 Analysis Based on Absolute Isometric Contraction Torque

Since the R^2 value did not change for each individual subject when only the scale of x-axis changed, i.e. from relative % MVC level to absolute isometric contraction torque, the quadratic regression model could be also used for examining the trend of the relationship between muscle shear modulus vs. absolute torque values. Quadratic regression was performed on the result of each individual subject at a given joint angle. Then the 10 sets of polynomial coefficients from each group were averaged for plotting curves. The achieved quadratic curves were plotted within a range from 0 Nm to the mean value of MVC torques achieved by each group of subjects and then compared to investigate the differences of their trends. The quadratic curves of each group were plotted to investigate the different trends at 90º and 60º knee joint angles, respectively. It was observed that with the increasing absolute torque value, the muscle shear modulus increased faster at 90º knee joint angle than at 60º knee joint angle, as demonstrated in Fig. 4.7. This result was similar to the relationship between muscle shear modulus vs. relative muscle contraction level (% MVC).

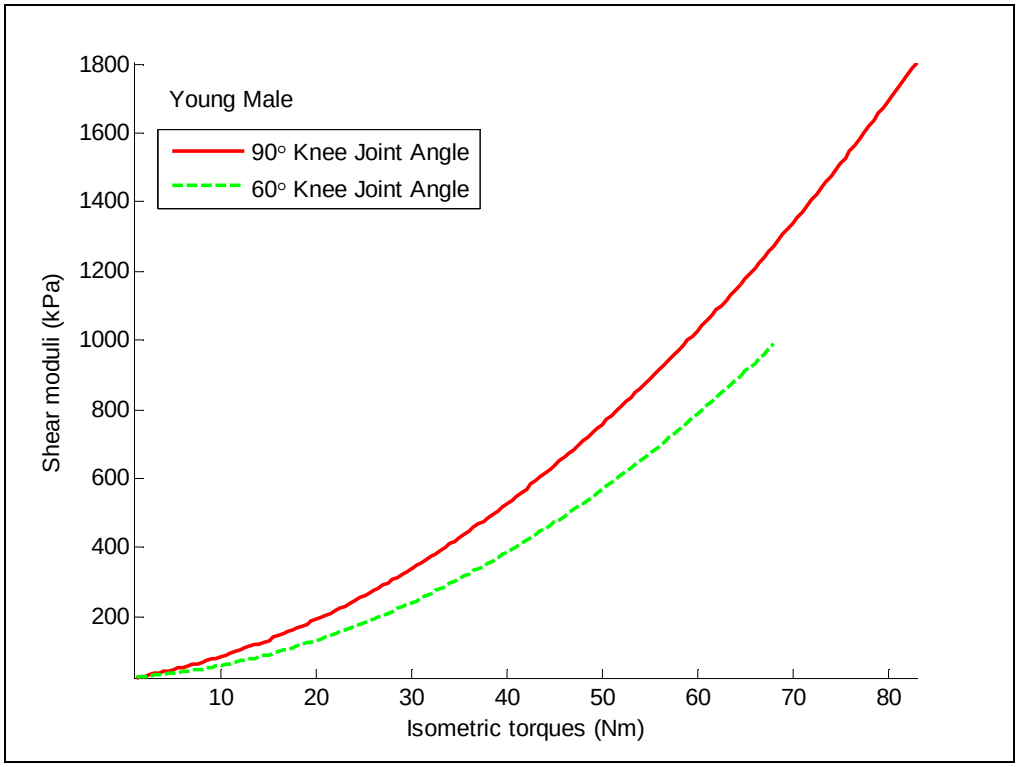
Young Male
90° Knee Joint Angle
60° Knee Joint Angle
Shear moduli (kPa)
Isometric torques (Nm)
1800
1600
1400
1200
1000
800
600
400
200
10
20
30
40
50
60
70
80

(a)

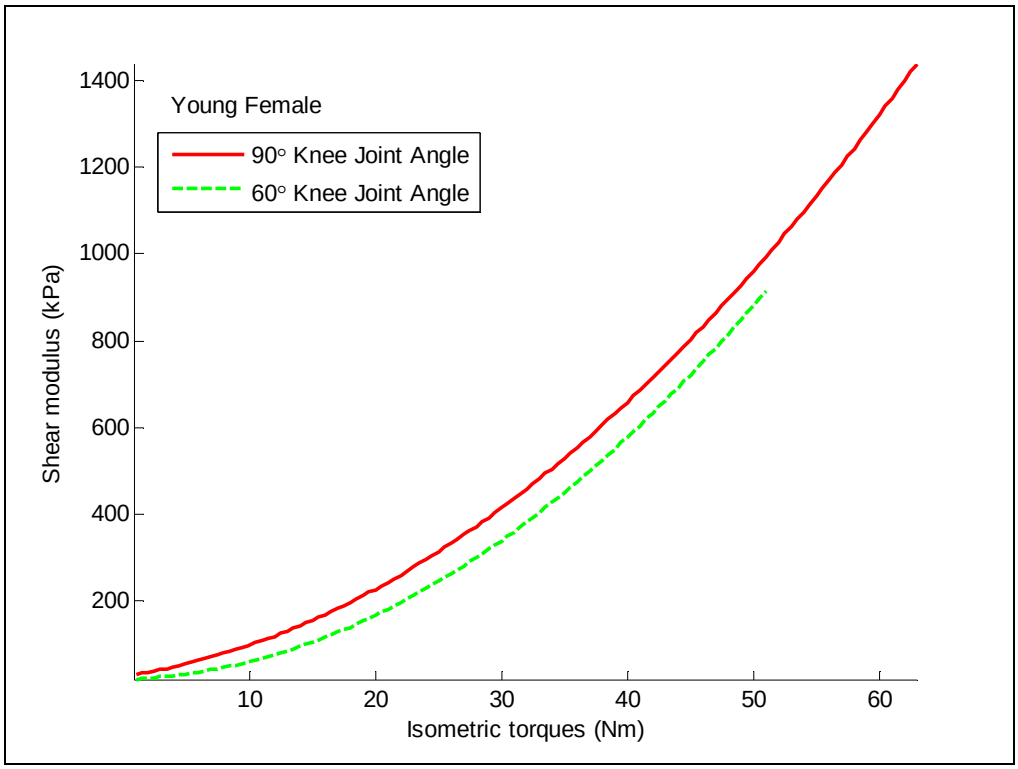
Young Female
90° Knee Joint Angle
60° Knee Joint Angle
Shear modulus (kPa)
Isometric torques (Nm)
1400
1200
1000
800
600
400
200
10
20
30
40
50
60

(b)

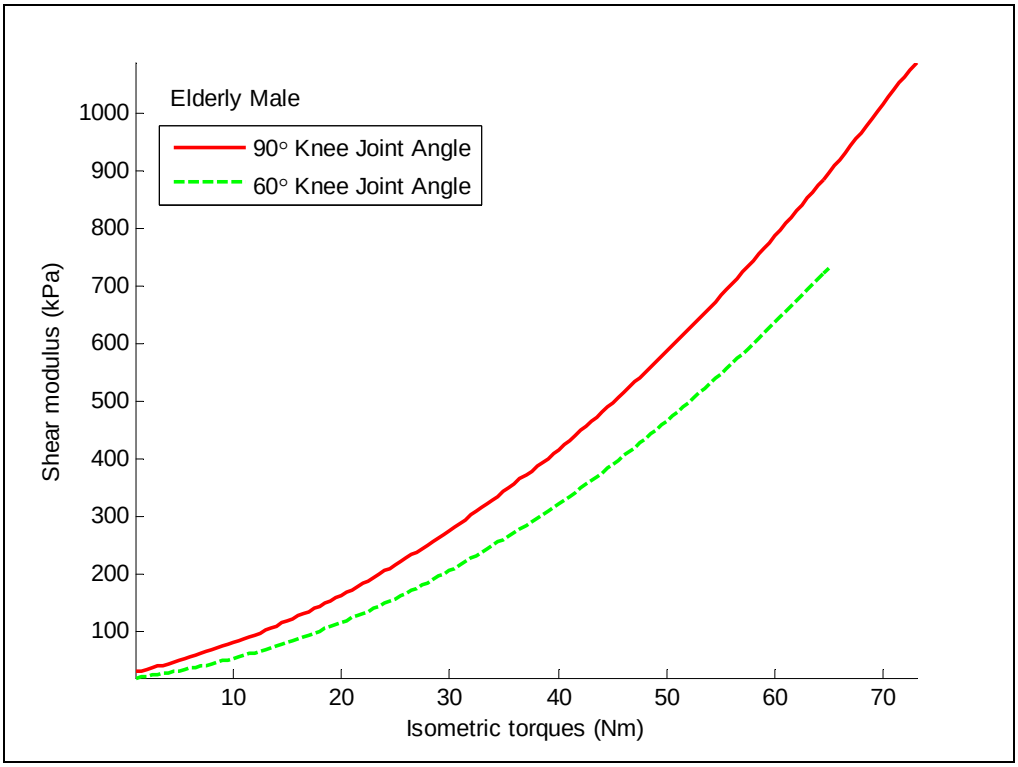

(c)

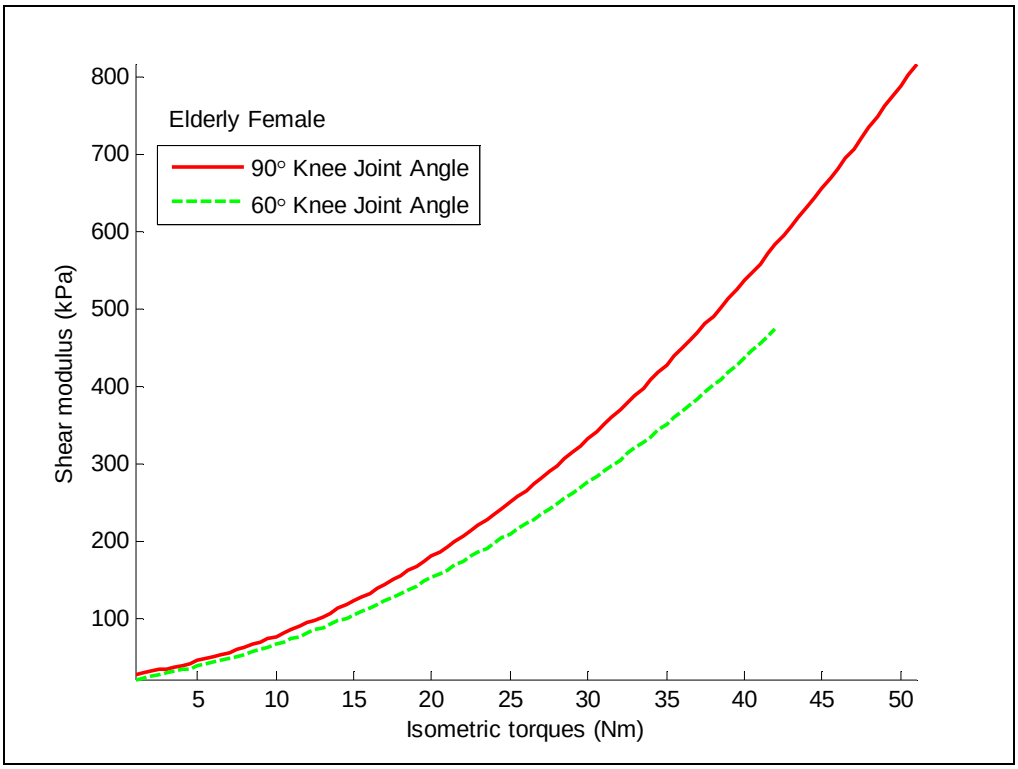

(d)

Fig. 4.7 Comparison of the relationships between the muscle shear modulus values and the absolute torque values at 90º and 60º knee joint angles for (a) young male subjects; (b) young female subjects; (c) elderly male subjects and (d) elderly female subjects.

The relationships between the muscle shear modulus and the absolute torque values with different age ranges and the same gender at a given knee joint angle were also plotted (Fig. 4.8). The results indicated that the shear modulus values of the young subjects increased faster compared with the elderly subjects, for both gender at the same knee joint angle. These relationships were the same as those between the muscle shear modulus and the relative muscle contraction level (% MVC).

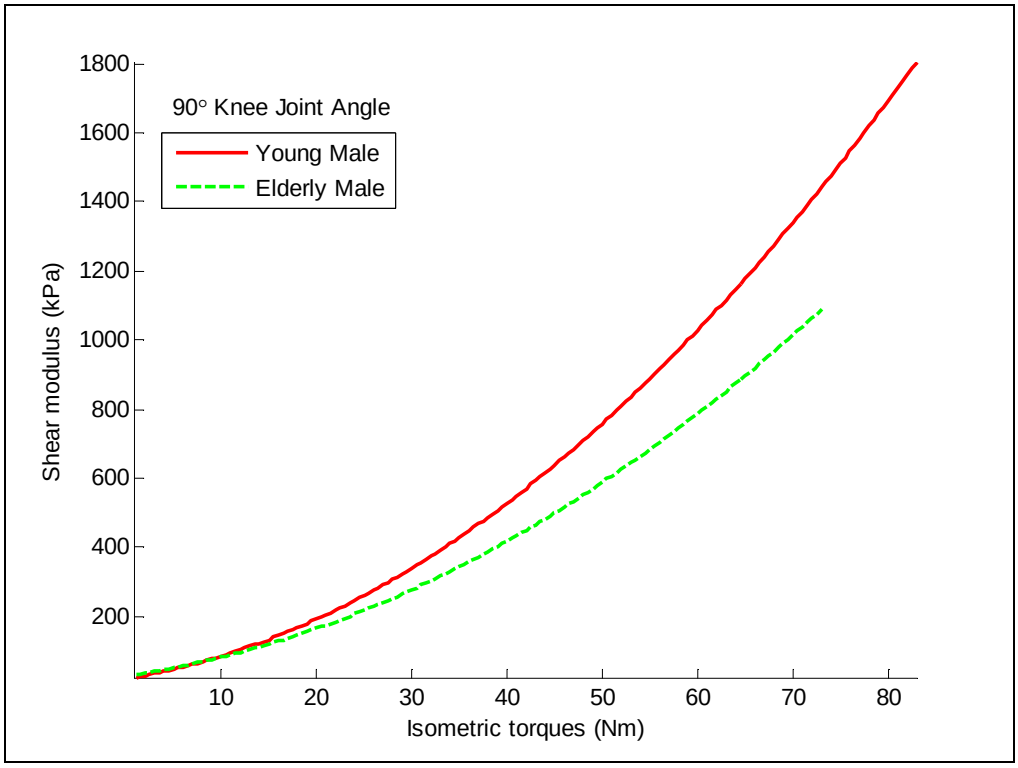

(a)

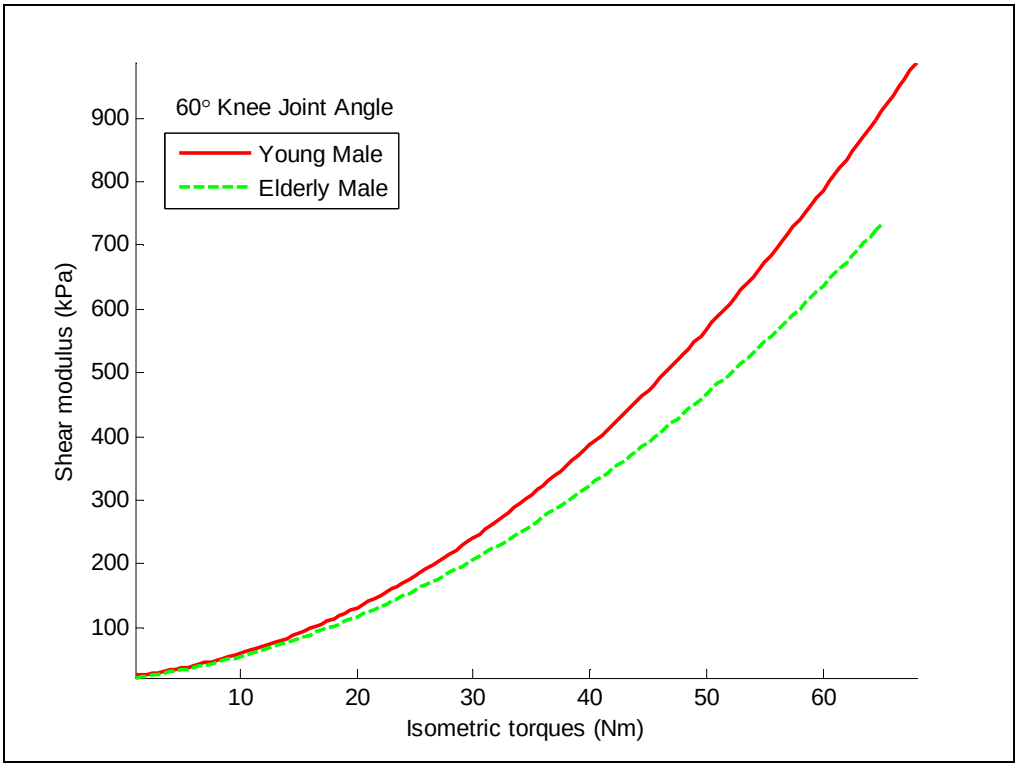
60° Knee Joint Angle
Young Male
Elderly Male
Shear modulus (kPa)
100
200
300
400
500
600
700
800
900
10
20
30
40
50
60
Isometric torques (Nm)

(b)

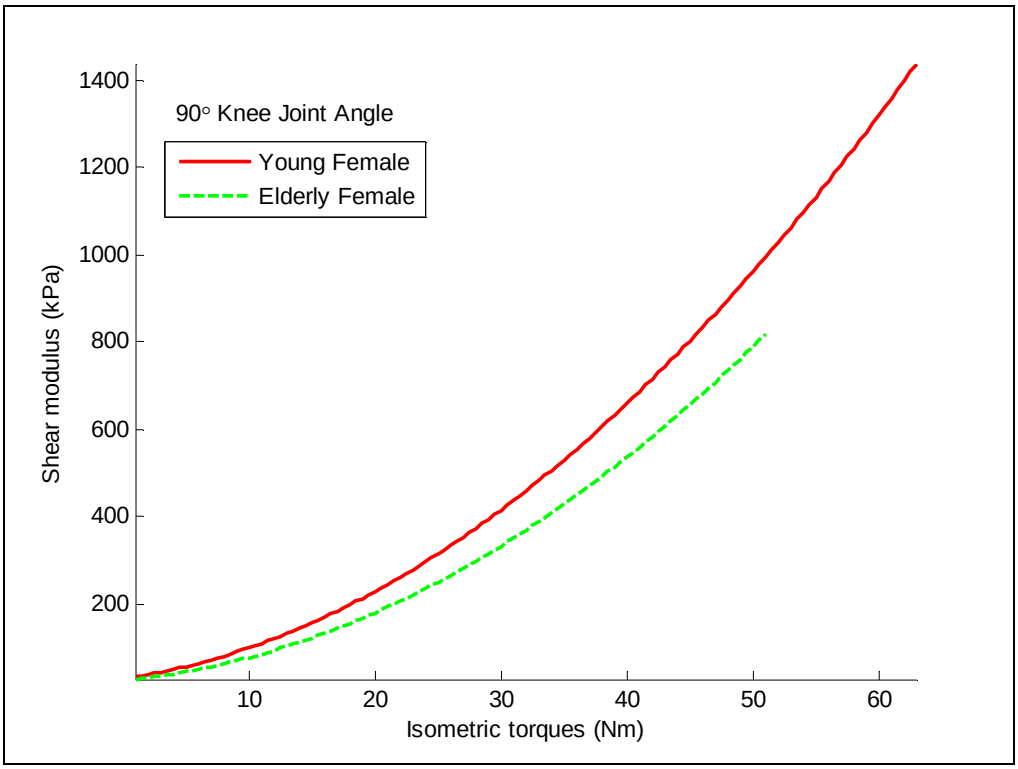
90° Knee Joint Angle
Young Female
Elderly Female
Shear modulus (kPa)
200
400
600
800
1000
1200
1400
10
20
30
40
50
60
Isometric torques (Nm)

(c)

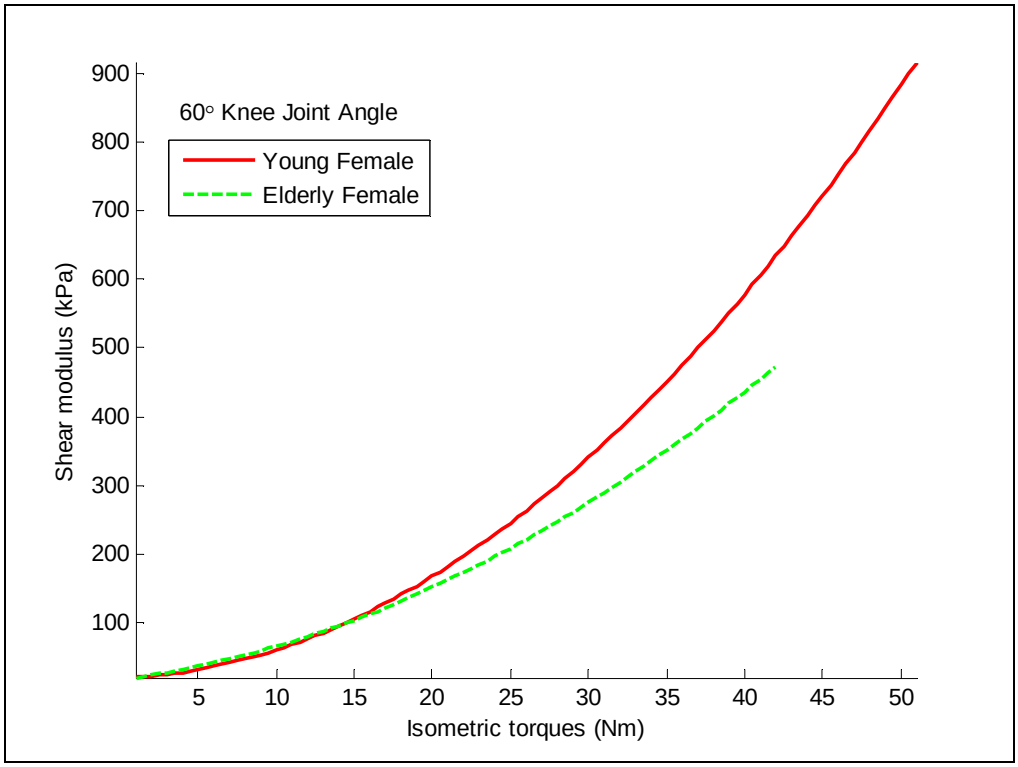

(d)

Fig. 4.8 Age dependences of the relationships between the muscle shear modulus values and the absolute torque values. Comparison were made between young and elderly male subjects at (a) 90º and (b) 60º knee joint angles, and between young and elderly female subjects at (c) 90º and (d) 60º knee joint angles.

Furthermore, the relationships between the muscle shear modulus and the absolute torque values of different genders and the same age range at a given knee joint angle were also compared, as shown in Fig. 4.9. The results showed that the shear modulus values of females increased faster than those of males, for both the age ranges and the knee joint angles. However, these results were opposite to the relationships between the muscle shear modulus and the relative muscle contraction level (% MVC). The reason of this conflict might be due to the relatively smaller MVC torque values of the female subjects, and would be further discussed in the Discussion chapter.

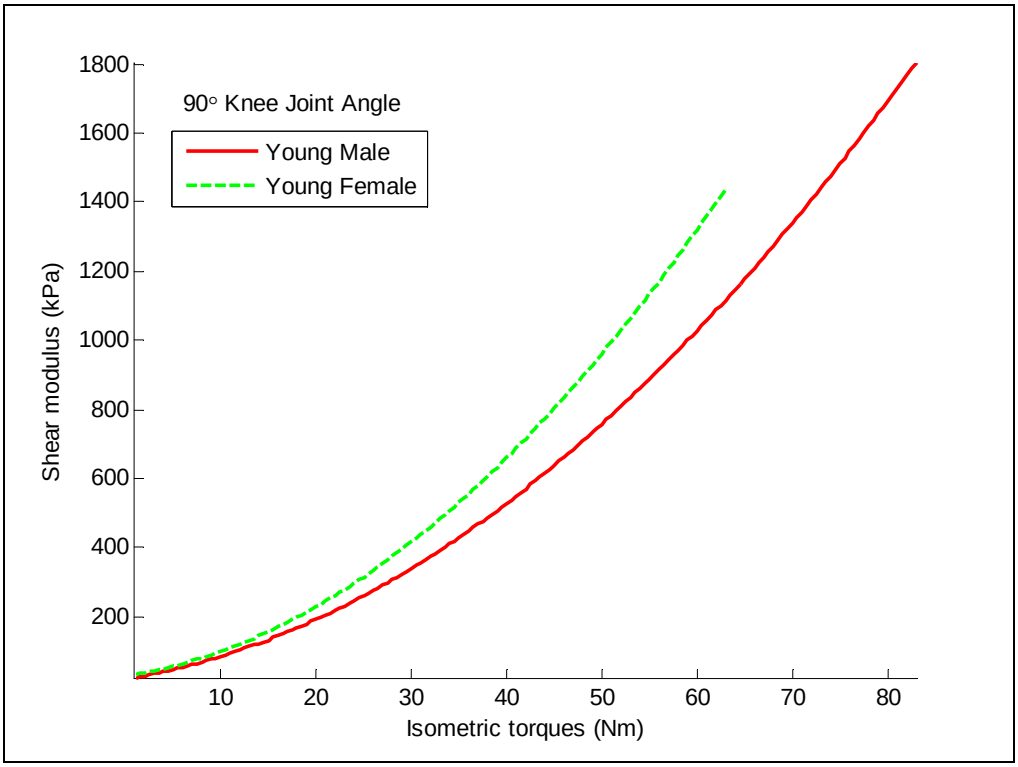
90° Knee Joint Angle
Young Male
Young Female
Shear modulus (kPa)
Isometric torques (Nm)
1800
1600
1400
1200
1000
800
600
400
200
10
20
30
40
50
60
70
80

(a)

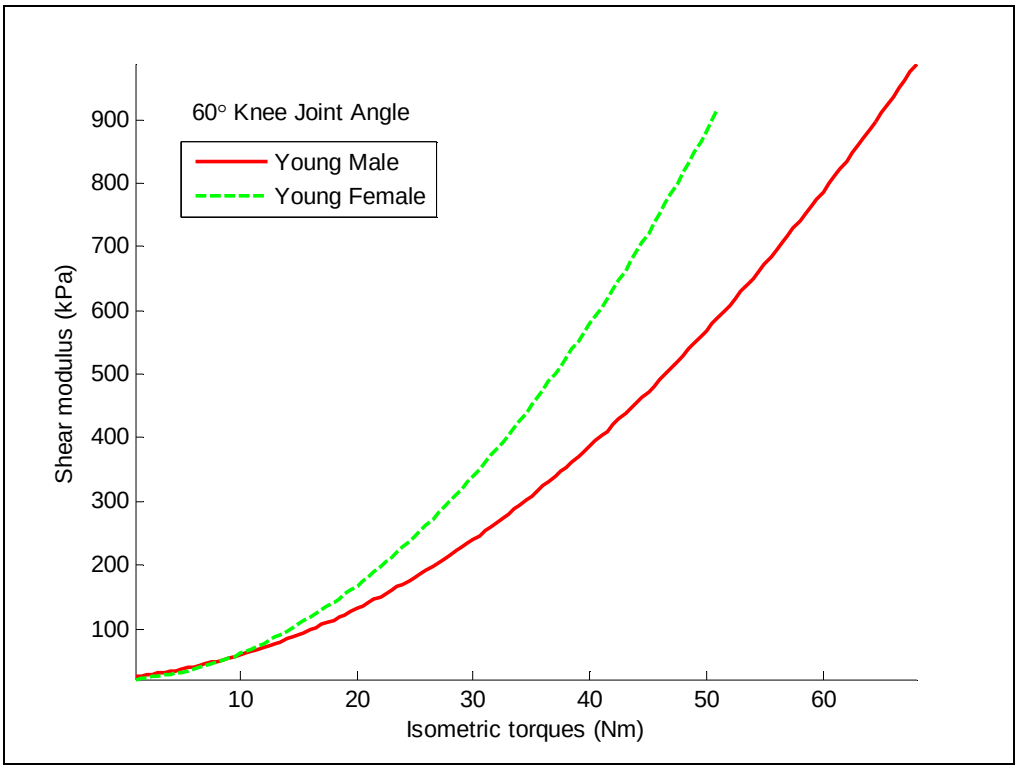
60° Knee Joint Angle
Young Male
Young Female
Shear modulus (kPa)
Isometric torques (Nm)
900
800
700
600
500
400
300
200
100
10
20
30
40
50
60

(b)

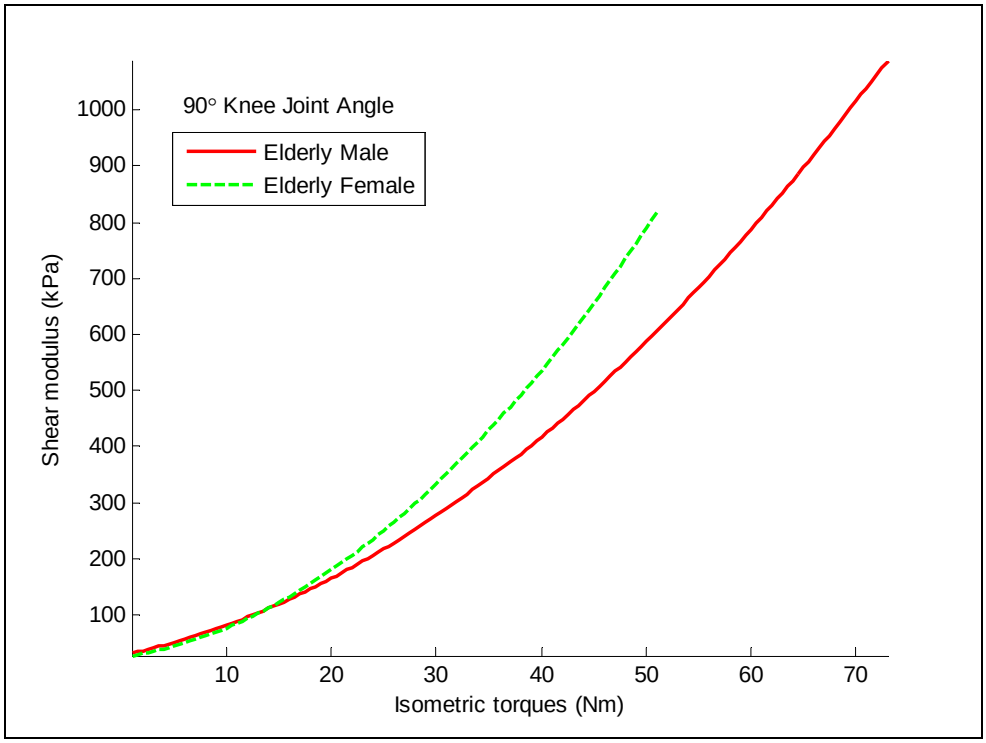

(c)

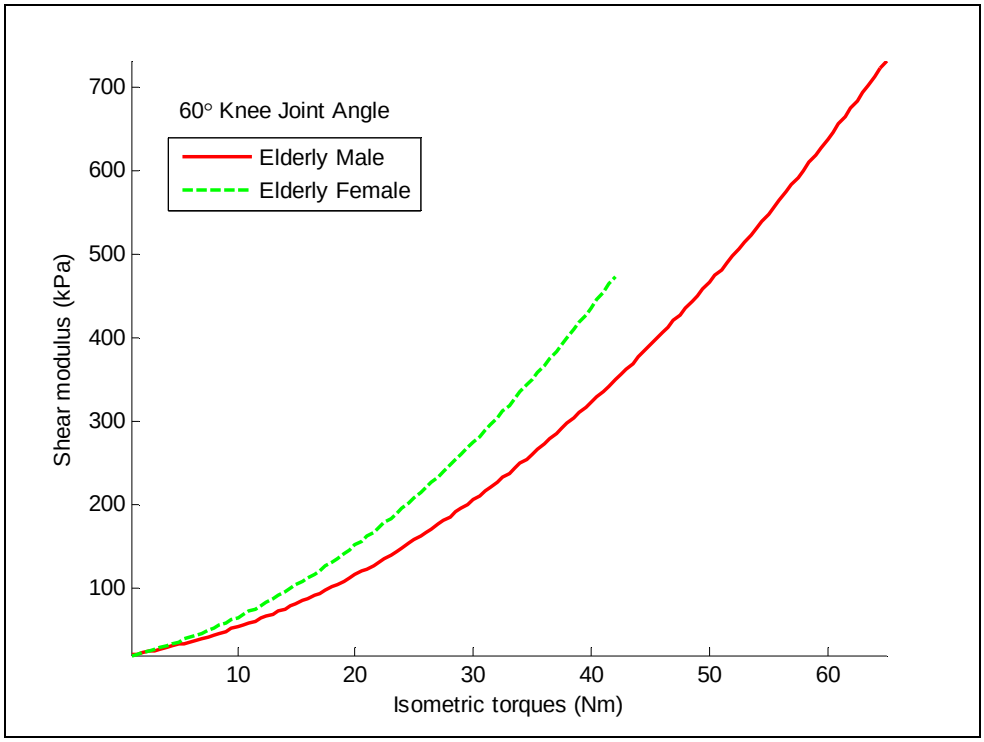

(d)

Fig. 4.9 Gender dependences of the relationships between the muscle shear modulus values and the absolute torque values. Comparison were made between young male and female subjects at (a) 90º and (b) 60º knee joint angles, and between elderly male and female subjects at (c) 90º and (d) 60º knee joint angles.

4.3.4 Correlation between Muscle Shear Modulus and EMG Magnitude

The Pearson's Correlation Coefficients (CC) between the mean shear modulus values of VI muscle and the normalized RMS values of the surface EMG signals obtained from VL muscle were listed in Table 4.6. The two signals were separately plotted according to the subject groups and knee joint angles, as shown in Fig. 4.10. Quadratic regression results were marked on the figures and all R^2 values were larger than 0.98. Since the EMG signal has been widely used as an index of muscle activity level, or to estimate the muscle stress *in vivo* via some mathematical models, our results indicated that the muscle shear modulus had potential to be used as the substitute for the surface EMG signal in research and clinical practice. Furthermore, it was found that, at 60º knee joint angle, the muscle shear modulus and the EMG magnitude were more linearly correlated compared with that at 90º knee joint angle.

Table 4.6 The Pearson's correlation coefficients between the mean shear modulus values of VI muscle and the normalized RMS values of surface EMG on VL muscle in each group and at different knee joint angles.

	Young male	Young female	Elderly male	Elderly female
90º knee joint angle	0.982	0.948	0.935	0.961
60º knee joint angle	0.994	0.995	0.994	0.993

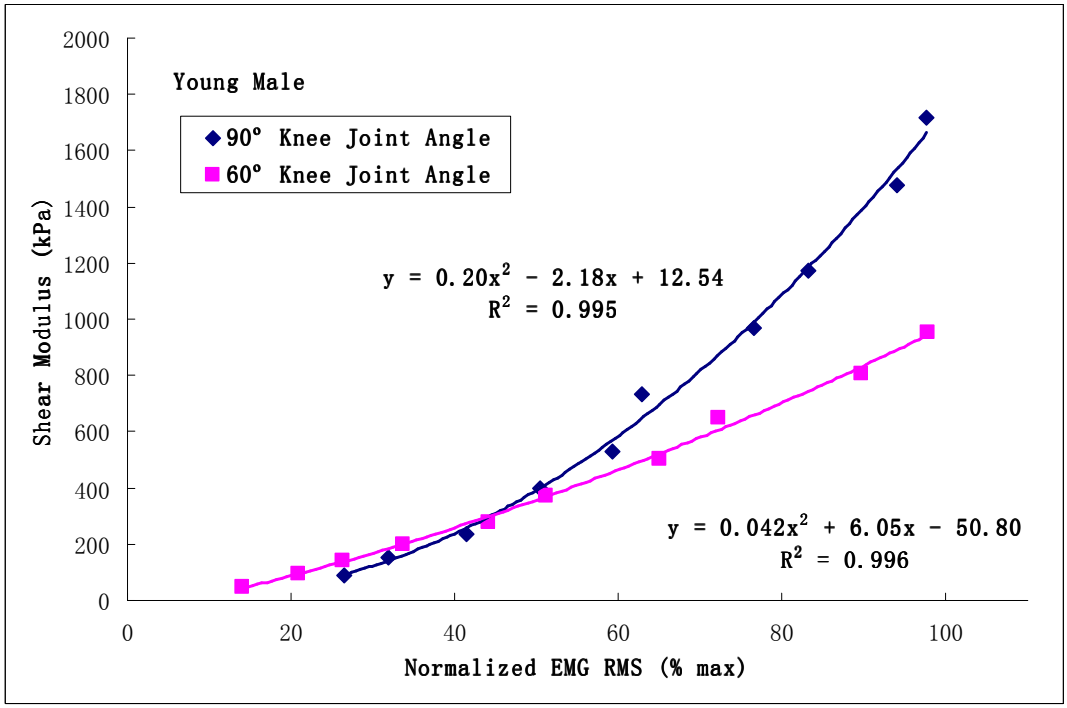
Young Male
90° Knee Joint Angle
60° Knee Joint Angle
y = 0.20x² - 2.18x + 12.54
R² = 0.995
y = 0.042x² + 6.05x - 50.80
R² = 0.996
Shear Modulus (kPa)
Normalized EMG RMS (% max)
0
200
400
600
800
1000
1200
1400
1600
1800
2000
0
20
40
60
80
100

(a)

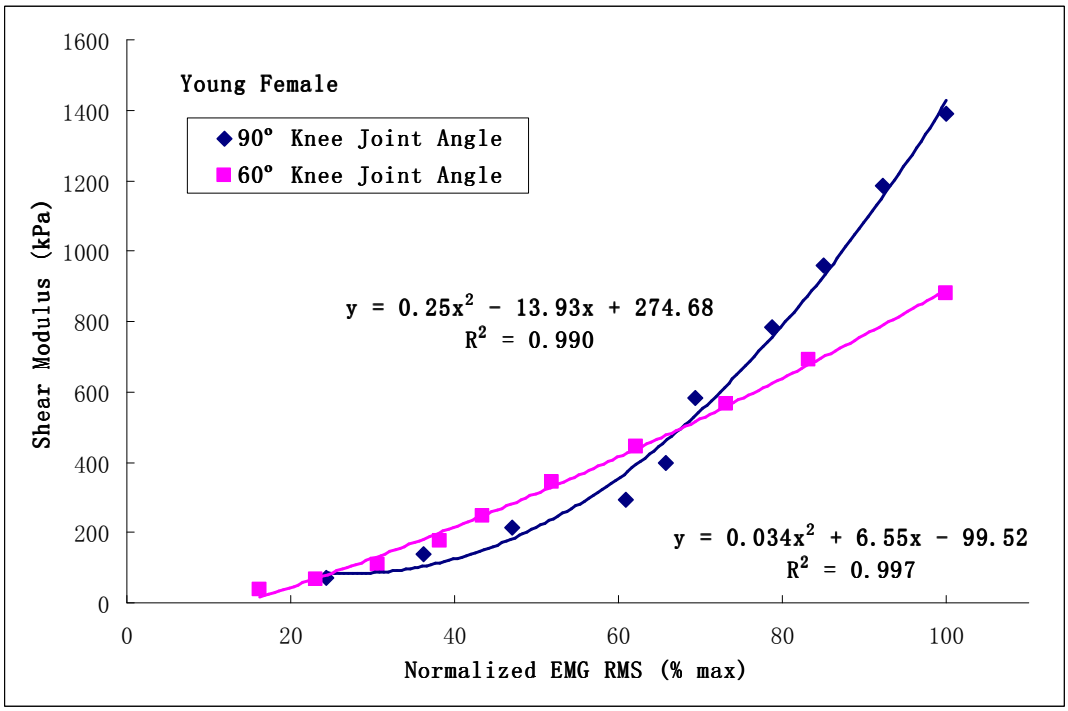
Young Female
90° Knee Joint Angle
60° Knee Joint Angle
y = 0.25x² - 13.93x + 274.68
R² = 0.990
y = 0.034x² + 6.55x - 99.52
R² = 0.997
Shear Modulus (kPa)
Normalized EMG RMS (% max)
0
200
400
600
800
1000
1200
1400
1600
0
20
40
60
80
100

(b)

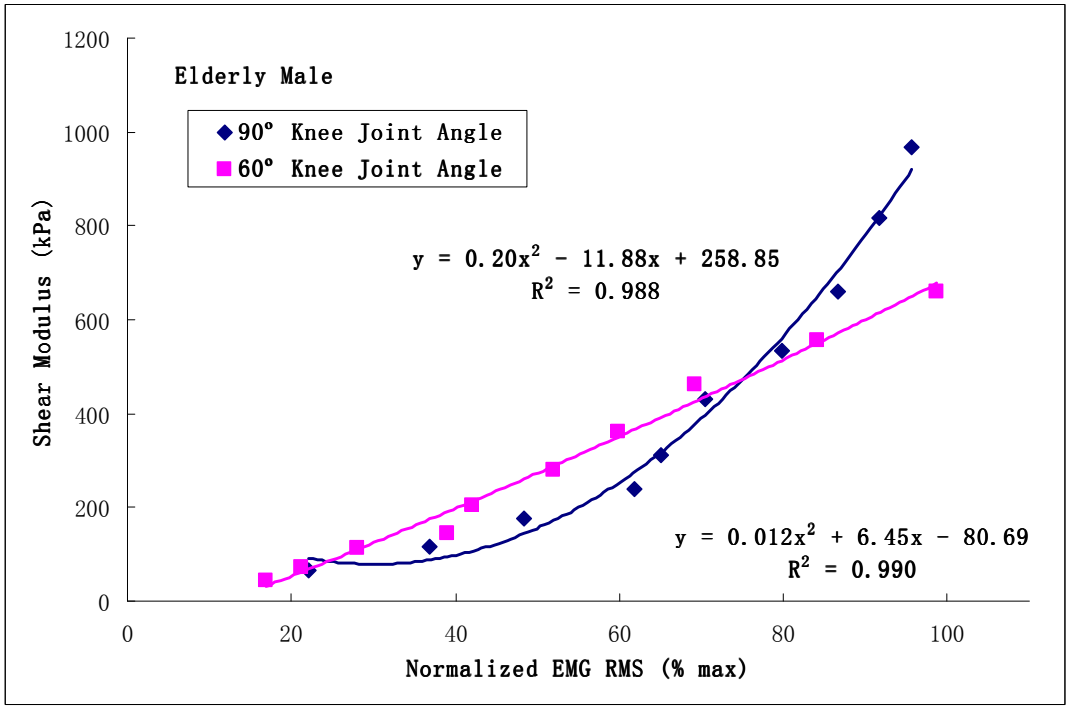

(c)

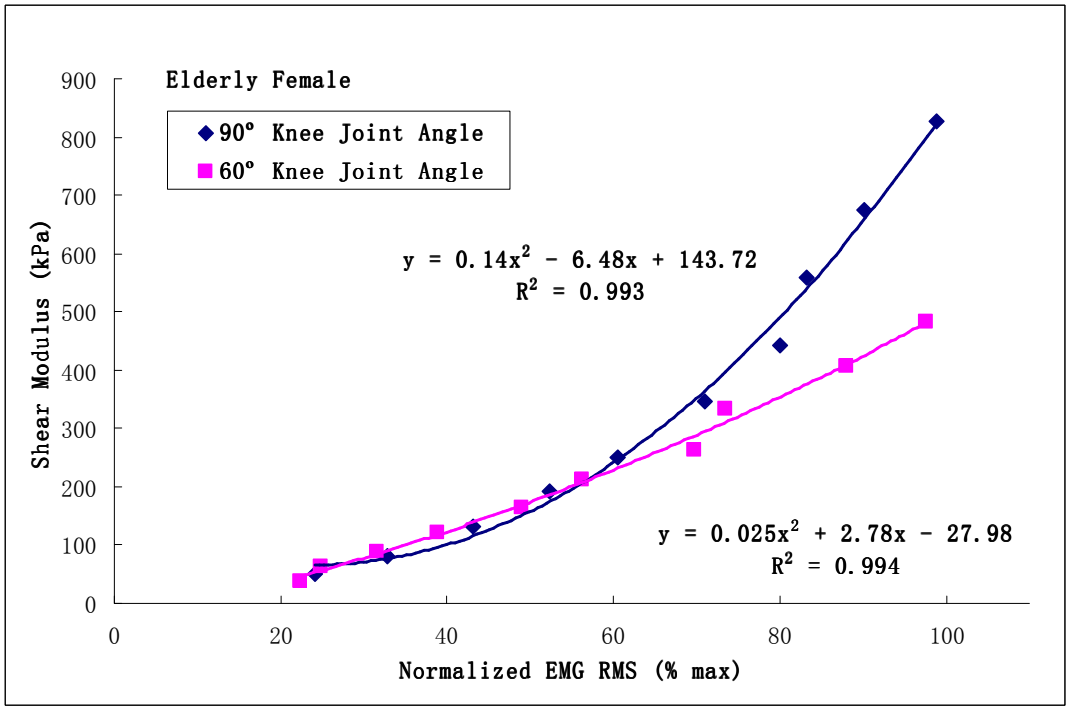

(d)

Fig. 4.10 The relationship between the mean shear modulus values of VI muscle and the normalized RMS values of surface EMG obtained from VL muscle. The figures were plotted for (a) young male subjects; (b) young female subjects; (c) elderly male subjects and (d) elderly female subjects.

CHAPTER 5 DISCUSSION

In this chapter, the newly developed vibro-ultrasound method for muscle stiffness assessment, the relationship between muscle stiffness of VI and contraction level of knee extensor, the gender and age dependences of muscle stiffness under different isometric contraction levels, and the correlation between the shear modulus of VI and the RMS value of surface EMG signal collected from VL, are discussed.

5.1 Development of Vibro-ultrasound Method for Muscle Stiffness Assessment

In this thesis, a vibro-ultrasound method for the measurement of muscle stiffness *in vivo* was developed and its feasibility was successfully tested on VI muscle. The accuracy of this new method might be influenced by several factors, including biomechanical model of soft tissues, wave propagation pattern in the skeleton muscle, and wave reverberation phenomena.

5.1.1 Tissue Biomechanical Model

In this vibro-ultrasound method, the simple tissue biomechanical model (i.e. Eq. 2.1 as described in Section 2.2.4.2) was adopted with an assumption that the skeleton muscle is a kind of pure elastic, locally homogeneous, isotropic and incompressible material. Thus the shear modulus μ_1 could be directly calculated with the shear wave velocity c_s and the material mass density ρ using the following well-known equation:

$$\mu_1 = \rho c_s^{\,2} \tag{5.1}$$

In this model, the reconstruction assumption of a pure elastic, homogeneous and

isotropic material is not valid for skeletal muscle, as the skeleton muscle has been proved to be anisotropic with higher stiffness along the muscle action direction than across the direction of muscle action. However, the assumption is generally assumed to yield an acceptable estimation of the muscle stiffness. This model has been widely used in the sonoelastography method, transient elastography method and MRE method for assessing the stiffness of various kinds of soft tissues. Previous studies have demonstrated that it is a promising model for estimating the stiffness of skeletal muscle (Bensamoun et al., 2006; Catheline et al., 1999; Gennisson et al., 2005; Hoyt et al., 2008; Levinson et al., 1995; Muthupillai et al. 1995; Ringleb et al., 2007).

Considering the viscosity of biological tissues, a more complicated model, Voigt model, has been used in the SDUV method and the SSI method to estimate the shear modulus and the shear viscosity of the soft tissues simultaneously, with a similar assumption that the tissues are homogeneous and isotropic mediums. However, it has been found that along the muscle action direction, the shear wave propagation is practically non-dispersive, at both relaxed and isometric contraction conditions (Catheline et al., 2004; Deffieux et al., 2009). This suggests that, along the muscle action direction which was studied using the vibro-ultrasound method in this study, the viscous effects could be neglected.

Furthermore, for minimizing the anisotropic effects in all the *in vivo* tests of our study, the mechanical vibrator (i.e. the short push-bar) was oriented under ultrasound guidance to ensure the direction of shear wave propagation was exactly along the muscle action direction (Gennisson et al., 2005; Hoyt et al., 2008; Kruse et al., 2000; Manduca et al., 2001).

5.1.2 Wave Propagation Pattern

Wave propagation pattern in the skeleton muscle is another important factor affecting stiffness measurement result and should be carefully studied and controlled during the measurement. In our method, the wave front was desired to be planar and vertical to the muscle action direction, since the shear wave velocity was estimated by directly dividing the distance between the two ultrasound scan lines by the corresponding time of shear wave propagation. If the wave front was a spherical surface or a sloppy plane, this distance would theoretically be longer than the real length of wave travelling path. Thus the measured shear modulus would be overestimated.

Previous studies have reported that when the external excitation was applied on the different positions of skeleton muscle, such as on the tendon or on the muscle belly, the shear wave pattern would be different. Sack et al. (2002) reconstructed the shear wave patterns using 3D coupled harmonic oscillator calculations (CHO) method and in vivo MRE data gotten from the biceps brachii muscle. In the CHO model, all muscle fibers were assumed to be simultaneously excited and the elements along the muscle action direction were coupled more strongly than those in the perpendicular direction. Planar waves were observed in their results when the external excitation was applied on the muscle belly using a short push-bar, of which the orientation was kept to be vertical to the muscle fibers to minimize the anisotropic effects (Hoyt et al., 2008; Kruse et al., 2000). The planar wave pattern along the muscle action direction can also be seen from the MRE images in the previous studies (Bensamoun et al., 2007; Bensamoun et al., 2008; Chen et al., 2008; Heers et al., 2003; Muthupillai et al. 1996; Ringleb et al., 2007).

Furthermore, it is also important to guarantee the wave front at ROI is a plane vertical to the muscle action direction. In wave theory, shear wave is a kind of transverse wave, which consists of oscillations perpendicular to the direction of wave propagation. The wave front is the locus of the points having the same phase, which is often described as a line/curve in a 2D wave propagating plane or a surface in 3D wave propagating model. In our experiments, lines were plotted by fitting the peak points of sinusoidal waveforms collected from the proximal and distal positions. The shape of these lines was straight and vertical to the time axis. So each fitting line could be seen as the wave front of shear wave at this depth and at a special time point. Hence in 3D space, the shape of wave front was a plane and the plane was parallel to the direction of ultrasound scan lines. The direction of scan lines had been positioned vertical to the muscle action direction with the help of B-mode ultrasound image guidance. In addition, each pair of wave fronts collected at the same time point but different positions was parallel. Thus, from the figures as interim results of echo-tracking procedure, e.g. Fig. 3.6, the wave fronts were shown to be vertical to the muscle action direction and hence the wave propagating direction was along the muscle action direction in the ROI region.

As mentioned in Section 3.3.1, whether the vibrator-beam distance would influence the measured shear modulus is a deductive problem caused by the shear wave patterns in the muscle. If the wave front pattern was planar, the vibrator-beam distance would not affect the measured shear wave velocity. If the wave front was a spherical surface or a sloppy plane, the direction of shear wave propagation would have an angle with the direction of muscle action, thus the measured shear modulus would be overestimated. Under this condition, when the vibrator-beam distance decreased, the angle between wave propagation direction and the muscle action direction would increase and hence

this kind of overestimation would also increase. Therefore, the above conclusion, i.e. in our study, the shear wave propagation pattern in the ROI of VI muscle was planar and the wave front was vertical to the muscle action direction, was also supported by the results of the experiment which evaluated the effects of different vibrator-beam distances on the measured muscle shear modulus, as described in Section 4.2.

5.1.3 Wave Reverberation Phenomena

Shear wave propagation in soft tissue has demonstrated several wave phenomena, such as refraction and reflection at the interface of aponeurosis or bone, and wave attenuation as it propagates through the tissue. All of these phenomena will affect the wave patterns in skeleton muscle (Muthupillai et al., 1996). In this study, efforts to avoid the negative influence of these wave phenomena had been considered when designing the experiment. In the case where the dimensions of the propagation medium are comparable to the wavelength, the boundary conditions may influence the measurements. For example, if the muscle shear modulus was measured as 16 kPa, which was a value close to the mean VI muscle shear modulus demonstrated in our study for the young male subjects under relaxed condition and 90º knee joint angle (14.5 ± 6.3 kPa), the shear wavelength would be 4 cm when the frequency of mechanical vibration was 100 Hz and it was much smaller than the dimension of the VI muscle along the direction of muscle action (about as long as femur, approximately 20-40 cm in adults). In our method, before the reflected wave echoed back along the muscle action direction, the data acquisition had been accomplished and would not be affected. Although high frequency could decrease the wavelength of shear wave and thus reduce the reflection effect, low-frequency mechanical vibration was used because the shear wave with high frequency would rapidly attenuate during the propagation in

the muscle. To increase the range of shear modulus measurement, a relatively larger distance between the two ultrasound scan lines was desired. This also required the wave attenuation on this distance to be small enough to make the tracking of the echoes displacements available at the distal position.

Most of the organs in the body can be seen as layered structures of tissues with different shear modulus. For example, in our study, the top layer is skin, followed by the fat layer, the RF muscle, the aponeurosis, the VI muscle and the bone, sequentially. Since the shear waves in the muscle were generated by the mechanical vibrator from the skin surface, the reverberation of the vertical vibrations also arose in the perpendicular direction from the boundaries of these layers. Although the boundaries were paralleled to the direction of shear wave propagation, the waveforms were still distorted by these reverberations, thus affecting the measured local shear wave velocity. However, this kind of distortion had been found to be relatively small and almost negligible at the upper part of the deeper muscle, just under its upper boundary (i.e. the aponeurosis in current study) (Suga et al., 2001), as the amplitude of reverberative waves from its deeper boundary (i.e. the femur bone in our study) was very small and quickly attenuated, as shown in Fig. 5.1. In this study, the ROI was selected as the upper part of the VI muscle. According to the wave patterns shown in the echo-tracking results in Fig. 3.6, the influence of the vertical wave reverberation on the measured muscle shear modulus would be very small.

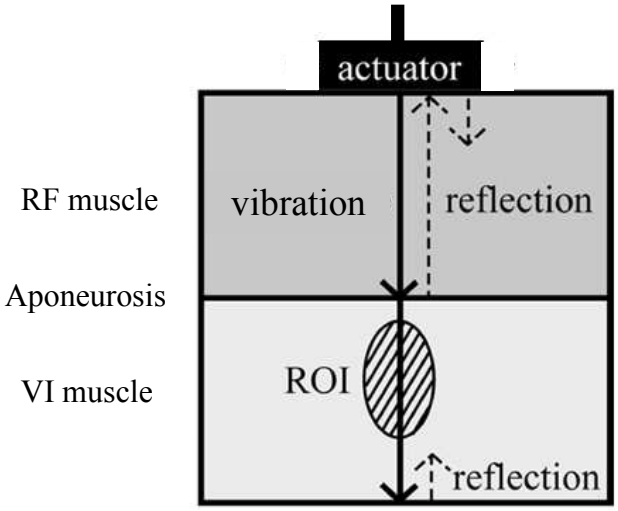

Fig. 5.1 Region of interest (ROI) in the soft tissues with layered structure. The arrow in the diagram indicated the vertical vibration (thick line) and reflection wave (dotted line) in the vertical direction. The reflections would interfere with the shear wave pattern and thus the shear wave velocity measurement. However, the effect of reflection could be mostly avoided in the ROI.

In addition, both the mechanical vibrator and ultrasound transducer were fixed rigidly to avoid their relative motion and to keep a consistent ROI for repeated measurements. Regarding the boundary conditions, our pilot studies had revealed that tissue surface stresses imposed by either the mechanical vibrator or ultrasound transducer could also influence the shear wave pattern by damping the vibration response of underlying tissues. Since the VI muscle is located deep in the layered structure, the effect of boundary condition on its stiffness measurement should be very little. In addition, the pennation angle of VI muscle at the anterior position, i.e. the position measured in this study, is small (7.1 ± 2.9º) (Blazevich et al., 2006), thus its muscle fiber direction was more in line with the muscle action direction which further guaranteed the accuracy of the shear wave velocity measurement.

5.1.4 Other Issues Related to the Vibro-ultrasound Method

The exact force exerted by a specific muscle cannot be directly measured in vivo. One solution is to use the joint torque measured by a dynamometer as an indication of the muscle activity intensity. This method has been widely used in the previous studies (Alkner et al., 2000; Guo et al., 2008; Kubo et al., 2001; Ryan et al., 2008; Wilson et al., 1994). Furthermore, since the quadriceps femoris muscle group is the sole contributor to generate force in the single-joint knee extension, and the neuromuscular activity vs. torque relationships of its four components, RF, VI, VL and VM, are similar in the step isometric contraciton exercises (Alkner et al., 2000), using the knee extension torque as an index for estimating the VI muscle activity was an acceptable approaching in our study. Furthermore, since the neuromuscular activity of the antagonistic muscle, hamstring, has been found to be much smaller than those of the four components of the quadriceps femoris muscle group during the step isometric contraciton exams (Alkner et al., 2000), the contribution of antagonistic muscular contraction has not been accounted for in this study. However, the activity and stiffness of hamstring during the knee extension should be further studied in the future.

In our method, all the time delay values at different depths in the ROI were averaged and the mean value was used to calculate the overall shear wave velocity, and then the overall shear modulus. A previous study using SSI method has reported the local spatial variablility of shear modulus in the biceps brachii muscle. However, very similar relationships between the shear modulus values and % MVC levels were also observed between the results obtained in different trials, of which the measured location slightly changed (Nordez and Hug, 2010). This justified the averaging of the measured shear modulus values in the ROI to be more representative of the mechanical properties of the

muscle belly. To understand better the site differences of skeleton muscle, the spatial variability of the muscle shear modulus should be investigated in future studies.

The influence of viscosity on shear wave velocity measurement in the muscle has been previously studied (Catheline et al., 2004; Deffieux et al., 2009). Using SSI, Deffieux et al. (2009) found that along the direction of muscle action, the shear wave propagation was practically non-dispersive, whereas in the direction perpendicular to the muscle action, the propagation was highly dispersive. In addition, at several different isometric contraction levels, the wave velocity along the muscle action direction remained quasi-constant versus frequency. In the vibro-ultrasound method of this study, as the muscle shear modulus along the muscle action direction was measured, the shear wave velocity was assumed to be almost independent of the exciting frequency and the viscous effects could be neglected.

The vibro-ultrasound method had been evaluated on the silicone phantoms using a conventional indentation method before it was performed on human muscle *in vivo*. MRE measurements were previously compared with static compression tests or dynamic mechanical analysis method on various kinds of phantoms (Hamhaber et al., 2003; Muthupillai et al., 1995; Ringleb et al., 2005) and the results measured with different methods showed good agreement. Our result on the tissue mimicking phantoms by the newly developed vibro-ultrasound method also agreed well with that by the traditional indentation method. This suggested that the methods based on the biomechanical models as mentioned in Section 5.1.1 could provide acceptable assessments of soft tissue stiffness. In addition, in the *in vivo* study, the overall ICC for the measured shear modulus of VI and the ICCs under different % MVC levels also indicated a high degree of intra-observer repeatability of this method.

5.2 Stiffness of VI Muscle in Relaxed Condition

The mean shear modulus of VI muscle in relaxed condition for all subjects were 16.2 ± 8.1 kPa (at 90º knee joint angle) and 11.1 ± 4.4 kPa (at 60º knee joint angle). Although several methods based on shear wave velocity measurement have been used to estimate the shear modulus of skeleton muscle, few studies have been done to assess the VI muscle stiffness. An earlier study using sonoelastography method by Levinson et al. (1995) yielded a Young's modulus of 79 ± 29 kPa in the quadriceps, corresponding to a shear modulus of about 27 kPa. However, in that study, which part of the quadriceps was examined was not clarified. From the figures in their paper, the muscle they studied should be the RF muscle. MRE method has also been used on the quadriceps femoris muscles, but only on VL and VM. Bensamoun et al. (2006) measured the shear modulus of VL and VM in relaxed condition on young healthy subjects. The mean values were 3.73 ± 0.85 kPa and 3.91 ± 1.15 kPa, respectively. The same group (Bensamoun et al., 2008) also assessed the stiffness of VM, using both 2D MRE and 1D MRE methods, and reported shear modulus values of 4.36 ± 0.98 kPa and 3.69 ± 0.80 kPa, respectively. The stiffness of other skeleton muscles in relaxed condition has also been measured in previous studies. The shear modulus for the biceps brachii was measured as 17.9 ± 5.5 kPa (Uffmann et al., 2004) and 27.3 ± 11.9 kPa using MRE (Dresner et al., 2001). Using SSI method, the shear modulus of biceps brachii measured at rest was 11.3 ± 3.8 kPa and 10.7 ± 4.5 kPa for two trials (Nordez and Hug, 2010). The stiffness of distal leg muscles was also investigated using MRE. Specifically, the shear modulus values were 8.7 ± 2.8 kPa (Uffmann et al., 2004) in the flexor digitorum profundus; 16.77 ± 0.24 kPa (Basford et al., 2002), 16.4 ± 0.2 kPa (Heers et al., 2003) and 12.5 ± 7.3 kPa (Uffmann et al., 2004) in the soleus (SL); 16.16 ± 0.19 kPa (Basford et al., 2002), 16.4

± 0.2 kPa (Heers et al., 2003), 9.9 ± 6.8 kPa (Uffmann et al., 2004) and 22.04 ± 3.46 kPa (Jenkyn et al., 2003) in the lateral gastrocnemius muscle (LG); 24.9 ± 0.7 kPa (Basford et al., 2002) and 20.3 ± 1.1 kPa (Heers et al., 2003) in the medial gastrocnemius muscle (MG); 12.03 ± 0.39 kPa (Basford et al., 2002), 11.9 ± 0.6 kPa (Heers et al., 2003) and 12.3 ± 4.5 kPa (Jenkyn et al., 2003) in the tibialis anterior (TA).

The different stiffness observed in different muscles may indicate that the propagation of shear waves is influenced by the muscle structure, such as muscle fiber orientation. The biceps brachii, gastrocnemius, RF and VI muscles, which are bipennate muscles, exhibit higher muscle stiffness than the VL and VM muscles, in which the fiber orientation is unipennate (Bensamoun et al., 2006). In addition, these differences might be also related to the muscle volume, muscle fiber type, muscle function or other specific muscle characteristics of different muscles. Although it is difficult to compare these results directly, the shear modulus values all fall into a similar range. Further studies are desired to more precisely determine the range of muscle stiffness under relaxed condition.

The results of muscle shear modulus measurement in relaxed condition might be also influenced by factors other than those discussed above. Although all the subjects were asked to fully relax their muscles during the exams, they might have slightly altered the tension in the muscle unconsciously. Since muscle stiffness is strongly influenced by the muscle contraction state, even this kind of slight tension might affect the measurement results. The muscle stiffness might also be affected by the state of the muscle itself. Little is known about the variation of muscle stiffness *in vivo* over time. The momentary stiffness might change due to the history of muscle use preceding the exams, which might also change the biochemical state of the subject's muscle (Uffmann

et al., 2004). That was why in our experiment, the subjects were asked not to participate in any strength or flexibility training one day before the measurement. The effects of sports and exercises on muscle stiffness should be further investigated in future studies.

It was found that the mean value of muscle shear modulus in relaxed condition at 90º knee joint angle (16.2 ± 8.1 kPa) was significantly larger than the value at 60º knee joint angle (11.1 ± 4.4 kPa) ($p < 0.001$). Few studies have been performed to investigate the relationship between the shear modulus of VI and the knee joint angle. The change of shear modulus of relaxed TA and LG muscles in distal leg with different foot position were studied using MRE by Jenkyn et al. (2003). Shear modulus of LG increased to 35.1 ± 0.4 kPa at 20º of dorsi-flexion from 22.1 ± 0.2 kPa at neutral, but decreased to 18.4 ± 0.1 kPa at 45º of plantar-flexion. The shear modulus of TA increased from 12.3 ± 0.5 kPa at neutral to 32.5 ± 0.2 kPa at 45º of plantar-flexion and was almost unchanged at 20º of dorsi-flexion (13.5 ± 0.4 kPa). The results indicated that the shear modulus increased with the increase of passive muscle stretching. Their results are in good agreement with ours. At the 90º knee joint angle, the VI muscle was more stretched than at the 60º knee joint angle, thus the shear modulus increased. Besides passive muscle stretching in this state, the difference of shear modulus might also be related to the morphology change with the different knee joint angles, such as fascicle length and pennation angle. When the knee was extended, the length of muscle-tendon complex and fascicle length of quadriceps femoris were reported to be shortened, and pennation angle increased in step with the changes of knee joint angle (Fukunaga et al., 1997; Ichinose et al. 2000). However, the detailed relationship between the changes of VI muscle shear modulus and the morphology changes with knee joint angle should be further studied.

5.3 Relationship between Muscle Stiffness and Step Isometric Contraction

As mentioned in Section 3.4.3, two methods have been used to exhibit the different contraction intensities, one is to use the relative muscle contraction level (% MVC), and the other one is to use the absolute torque value of the joint extensor or flexor. The focused aspects of these two methods are different. However, both of these two methods can help us to further understand the muscle function and recruitment strategies from different perspectives.

Besides two methods mentioned above, some previous studies also used different weight loads to represent the different muscle contraction levels, such as on the knee extensor (Levinson et al. 1995) and on the elbow flexor (Dresner et al., 2001). In the study of Levinson et al. (1995), 0, 7.5 kg and 15 kg weights were applied to the ankle and the sonoelastography method was used. The corresponding values of Young's modulus of quadriceps femoris muscle were 79 ± 29 kPa, 103 ± 26 kPa and 126 ± 26 kPa, respectively. The shear modulus values estimated from the Young's modulus were about 26 kPa, 34 kPa and 42 kPa, assuming a Poisson's ratio of 0.5. In the study of Dresner et al. (2001), various weight loads from 0 kg to 10 kg were applied on the wrist of subjects when the elbow joint angle was 90º and the shear modulus of biceps brachii muscle was measured using MRE. Linear regression was performed on the relationship between shear modulus and weight loads among 5 male subjects (age: 18 – 55). The slope values were from 7.9 ± 0.4 kPa/kg to 34.0 ± 3.5 kPa/kg. However, the method using weight load as an indicator of isometric contraction level was not accurate

enough, since the length of limbs was different among the subjects and the lever of force was not counted. Thus these results can hardly be compared with ours.

5.3.1 Previous Studies Based on Relative Isometric Contraction Levels

Our results demonstrated that the stiffness of the VI muscle along the direction of muscle action was positively correlated to the relative muscle contraction level (% MVC) at two different knee joint angles and in the full range of isometric contraction. Some previous studies have been reported about the positive correlation between the muscle stiffness and the non-fatiguing muscle contraction level on different muscles.

For the VM muscle, the shear modulus values measured under a contraction of 20% MVC using 2D MRE and 1D MRE were 9.22 ± 1.29 kPa and 9.52 ± 2.74 kPa, while the values in the relaxed position were 4.36 ± 0.98 kPa and 3.69 ± 0,80 kPa, respectively (Bensamoun et al., 2008). In another MRE study by Bensamoun et al. (2006), the reported shear modulus values of the VL and VM were 6.11 ± 1.15 kPa and 4.83 ± 1.68 kPa when the subjects were asked to contract their thighs at 10% MVC. With a contraction of 20% MVC, the shear modulus values of the VL and VM were reported to be 8.49 ± 4.02 kPa and 6.40 ± 1.79 kPa，respectively. They also reported that the shear modulus values of VL and VM at relaxed condition were 3.73 ± 0.85 kPa and 3.91 ± 1.15 kPa. Their results showed a significant increase ($p < 0.05$) in the shear modulus of VL and VM muscles with the increase of % MVC (Bensamoun et al., 2006).

Since the subjects in their studies were young males and young females (but were not distinguished), for a comparison, the averaged shear modulus values of the VI muscle of the young male subjects at 10% MVC in our study were 88.5 ± 53.8 kPa at 90º knee

joint angle and 46.7 ± 18.2 kPa at 60º knee joint angle, and for the young female subjects, the values were 152.9 ± 92.5 kPa at 90º knee joint angle and 93.4 ± 30.9 kPa at 60º knee joint angle. At 20% MVC, the corresponding shear modulus values were 69.8 ± 31.5 kPa, 37.7 ± 14.0 kPa for the young males, and 138.7 ± 54.6 kPa and 68.5 ± 33.8 kPa for the young females, respectively. As mentioned in the Section 5.2, since the structure of VI muscle is different from those VL and VM muscles, their stiffness is different even under the same contraction conditions. Furthermore, the position of the subjects in their studies was supine and the knee joint angle was 30º, which were both different from the conditions in our study, the muscle contraction strategies would also be different. Thus it was hard to compare the shear modulus values they measured with ours. However, our conclusion of a significant increase of muscle stiffness with the increase of isometric contraction level from 10% to 20% MVC is in good agreement with their finding.

5.3.2 Previous Studies Based on Absolute Torques

It was demonstrated in this study that the shear modulus of the VI muscle along the direction of muscle action was also positively correlated to the absolute torques. Some previous studies have reported the shear modulus measured under different absolute torques of joint extensors or flexors, but not on the quadriceps femoris muscle

Several studies have been reported to assess the stiffness of distal leg muscles, such as TA, MG, LG and SL, as groups of agonist and antagonist. The muscle shear modulus was measured under isometric contraction when the subject resisted ankle plantar-flexing and dorsi-flexing moments, of which the directions of applied moments were opposite. In the study of Heers et al. (2003) using MRE method, the shear

modulus in the TA increased significantly ($p < 0.0001$) from 70.6 ± 1.8 kPa to 126.6 ± 5.1 kPa as the plantar-flexing moment increased from 8.2 Nm to 16.4 Nm. On the other hand, the shear modulus measured in the posterior muscles, i.e. the MG, LG and SL, did not show significant changes ($p > 0.05$). In addition, as dorsi-flexing loads increased from 20.2 Nm to 40.4 Nm, shear modulus increased significantly from 41.6 ± 5.1 kPa to 63.2 ± 5.1 kPa in the MG ($p < 0.01$), from 27.6 ± 1.1 kPa to 73.1 ± 7.3 kPa in the LG ($p < 0.003$), and from 36.0 ± 0.4 kPa to 65.6 ± 1.8 kPa in the SL ($p < 0.001$) as the muscles resisted the dorsi-flexing moment of the plate. However, the shear modulus measured in the TA did not change with load ($p > 0.05$). A similar study was performed by Jenkyn et al. (2003) on the distal leg muscles. Shear modulus of relaxed TA and LG with the foot in neutral was 12.4 ± 0.5 kPa and 22.1 ± 0.2 kPa, respectively. Shear modulus of TA increased to 133.7 ± 2.1 kPa during a 16 Nm dorsi-flexing effort, but was relatively unchanged during a 48 Nm plantar-flexing effort (30.1 ± 0.5 kPa). Shear modulus of LG decreased slightly during a 16 Nm dorsi-flexing effort (15.0 ± 0.3 kPa), but significantly increased with a 48 Nm plantar-flexing effort (140.4 ± 0.3 kPa).

Since the muscles they studied were different with ours, their measured shear modulus values based on the absolute isometric contraction torques could not be directly compared with ours. However, our result of the relationship between the increasing muscle stiffness and the increasing absolute torques was the same as theirs.

5.3.3 Regression Analysis of the Relationship between Muscle Stiffness and Activity

Our results showed that in the full range of isometric contraction, the stiffness of VI muscle along the direction of muscle action was positively correlated to both the relative contraction level (% MVC) and the absolute torques (Nm). The above two

relationships were both close to be quadratic curves. In previous studies, the results of regression analysis were mostly reported as a linear relationship (Levinson et al. 1995; Dresner et al., 2001). However, they only measured the muscle shear modulus with 3 or 5 isometric contraction levels. Furthermore, their results were also limited by the relatively small measurement range of the methods they used. It is well known that, a small range of the quadratic curve can be treated as being linear. That might be the reason for the different conclusions between theirs and ours. In addition, from the results reported by Nordez et al., (2010), the relationship between the shear modulus of biceps brachii muscle and the isometric contraction torques seemed to be similar to a quadratic curve. However, they didn't perform a quantitative regression analysis, hence it was difficult to compare theirs results with ours.

5.3.4 Previous Studies Based on Muscle EMG Activity

In this study, a high correlation was observed between the mean shear modulus values of VI muscle and the normalized RMS values of surface EMG obtained on VL muscle. The relationship was close to a quadratic polynomial curve.

Since VI muscle lies between VL and VM muscles and right under the RF muscle, surface EMG can be hardly collected directly from it. Few studies have been reported to collect EMG from VI muscle, including using surface EMG or fine wire EMG. Watanabe et al. (2008) reported that they had successfully collected the surface EMG from the distal region of the VI muscle. However, the surface region of VI is very small and the EMG signal was recorded from the distal end of a muscle near the joint but not the muscle belly, which would affect the amplitude and frequency of the collected signals. In addition, the surface EMG is sensitive to the location of electrodes (Ramirez

et al., 2008). This makes it difficult to compare the results of their studies to those obtained in our study. We found that sometimes the EMG signal recorded from VL muscle was assumed to be representative for the VI muscle activity (Nene et al., 2004; Byrne et al., 2005). Since the vasti muscles, including VI, VL and VM, work in unison and the amount of fusion between VI and VL was reported up to be 60% to 77% (Willan et al., 2002), it is reasonable to use the activity of VL muscle to represent the activity of VI muscle in our study. Further studies are necessary on how to more accurately measure the EMG signal for VI muscle.

Comparison between the muscle stiffness and the surface EMG signals has been made in previous studies. In the study of Nordez and Hug (2010) using SSI method, a linear relationship was demonstrated between the biceps brachii muscle shear modulus and the corresponding EMG activity level. During an increasing ramp type isometric contraction, shear modulus was estimated simultaneously with the measurement of surface EMG for two trials. The shear modulus estimated at 3% and 7% of the maximum EMG activity (by RMS values) was 21.7 ± 6.7 kPa (3%, trial 1), 23.2 ± 7.2 kPa (3%, trial 2) and 42.6 ± 14.1 kPa (7%, trial 1), 44.8 ± 15.8 kPa (7%, trial 2), respectively. A significant main effect of muscle contraction intensity ($p < 0.01$) was found, indicating that the shear modulus was higher at 7% of the maximum EMG activity than that at 3% EMG activity. However, the range of activity used in this comparison was limited to 30% of the maximum EMG activity. The muscle recruitment strategies of ramp type isometric contraction they used might differ from the step type that we used in this study (Sanchez et al., 1993). In another study of Heers et al. (2003) using MRE method, it was reported that changes in the EMG activity and muscle stiffness with different loads were linearly related for the distal leg muscles (TA, MG,

LG and SL). However, they only used three different loads (0, 8.2 Nm and 16.4 Nm for plantar-flexion and 0, 20.2 Nm and 40.4 Nm for doris-flexion) to indicate different muscle isometric contraction level and thus the results may not be accurate enough. In addition, the corresponding relative EMG activity level, which was expressed as the percentage of the maximum EMG RMS value, was mostly not larger than 40% (only for SL, the upper limit of EMG activity level was 63.5 ± 44.1%; for TA, 33 ± 11.8%; for MG, 27.4 ± 13.7%; for LG, 23.1 ± 15.5%). Their result of the highly positive correlation between the muscle stiffness and the relative EMG activity level was the same as ours. However, the linear relationship they reported was different from the quadratic relationship we observed. This different result may be caused by two reasons: (1) In a lower and smaller range of contraction level, the relationship of the two signals may be closer to linear rather than quadratic; (2) The different muscles studied in the two studies may behave differently. Moreover, we also found that, at 60º knee joint angle, the fitting curves were closer to be linear than the curves at 90º knee joint angle. The reason for this phenomenon should be further studied. Furthermore, the differences of muscle stiffness change under different contraction types, such as ramp and step types, should be further investigated.

The estimation of the force exerted by a specific muscle has important meaning in both biomechanical studies and clinical applications (Nordez and Hug, 2010). However, it cannot be directly measured *in vivo*. Several mathematical models based on EMG signal have been developed to estimate the muscle stress (Disselhorst-Klug et al., 2009; Erdemir et al., 2007). Nevertheless, their accuracy was affected by various physiological or non-physiological factors (Farina et al., 2004). Our results indicate that the muscle shear modulus had potential to be used to estimate the muscle activity level

or muscle stress, in addition to the traditional method using surface EMG. However, the accuracy of this kind of indirect estimation method needs to be further tested in future studies.

5.3.5 Previous Studies Based on Different Joint Angles

In our study, the results of the mean MVC torque values of different knee joint angles showed that, the MVC torque values measured at 90º knee joint angle were larger than those measured at 60º ($p = 0.001$). This result was in agreement with the results of previous studies (Altenburg et al., 2009; Papadopoulos et al., 2008; Ruiter et al., 2008; Suter and Herzog, 1997).

We also found that the mean value of muscle shear modulus under step isometric contraction at 90º knee joint angle was larger than that measured at 60º ($p < 0.001$). Furthermore, for the two factors interaction of joint angles vs. % MVC, with the increase of % MVC, differences between the muscle shear modulus measured at 90º knee joint angle and those measured at 60º increased. This indicated that, the influence of knee joint angle on the muscle stiffness was larger for higher isometric contraction levels compared with the lower levels. Few studies have been reported to investigate the relationship between the VI muscle shear modulus and the knee joint angle, especially under different step isometric contraction levels. However, EMG activity of VL muscle has been studied with different knee joint angles and the results can be used as a reference. Suter and Herzog (1997) studied the EMG activity of the VL muscle at 15º, 30º, 45º, 60º and 90º knee joint angles (0º for full extension). They reported that muscle activity measured as the RMS values of the EMG of VL was the same for four out of the five knee joint angles. Only at the knee joint angle of 90º, the RMS values were

significantly higher than those of other angles. However, some other studies indicated that at a joint angle where the MVC torque value was relatively larger, the corresponding EMG activity was also relatively larger (Ruiter et al., 2008; Altenburg et al., 2009). Considering the highly positive correlation between the muscle stiffness and the EMG activity observed in our study, our results about the VI muscle stiffness at different knee joint angles was considered to be reasonable.

Furthermore, similar as described in Section 5.2, the reason for larger muscle stiffness at 90º knee joint angle might be also related to the larger passive stretching on the VI muscle compared with the passive stretching at 60º knee joint angle. On the other hand, the morphological changes with different joint angles might also contribute to the knee joint angle dependence of the VI muscle stiffness. However, all these hypotheses should be further tested in future studies.

5.3.6 Other Issues on the Relationship between Muscle Stiffness and Activity

All the previously reported methods of muscle shear modulus assessment were restricted by the limitation of their measurement range. No study has been conducted at a contraction level larger than 50% MVC. Acceptable quantitative results of MRE can be only achieved under approximately 20% level (Bensamoun et al., 2008). At higher levels, the SNR of MRE images was significantly reduced due to the long acquisition time and muscle fatigue. The SSI method also had the similar limitation and its measured shear modulus values saturated at 100 kPa (Nordez and Hug, 2010; Shinohara et al., 2010). However, this gap was now filled by our newly developed vibro-ultrasound method. With a frame rate up to 4.6 kHz for a measurement depth of 65 mm and using the 15 mm distance apart from the two ultrasound scan lines for the

shear wave propagation，we achieved a theoretical upper limit of shear wave velocity up to 69 m/s. The theoretical upper limit for the shear modulus measurement was larger than 4000 kPa, which can fully satisfy the requirement of muscle stiffness assessment at high isometric contraction levels, even up to 100% MVC. In addition, the data acquisition of our method was almost instantaneous, thus the fatigue issue could be avoided even at a 100% MVC level.

Our study has successfully extended the range of shear modulus measurement to 100% MVC and provided a full picture of the relationship between the muscle stiffness and the muscle isometric contraction activity. However, the deviations of the muscle shear modulus at the levels larger than 60% MVC showed an increasing trend among any groups of the subjects. It may be related to several possible reasons. First, during a high intensity contraction, changes of the structure, location and orientation of the VI muscle may be large enough to affect the muscle shear modulus results. Particularly, changes in the pennation angle, fascicle length and anisotropy of the contracted muscle may produce complicated effects on the shear wave propagation pattern and the measured shear wave velocity. To reduce the effects of human body motions during the high intensity muscle contraction in this study, besides fixing the subject's leg on the dynamometer, the vibrator and the transducer were also rigidly fixed, and the subject's body was fixed on the chair with straps restricting the movement of waist and shoulders. However, the gliding motions of muscle fibers under the skin were not able to be avoided during contraction particularly under high contraction levels. Another possible reason may be that, the shear wave velocity increased dramatically at high intensity contraction levels, thus the measured time delay values became much smaller in comparison with those at relaxed condition. Since the time resolution was limited by the

frame rate of the ultrasound signals, the experimental error would increase at high intensity isometric contraction levels. However, this trend of larger deviations under high contraction levels might also be caused by the inherent property of VI muscle itself. For maintaining the high intensity isometric contraction, the dynamic range of muscle activity level within this period would also increase and subsequently cause the increase of the deviations in the results. Further studies are required to investigate whether these larger deviations were due to the inherent property of the muscle or caused by the limitation of our assessment system.

5.4 Gender Dependences of the Relationship between Muscle Stiffness and Step Isometric Contraction

The mean MVC torque values obtained from different genders with different knee joint angles showed that the MVC torque values of males were larger than females ($p < 0.001$). This result was in agreement with those of many previous studies (Granata et al., 2001; Ochala et al., 2004; Staron et al., 2000; Uffmann et al., 2004).

It was found that, at both knee joint angles, there was no significant main effect of gender ($p > 0.5$) on the muscle shear modulus at relaxed condition. However, when performing the step isometric contraction, the effect of gender factor was significant. The estimated marginal mean value of males was larger than that of females ($p < 0.001$). On the other hand, by comparing the trends of the relationship between the muscle shear modulus and the absolute torque values of the two genders, it was found that the shear modulus of females increased faster than that of males under the same

knee joint angle. However, this relationship was opposite to the relationship between the muscle shear modulus and the relative contraction levels (% MVC).

Muscle stiffness links both the primary functions of skeleton muscle, force generation and body movements. The gender difference of muscle stiffness may also contribute to the sex discrepancy of ACL injury, such as the other mechanical factors including muscular strength and tendon stiffness (Aune et al., 1996; Padua et al., 2005; Withrow et al., 2006). However, rarely study has been performed to investigate this relationship. Our vibro-ultrasound method has a potential to be used to provide additional information about the reasons for the higher risk of ACL injury among females. Nevertheless, further experimental studies or model calculations are needed for this purpose.

The gender dependences of the muscle stiffness in relaxed and step isometric contraction conditions have been rarely studied using methods based on shear wave velocity measurement, such as MRE or SSI. Uffmann et al. (2004) measured the stiffness of four different muscles (biceps brachii, the flexor digitorum profundus, the soleus and the gastrocnemius) at relaxed condition on 8 young male and 4 female subjects using MRE. They reported that the comparisons between females and males did not reveal statistically significant differences for any muscles. Our result agreed well with theirs. In addition, two other methods have often been used to evaluate the muscle stiffness in the muscle-tendon structure or in the muscle-joint structure, i.e. measuring the musculotendinous stiffness using quick-release movement method or measuring the musculoarticular stiffness using sinusoidal perturbations method. Although these methods cannot provide numerical values of elastic modulus, they are simple and relatively accurate methods for estimating effective stiffness. The slopes of

the linear relationship of stiffness vs. absolute torque were defined as stiffness indexes: SI_{MT} and SI_{MA}, respectively (Blackburn et al., 2003; Granata et al., 2001; Ochala et al., 2004). They were reported to be both higher in elderly females than elderly males for the plantar flexor muscles (Ochala et al., 2004). Furthermore, their results showed that the musculotendinous and musculoarticular stiffness were both higher in females than those in males at the same absolute torque value. In another study of Blackburn et al. (2003), young males showed higher active stiffness for the knee flexor, evaluated by the sinusoidal perturbations method with a load of 10% body mass. The simultaneously collected EMG signal proved that this load was a relatively similar activity level from a neural perspective, corresponding to 26% and 31% of the maximum EMG activity in males and females, respectively. The relationship between muscle stiffness and relative isometric contraction levels obtained in this study was in agreement with theirs. Granata et al. (2001) found that at 0% and 20% MVC levels, the musculoarticular stiffness of quadriceps muscles and hamstring muscle in young males was larger than that in young females. This result also echoed with our findings in this study. However, from the scatter figures of musculoarticular stiffness vs. absolute joint torque reported by Granata et al. (2001), the stiffness was slightly higher for males than that for females at the same torque value, which was opposite to our findings. This difference may result from the differences in methodology, sample size or physical activity condition of the subjects in the studies. Blackburn et al. (2006, 2009) performed two similar studies on the triceps surae muscle and the hamstring muscle using perturbations method to assess the musculoarticular stiffness and calculated the Young's modulus using additional morphology parameters and a mathematical model developed by themselves. The load they used was 10% body mass. They found the results were different for different muscles. For both muscles, the musculoarticular stiffness was greater in males than in

females. For triceps surae muscle, the Young's modulus was greater in males than in females, and this result was in agreement with ours. But for hamstring muscle, they found there was no significant difference between the Young's moduli of males and females. Their results indicated that for different muscles, the gender dependence of the relationship of muscle stiffness and relative contraction level may be not the same.

The results of musculotendinous stiffness which looks the muscle and tendon as a whole structure are more valuable to us for reference than the musculoarticular stiffness. In humans, the stiffness of tendon structures in females has been found to be significantly lower than that in males (Kubo et al., 2003). Consequently, the higher musculotendinous stiffness observed in females would mainly originate from the active stiffness of muscle fibers. On the other hand, for the results of musculoarticular stiffness, when the two components of knee joint stiffness were compared, i.e. stiffness from active muscle recruitment and stiffness from passive joint structures, the active muscles were the dominant component (Crisco et al., 1991). Thus the results of musculoarticular stiffness could also have values for us to refer to.

Gender differences on morphology parameters may be one of the reasons for the different muscle stiffness between males and females when performing isometric contraction. Previous research reported that the muscle mass and the cross-sectional area were greater in males than in females (Miller et al., 1993; Staron et al., 2000). In addition, females were found to have longer muscle fiber length and males have thicker muscles and larger pennation angles (Chow et al., 2000). However, these geometric factors would result in a complex relationship with muscle stiffness and the detailed influence of morphology parameters on the muscle stiffness is still unclear. The detailed causal connections between them need to be further studied.

Another possible reason is the gender difference of fiber type distribution. Although the fiber type distribution of VI muscle has been seldom studied, VL muscle has been widely studied in previous studies. However, conflicting results have been reported. In some studies, the differences of muscle fiber type distribution between young male and female subjects were found to be not significant for type I fibers (Gollnick et al., 1972; Glenmark et al., 1992; Oertel 1988; Staron et al., 2000), for type IIa fibers (Glenmark et al., 1992; Simoneau and Bouchard, 1989; Simoneau et al., 1985; Staron et al., 2000) and for type IIb fibers (Essen-Gustavsson and Borges, 1986; Glenmark et al., 1992; Simoneau et al., 1985; Staron et al., 2000). However, in other studies, the distribution of type I fibers of males was reported to be larger (Essen-Gustavsson and Borges, 1986; Komi and Karisson, 1978) or smaller than that of females (Simoneau and Bouchard, 1989; Simoneau et al., 1985). For type IIa fibers, the distribution of males was also reported to be smaller than that of females (Essen-Gustavsson and Borges, 1986). And for type IIb fibers, the distribution of males was reported to be larger compared with females (Simoneau and Bouchard, 1989). However, the cross-sectional area of all three fiber types was found to be larger for males compared to females (Simoneau and Bouchard, 1989; Staron et al., 2000). In addition, the area of type IIa fibers was found to be the larger for males, whereas the area of type I fibers tended to be larger for females (Simoneau and Bouchard, 1989; Simoneau et al., 1985; Staron et al., 2000). As mentioned in Section 2.1.6, the slow-twitch (type I) and fast-twitch fibers (type II) have different stiffness characteristics. For instance, in rats, type I fibers have been observed to be stiffer than type II fibers when generating the same active contraction force (Toursel et al., 1999). Therefore, the greater area occupied by type I fibers in females and the greater area occupied by type II fibers in males (Simoneau and Bouchard, 1989; Simoneau et al., 1985; Staron et al., 2000) can at least partially explain the higher

muscle stiffness in females than in males at the same absolute torque value. And gender differences in muscle stiffness may also be related to the gender differences in hormone concentration (Blackburn et al., 2003).

5.5 Age Dependences of the Relationship between Muscle Stiffness and Step Isometric Contraction

Analysis of the age dependences of the mean MVC torque values at different knee joint angles revealed that the MVC torque values of young subjects were larger than those of the elderly subjects ($p = 0.01$). The same result has been reported by many previous studies (Abernethy et al., 2005; Karamanidis and Arampatzi, 2006; Karamanidis et al., 2008; MacIntosh et al., 2005; Ochala et al., 2004).

Our results showed that, at both knee joint angles, there was no significant effect of age (both $p > 0.1$) on the muscle shear modulus at relaxed condition. However, when performing step isometric contraction, the effect of age factor was significant. The estimated marginal mean value of young subjects was larger than the value of the elderly participants ($p < 0.001$). Furthermore, the two-way interaction effects of age vs. % MVC and age vs. angles were significant (both $p < 0.001$). For age vs. % MVC, with % MVC increasing, the difference between the muscle shear modulus of young subjects and that of the elderly subjects became larger. This indicated that at higher isometric contraction levels, the age difference of muscle active stiffness was larger. For age vs. angles, the difference between the muscle shear modulus of the two knee joint angles was larger in the young subjects compared with the elderly subjects. This suggested that the influence of knee joint angle on the muscle stiffness was larger for the young

subjects than for the elderly subjects. On the other hand, by comparing the trends of muscle shear modulus vs. absolute torque values with different age and same gender, it was showed that the shear modulus values of the young subjects increased faster than the elderly subjects at the same knee joint angle. This relationship was the same as the relationship between the muscle shear modulus and the relative muscle contraction levels (% MVC).

Previous studies on the age differences of muscle stiffness in relaxed and step isometric contraction conditions have been even rarer than those on the gender differences. Domire et al. (2009) measured the stiffness of tibialis anterior muscle using MRE at a relaxed condition on 20 female subjects with an age range of 50 to 70 years. They found that there was no significant relationship between age and muscle shear modulus. This is in agreement with our results. Musculotendinous stiffness and musculoarticular stiffness have also been widely used to study the age difference of muscle stiffness. The stiffness index, SI_{MT}, was found to be higher for elderly subjects than for young ones for the plantar flexor muscles, whereas SI_{MA} was not significantly different between two groups with different ages (Ochala et al., 2004). The stiffness values of their study were measured at 20 %, 40%, 60% and 80% MVC levels. From the figures they published, it was clearly shown that the musculotendinous stiffness of elderly subjects was smaller than that of young subjects when measured at the same relative isometric contraction level. Although it was reported that the stiffness of tendon structures in elderly subjects was significantly lower than that in young subjects (Karamanidis and Arampatzi, 2006; Karamanidis et al., 2008; Narici et al., 2005), this result of reduced musculotendinous stiffness due to muscle ageing is still valuable as a reference for our study and also in agreement with our results. In addition, there are many other studies which focused on

the structure stiffness of knee joint or whole leg when performing a special gait, such as fast/slow walk, upward/downward stepping, etc (Cenciarini et al., 2010; DeVita et al., 2000; Hoffren et al., 2007; Hsu et al., 2007; Wang et al., 2008). Since under these conditions, the contraction level of a single muscle could not be exactly examined, it was difficult to compare their results with ours. However, some of their findings were useful to explain our results, such as the age difference of muscle coactivation level.

The age differences of morphology factors are related to the sarcopenia caused by muscle ageing process and have been studied by many previous studies. Corresponding to the loss of muscle strength, the muscle size estimated from the muscle CSA has also been proved to be about 20% smaller in older adults compared to young adults (Klein et al. 2001; Narici et al. 2003). In addition, Lexell et al. (1983) found that the VL muscle of elderly men contained about 25% fewer fibers than the corresponding muscle of young men. Furthermore, muscle ageing also leads to marked alterations in muscle architecture that potentially contributes to strength loss. Muscle fascicle lengths and pennation angles in elderly individuals were reported to be significantly smaller than those in younger adults (Morse et al., 2005; Narici et al., 2003; Narici et al., 2008). However, few studies were performed to evaluate the relationship between the changes of these morphology factors and muscle stiffness. The influence of sarcopenia on the muscle stiffness should be further studied in the future.

Larsson et al. (1978) found that the relative percentage of type I fibers increased with ageing and the fiber atrophy was most pronounced for type II fibers. As mentioned in Section 5.4, it was reported that type I fibers were stiffer than type II fibers when generating the same active contraction force (Toursel et al., 1999). Therefore, the increasing percentage of type I fibers in elders should make the muscle stiffer in

comparison with the young people when performing the same absolute contraction torque. However, this is opposite to the result we observed in our study. The reason may be related to the increasing muscle coactivation level for the elders. The level of muscle coactivation has been observed increasing with age. In the elders, the EMG activity, i.e. the neural driving activity, was found to be reduced in agonist muscles and increased in antagonist muscles (Hortobagyi et al., 2000; Klein et al., 2001). And in a recent study, muscle coactivation in elderly adults was reported to be increasing, independent of the different muscle groups and the types of muscle contraction (Hortobagyi et al., 2009). The coactivation can increase the joint stability and safety to compensate for the reduction of muscle strength in elderly adults (Ochala et al., 2004). For knee joint extensor, quadriceps muscles act as agonist and hamstring act as antagonist. Hence in our study, when the elderly subjects performed the knee extension with the same absolute torque, the EMG activity level of their VI muscle, one of the quadriceps muscles, would be smaller compared with the young subjects. Since the muscle stiffness has a positive correlation with the EMG activity, which has been proved by the results of our study and several previous studies, reduction in the neural activity of a special muscle would decrease its stiffness during contraction. These two competing factors, i.e. the increasing distribution of type I fibers and the increasing muscle coactivation, result in a complex relationship between the muscle stiffness and the sarcopenia caused by muscle ageing process. According to our result that the VI muscle stiffness of young subjects was larger than that of the elderly subjects at the same absolute torque value, the effect of increasing coactivation may play a dominant role in this process. In addition, the age dependence in muscle stiffness may also be associated with the age differences in hormone concentration. Further studies are required to better understand the effects of different factors contributing to the ageing effects of muscle stiffness.

5.6 Summary

In this chapter, discussion has been made on the advantages and limitations of our newly developed vibro-ultrasound method for muscle stiffness assessment, and on the relationship between VI muscle stiffness and the relative muscle isometric contraction level (in a full range from 0% to 100% MVC), and also the trend of the relationship between VI muscle stiffness and the absolute torque of knee extensor. The gender and age dependences of these relationships have also been discussed and compared with the results of previous studies. Possible reasons leading to these results have been explored in detail. Important findings obtained in this study, limitations of the experiment and suggested future works will be introduced in the next chapter.

CHAPTER 6 CONCLUSIONS AND FUTURE STUDIES

6.1 Conclusions

In this study, a new vibro-ultrasound method for muscle shear modulus measurement was developed and evaluated on phantoms, and then applied for *in vivo* tests on human subjects. For the first time, the relationship between VI muscle stiffness and the relative isometric contraction level was studied in a full range, i.e. from 0% to 100% MVC. The gender, age and knee joint angle dependences of this relationship were also investigated. Furthermore, the trends of the relationship between VI muscle stiffness and the absolute torque values of knee extensor were also compared between subjects with different genders, different age ranges and two knee joint angles. The correlation between VI muscle stiffness and the RMS of EMG signal obtained from VL muscle was also studied. The findings of this study are summarized as follows.

1. A new vibro-ultrasound method for muscle stiffness measurement was successfully developed and evaluated. It provided, for the first time, the measurement of muscle shear modulus for a full range of isometric contraction, from 0% to 100% MVC. This new system had potential to be a unique tool for muscle assessment in research and clinical applications.

2. For the first time, the positive correlation between the shear modulus of VI muscle and the relative isometric contraction level (% MVC) of the knee extensor, as well as the positive correlation between the shear modulus of VI muscle and the absolute contraction torque (Nm) of the knee extensor, were verified in a full range of isometric contraction. Both the relationships were proved to be close to quadratic polynomial

curves. These results can help us to better understand the muscle function and recruitment strategies under step type isometric contraction.

3. The positive correlation between the shear modulus of VI muscle and the normalized EMG RMS value obtained from VL muscle was verified in a full range of isometric contraction. The relationship was found to be close to a quadratic polynomial curve. These results indicated that the muscle shear modulus had potential to be used as an index for the muscle activity level or muscle stress, in addition to the traditional method using surface EMG.

4. The shear modulus of VI muscle measured at 90º knee joint angle was found to be larger than that measured at 60º knee joint angle in a full range of isometric contraction. It was also observed that the effect of knee joint angle on the shear modulus of VI muscle was larger under high contraction levels. These results provided a new perspective to further investigate the effects of different joint angles on the muscle structure and the recruitment strategies of muscle contraction.

5. There was no significant difference between the muscle shear moduli of the male and female subjects at relaxed condition. However, when performing the step isometric contraction, the muscle shear modulus of males was found to be larger than that of females measured at the same % MVC. On the other hand, for the relationship between the muscle shear modulus and the absolute torque, the muscle shear modulus of females increased faster than that of males. Studying the gender dependences of muscle shear modulus could provide additional information to understand better the reasons for the higher risk of anterior cruciate ligament (ACL) and cartilage injury among females.

6. No significant difference was observed between the muscle shear moduli of the subjects with different age ranges at relaxed condition. However, when performing the step isometric contraction, the muscle shear modulus of young subjects was found to be larger than that of the elderly subjects measured at the same % MVC. For the relationship between the muscle shear modulus and the absolute torque, the muscle shear modulus of young subjects increased faster when compared with the elderly subjects. Investigating the age dependences of muscle shear modulus would be useful for us to better understand the cause and process of muscle ageing.

6.2 Further Studies

Based on the findings of the present study, it is necessary to further improve our methods in some aspects, and to conduct more experiments to comprehensively assess the relationship between the stiffness and other properties of specific muscles. The effects or influences of the muscle stiffness on the muscle functions should be also included in future studies.

1. To improve the vibro-ultrasound method

Although the current vibro-ultrasound method could provide successful muscle stiffness measurement under a full range of muscle contraction levels with satisfying reliability and intra-observer repeatability, it still had some limitations. In the preliminary study, it was observed that, the echo-tracking results showed some wave patterns not good enough for further analysis when a muscle with small dimension or complex structure was measured. This might be caused by the multiple reflection and refraction phenomena at the interface of different tissues. The solution to this problem is to further

increase the frame rate of ultrasound acquisition system, and accurately control the position, frequency and amplitude of the shear wave generated in the soft tissue. Another limitation was that the current system could not provide the estimation of viscosity modulus simultaneously with the elastic shear modulus. Although along the direction of muscle action the shear wave propagation is practically non-dispersive and does not affect our current results according to the results of previous studies (Catheline et al., 2004; Deffieux et al., 2009), the viscosity evaluation is still important, especially for other kinds of soft tissues. Therefore, different excitation frequency of the vibration may be used in future studies to extract the viscosity as well.

2. The relationship between muscle stiffness and relative isometric contraction level or absolute torque value

Our results provided a whole picture of the relationship between the muscle stiffness and the relative isometric contraction level (% MVC) in a full range. However, the deviations of the muscle shear modulus at the levels larger than about 60% MVC showed an increasing trend for all the groups of subjects. The reason for the increasing deviations needs to be further studied. In the current study, only two knee joint angles were included in the tests. More experiments are required to be performed at other knee joint angles. In addition, how these factors, i.e. knee joint angle, gender and age, would influence the muscle stiffness at relaxed condition and different isometric contraction levels should be further investigated, e.g. with simultaneous measurement of some morphology characteristics using B-mode ultrasound images.

3. More comparison between the muscle stiffness of different kinds of groups of subjects

Using our method, more comparisons in the muscle stiffness among different groups of subjects can be performed, e.g. well-trained athletes vs. those without or with little physical training. In addition, for patients with some muscle diseases such as the sarcopenia and the muscle atrophy caused by stroke, some rehabilitation programs are desired to assess their recovering. Our method had potential to be used to evaluate the effectiveness of these treatments. Further collaboration between our new technology and clinical practice will be a very important task in the future.

4. Combination of the muscle stiffness measurement with sonomyography (SMG)

Our another aim is to provide real-time muscle stiffness values simultaneously with the sonomyography (SMG) signals, which are the sonographically detected signals of the morphology change of muscles. A system which can record and analyze ultrasound images, force/torque, joint angle and surface EMG simultaneously has been successfully used in several previous studies. By combining the muscle stiffness measurement device into the existing SMG system can provide more information about the functions of skeleton muscles, and help us to further understand the recruitment strategies of different types of muscle contraction.

REFERENCES

Abernethy B, Mackinnon S, Kippers V, Hanrahan S, Pandy M. The biophysical foundations of human movement. 2nd ed. Champaign, IL: Human Kinetics, 2005; 169-196.

Akataki K, Mita K, Itoh K, Suzuki N and Watakabe M. Acoustic and electrical activities during voluntary isometric contraction of biceps brachii muscles in patients with spastic cerebral palsy. Muscle and Nerve 1996; 19:1252-7.

Akataki K, Mita K, Watakabe M and Itoh K. Mechanomyogram and force relationship during voluntary isometric ramp contractions of the biceps brachii muscle. European Journal of Applied Physiology 2001; 84:19-25.

Akasaka K, Onishi H, Momose K, Ihashi K, Yagi R, Handa Y and Hoshimiya N. EMG power spectrum and integrated EMG of ankle planterflexors during stepwise and ramp contractions. Tohoku Journal of Experimental Medicine 1997; 182:207-16.

Al-Assaf Y. Surface myoelectric signal analysis: Dynamic approaches for change detection and classification. IEEE Transactions on Biomedical Engineering 2006; 53: 2248-56.

Alkner BA, Tesch PA, and Berg HE. Quadriceps EMG/force relationship in knee extension and leg press. Medicine and Science in Sports and Exercise 2000; 32: 459-463.

Altenburg TM, de Haan A, Verdijk PWL, van Mechelen W, and de Ruiter CJ. Vastus lateralis single motor unit EMG at the same absolute torque production at different knee angles. Journal of Applied Physiology 2009; 107: 80-89.

Andrade AS, Gaviao MBD, Derossi M and Gameiro GH. Electromyographic activity and thickness of masticatory muscles in children with unilateral posterior crossbite. Clinical Anatomy 2009; 22: 200-6.

Arampatzis A, Karamanidis K, and Mademli L. Deficits in the way to achieve balance related to mechanisms of dynamic stability control in the elderly. Journal of Biomechanics 2008; 41: 1754-1761.

Arts IMP, Pillen S, Schelhaas HJ, Overeem S, Zwarts MJ. Normal Values For Quantitative Muscle Ultrasonography in Adults. Muscle & Nerve. 2010; 41:32-41.

Arendt-Nielsen L, Gantchevb N and Sinkjæra T. The influence of muscle length on muscle fiber conduction velocity and development of muscle fatigue. Electroencephalography and Clinical Neurophysiology 1992; 85: 166-172

Aune AK, Nordsletten L, and Ekeland A. Structural capacity of the knee to anterior cruciate ligament failure during quadriceps contraction. An in vivo study in the rat. Journal of Biomechanics 1996; 29: 891-897.

Basford JR, Jenkyn TR, An KN, Ehman RL, Heers G, Kaufman KR. Evaluation of healthy and diseased muscle with magnetic resonance elastography. Archives of Physical Medicine and Rehabilitation 2002; 83: 530-1536.

Beck TW, Housh TJ, Johnson GO, Weir JP, Cramer JT, Coburn JW and Malek MH. Mechanomyographic amplitude and mean power frequency versus torque relationships during isokinetic and isometric muscle actions of the biceps brachii. Journal of Electromyography and Kinesiology 2004; 14:555-64.

Beck TW, Housh TJ, Johnson GO, Weir JP, Cramer JT, Coburn JW and Malek MH. Gender comparisons of mechanomyographic amplitude and mean power frequency versus isometric torque relationships. Journal of Applied Biomechanics 2005; 21:96-109.

Benoit DL and Dowling JJ. *In vivo* assessment of elbow flexor work and activation during stretch-shortening cycle tasks. Journal of Electromyography and Kinesiology 2006; 16: 352-64.

Bensamoun SF, Ringleb SI, Littrell L, et al. Determination of thigh muscle stiffness using magnetic resonance elastography. Journal of Magnetic Resonance Imaging 2006; 23(2):242-247.

Bensamoun SF, Glaser KJ, Ringleb SI, Chen Q, Ehman RL, An KN. Rapid magnetic resonance elastography of muscle using one-dimensional projection. Journal of Magnetic Resonance Imaging 2008; 27(5):1083-1088.

Bernathova M, Felfernig M, Rachbauer F, Barthi SD, Martinoli C, Zelger B and Bodner G. Sonographic Imaging of Abdominal and Extraabdominal Desmoids. Ultraschall in Der Medizin 2008; 29: 515-9.

Bilodeau M, Arsenault AB, Gravel D and Bourbonnais D. EMG power spectra of elbow extensors during ramp and step isometric contractions. European Journal of Applied Physiology and Occupational Physiology 1991; 63: 24-8.

Bilodeau M, Cincera M, Arsenault AB and Gravel D. Normality and stationarity of EMG signals of elbow flexor muscles during ramp and step isometric contractions. Journal of Electromyography and Kinesiology 1997; 7: 87-96.

Blackburn JT, Riemann BL, Padua DA, Guskiewicz KM. Sex comparison of extensibility, passive, and active stiffness of the knee flexors. Clinical Biomechanics 2004; 19: 36-43.

Blackburn JT, Padua DA, Weinhold PS, Guskiewicz KM. Comparison of triceps surae structural stiffness and material modulus across sex. Clinical Biomechanics 2006; 21: 159-167.

Blackburn JT, Bell DR, Norcross MF, Hudson JD, Kimsey MH. Sex comparison of hamstring structural and material properties. Clinical Biomechanics 2009; 24: 65-70.

Blazevich AJ, Gill ND, Zhou S. Intra- and intermuscular variation in human quadriceps femoris architecture assessed *in vivo*. Journal of Anatomy 2006; 209:289-310

Bojsen-Moller J, Hansen p, Aagaard p, Kjaer M and Magnusson SP. Measuring mechanical properties of the vastus lateralis tendon-aponeurosis complex *in vivo* by ultrasound imaging. Scandinavian Journal of Medicine & Science in Sports 2003; 13:259-65.

Botteron S, Verdebout CM, Jeannet PY and Kiliaridis S. Orofacial dysfunction in Duchenne muscular dystrophy. Archives of Oral Biology 2009; 54: 26-31.

Brown SHM, McGill SA. The intrinsic stiffness of the *in vivo* lumbar spine in response to quick releases: Implications for reflexive requirements. Journal of Electromyography and Kinesiology 2009; 19:727-736.

Byrne CA, Lyons GM, Donnelly AE, O'Keeffe DT, Hermens H, and Nene A. Rectus femoris surface myoelectric signal cross-talk during static contractions. Journal of Electromyography and Kinesiology 2005; 15: 564-575.

Catheline S, Thomas JL, Wu F, Fink MA. Diffraction field of a low frequency vibrator in soft tissues using transient elastography. IEEE Transactions on Ultrasonics Ferroelectrics and Frequency Control 1999; 46(4):1013-1019.

Catheline S, Wu F, Fink M. A solution to diffraction biases in sonoelasticity: The acoustic impulse technique. Journal of the Acoustical Society of America 1999; 105(5):2941-2950.

Catheline S, Gennisson JL, Delon G, Fink M, Sinkus R, Abouelkaram S, and Culioli J. Measurement of viscoelastic properties of homogeneous soft solid using transient elastography: An inverse problem approach. Journal of the Acoustical Society of America 2004; 116:3734 – 3741.

Cenciarini M, Loughlin PJ, Sparto PJ, and Redfern MS. Stiffness and Damping in Postural Control Increase With Age. IEEE Transactions on Biomedical Engineering 2010; 57: 267-275.

Cespedes I, Huang Y, Ophir J, Spratt S. Methods for Estimation of Subsample Time Delays of Digitized Echo Signals. Ultrasonic Imaging 1995; 17: 142-171.

Chen SG, Urban MW, Greenleaf JF, Zheng Y, Yao AP. Quantification of Liver Stiffness and Viscosity with SDUV: *In Vivo* Animal Study. 2008 IEEE Ultrasonics Symposium, Vols 1-4 and Appendix 2008:654-657.

Chen SG, Urban MW, Pislaru C, et al. Shearwave Dispersion Ultrasound Vibrometry (SDUV) for Measuring Tissue Elasticity and Viscosity. IEEE Transactions on Ultrasonics Ferroelectrics and Frequency Control 2009; 56 (1):55-62.

Chen QS, Basford J, and An KN. Ability of magnetic resonance elastography to assess taut bands. Clinical Biomechanics 2008; 23: 623-629.

Chester R, Costa ML, Shepstone L, Cooper A and Donell ST. Eccentric calf muscle training compared with therapeutic ultrasound for chronic Achilles tendon pain-A pilot study. Manual Therapy 2008; 13: 484-91.

Chow RS, Medri MK, Martin DC, Leekam RN, Agur AM, McKee NH. Sonographic studies of human soleus and gastrocnemius muscle architecture: gender variability. European Journal of Applied Physiology 2000; 82: 236-244.

Cornu C, Goubel F. Musculo-tendinous and joint elastic characteristics during elbow flexion in children. Clinical Biomechanics 2001; 16: 758-764.

Cope TC and Pinter MJ. The size principle: still working after all these years, News in Physiological Sciences 1995; 10: 280-86.

Crisco JJ, Panjabi MM. The intersegmental and multisegmental muscles of the lumbar spine: a biomechanical model comparing lateral stabilizing potential. Spine 1991; 16:793–9.

De Luca CJ, LeFever RS, McCue MP and Xenakis AP. Behaviour of human motor units in different muscles during linearly varying contractions. The Journal of physiology 1982; 329:113-28.

De Luca CJ. The use of surface electromyography in biomechanics. Journal of Applied Biomechanics 1997; 13: 135-63.

De Luca CJ. Surface electromyography: detection and recording. Boston: DelSys Inc.; 2002. pp. 1-6.

De Ruiter CJ, Hoddenbach JG, Huurnink A, and de Haan A. Relative torque contribution of vastus medialis muscle at different knee angles. Acta Physiol (Oxf) 2008; 194:223-237.

De Vita P, and Hortobagyi T. Age increases the skeletal versus muscular component of lower extremity stiffness during stepping down. Journals of Gerontology Series a-Biological Sciences and Medical Sciences 2000; 55: B593-B600.

Deffieux T, Montaldo G, Tanter M, Fink M. Shear Wave Spectroscopy for *In Vivo* Quantification of Human Soft Tissues Visco-Elasticity. IEEE Transactions on Medical Imaging 2009; 28: 313-322.

Diaz JFJ, Rey GA, Matas RB, De La Rosa FJB, Padilla EL and Vicente JGV. New technologies applied to ultrasound diagnosis of sports injuries. Advances in Therapy 2008; 25:1315-30.

Disselhorst-Klug C, Schmitz-Rode T, and Rau G. Surface electromyography and muscle force: Limits in sEMG-force relationship and new approaches for applications. Clinical Biomechanics 2009; 24: 225-235.

Domire ZJ, McCullough MB, Chen QS, and An KN. Feasibility of Using Magnetic Resonance Elastography to Study the Effect of Aging on Shear Modulus of Skeletal Muscle. Journal of Applied Biomechanics 2009; 25: 93-97.

Dresner MA, Rose GH, Rossman PJ, Muthupillai R, Manduca A, Ehman RL. Magnetic resonance elastography of skeletal muscle. Journal of Magnetic Resonance Imaging 2001;13(2):269-276.

Ebersole KT, Housh TJ, Johnson GO, Evetovich TK, Smith DB, Perry SR. MMG and EMG responses of the superficial quadriceps femoris muscles. Journal of Electromyography and Kinesiology 1999; 9: 219-227.

Eiling E, Bryant AL, Petersen W, Murphy A, and Hohmann E. Effects of menstrual-cycle hormone fluctuations on musculotendinous stiffness and knee joint laxity. Knee Surgery Sports Traumatology Arthroscopy 2007; 15: 126-132.

Engelhart K, Hudgins B, Parker PA andStevenson M. Classification of the myoelectric signal using time-frequency based representations. Medical Engineering & Physics 1999; 21: 431-438

Erdemir A, McLean S, Herzog W, and van den Bogert AJ. Model-based estimation of muscle forces exerted during movements. Clinical Biomechanics 2007; 22: 131-154.

Essén–Gustavsson B, Borges O. Histochemical and metabolic characteristics of human skeletal muscle in relation to age. Acta Physiol Scand 1986; 126:107–111.

Farella M, Bakke M, Michelotti A, Rapuano A and Martina R. Masseter thickness, endurance and exercise-induced pain in subjects with different vertical craniofacial morphology. European Journal of Oral Sciences 2003; 111:183-88.

Farina D, Merletti R, and Enoka RM. The extraction of neural strategies from the surface EMG. Journal of Applied Physiology 2004; 96: 1486-1495.

Feit H, Kawai M, Schulman MI. Stiffness and Contractile Properties of Avian Normal and Dystrophic Muscle Bundles as Measured by Sinusoidal Length Perturbations. Muscle & Nerve 1985; 8: 503-510.

Ferreira PH, Ferreira ML and Hodges PW. Changes in recruitment of the abdominal muscles in people with low back pain - Ultrasound measurement of muscle activity. Spine 2004; 29:2560-6.

Fukunaga T, Kubo K, Kawakami Y, Fukashiro S, Kanehisa H and Maganaris CN. *In vivo* behaviour of human muscle tendon during walking. In: Proceedings of the Royal Society of London Series B-Biological Sciences 2001; 268: 229-33.

Fukunaga T, Ichinose Y, Ito M, Kawakami Y, and Fukashiro S. Determination of fascicle length and pennation in a contracting human muscle *in vivo*. Journal of Applied Physiology 1997; 82: 354-358.

Fung YC. Biomechanics, Mechanical Properties of Living Tissues. 2nd ed. Springer, New York, 1993; 392–424.

Gao L, Parker KJ, Lerner RM, Levinson SF. Imaging of the elastic properties of tissue - A review. Ultrasound in Medicine and Biology 1996; 22(8):959-977.

Gennisson JL, Cornu C, Catheline S, Fink M, Portero p. Human muscle hardness assessment during incremental isometric contraction using transient elastography. Journal of Biomechanics 2005; 38(7):1543-1550.

Georgiakaki I, Tortopidis D, Garefis p and Kiliaridis S. Ultrasonographic thickness and electromyographic activity of masseter muscle of human females. Journal of Oral Rehabilitation 2007; 34:121-8.

Glenmark B, Hedberg G, Jansson E. Changes in muscle fiber type from adolescence to adulthood in women and men. Acta Physiol Scand 1992; 146:251–259.

Griffiths RI. Ultrasound transit time gives direct measurement of muscle fiber length *in vivo*. Journal of Neuroscience Methods 1987; 21: 159-65.

Gollnick PD, Armstrong RB, Saubert CW IV, Piehl K, Saltin B. Enzyme activity and fiber composition in skeletal muscle of untrained and trained men. J Appl Physiol 1972; 33:312–319.

Goubel F, Marini JF. Fiber type transition and stiffness modification of soleus muscle of trained rats. Pflugers Archives 1987; 410: 321-325.

Grabiner MD, Owings TM, Pavol MJ. Lower extremity strength plays only a small role in determining the maximum recoverable lean angle in older adults. Journals of Gerontology A - Biological Sciences and Medical Sciences 2005; 60: M1447–M1450.

Granata KP, Wilson SE, Padua DA. Gender differences in active musculoskeletal stiffness. Part I. Quantification in controlled measurements of knee joint dynamics. J. Electromyo. Kinesiol 2002; 12: 119 – 126.

Guo JY, Zheng YP, Huang QH and Chen X. Dynamic monitoring of forearm muscles using 1D sonomyography (SMG) system. Journal of Rehabilitation Research and Development 2008; 45:187-96.

Guo JY, Zheng YP, Huang QH, Chen X, He JF and Chan H. Performances of one-dimensional sonomyography and surface electromyography in tracking guided patterns of wrist extension. Ultrasound in Medicine and Biology 2009; 35: 894-902.

Guo JY, Zheng YP, Xie HB, and Chen X. Continuous monitoring of electromyography (EMG), mechanomyography (MMG), sonomyography (SMG) and torque output during ramp and step isometric contractions. Medical Engineering & Physics 2010; 32: 1032-1042.

Häkkinen K and Häkkinen A. Muscle cross-sectional area, force production and relaxation characteristics in women at different ages. European journal of applied physiology and occupational physiology 1991; 62:410-4.

Hahn M E. Feasibility of estimating isokinetic knee torque using a neural network model. J. Biomech 2007; 40: 1107–14.

Hamhaber U, Grieshaber F, Nagel J, Klose U. Comparison of quantitative shear wave MR-elastography with mechanical compression tests. Magn Reson Med 2003; 49: 71–77.

Hayes WC, Herrmann G, Mockros LF, and Keer LM. A mathematical analysis for indentation tests of articular cartilage. J. Biomech 1972; 5: 541–551.

Heers G, Jenkyn T, Dresner MA, et al. Measurement of muscle activity with magnetic resonance elastography. Clinical Biomechanics 2003;18(6):537-542.

Henneman E, and Mendell LM. Functional organization of motoneuron pool and its inputs. In: Brooks VB, editor. Handbook of physiology, the nervous system, motor control. Bethesda (MD): American Physiological Society, 1981.

Hides JA, Stokes MJ, Saide M, Jull GA and Cooper DH. Evidence of lumbar multifidus muscle wasting ipsilateral to symptoms in patients with acute/subacute low back pain. Spine 1994; 19:165-72.

Hodges PW, Pengel LHM, Herbert RD and Gandevia SC. Measurement of muscle contraction with ultrasound imaging. Muscle and Nerve 2003; 27:682-92.

Hoffren M, Ishikawa M, and Komi PV. Age-related neuromuscular function during drop jumps. Journal of Applied Physiology 2007; 103: 1276-1283.

Hook P, Li X, Sleep J, Hughes S, Larsson L. In vitro motility speed of slow myosin extracted from single soleus fibers from young and elderly rats. J. Physiol 1999; 15: 463–471.

Hortobagyi T, DeVita P. Muscle pre- and coactivity during downward stepping are associated with leg stiffness in aging. Journal of Electromyography and Kinesiology 2000; 10: 117-126.

Hortobagyi T, Solnik S, Gruber A, et al. Interaction between age and gait velocity in the amplitude and timing of antagonist muscle coactivation. Gait & Posture 2009; 29: 558-564.

Housh TJ, Perry SR, Bull AJ, Johnson GO, Ebersole KT, Housh DJ and deVries HA. Mechanomyographic and electromyographic responses during submaximal cycle ergometry. European Journal of Applied Physiology 2000; 83: 381-7.

Hoyt K, Parker KJ, Rubens DJ, and Ieee. Sonoelastographic Shear Velocity Imaging: Experiments on Tissue Phantom and Prostate. In: 2006 Ieee Ultrasonics Symposium, Vols 1-5, Proceedings 2006, p. 1686-1689.

Hoyt K, Kneezel T, Castaneda B, Parker KJ. Quantitative sonoelastography for the *in vivo* assessment of skeletal muscle viscoelasticity. Physics in Medicine and Biology 2008; 53:4063-4080

Hsu MJ, Wei SH, Yu YH, and Chang YJ. Leg stiffness and electromyography of knee extensors/flexors: Comparison between older and younger adults during stair descent. Journal of Rehabilitation Research and Development 2007; 44: 429-435.

Huang QH, Zheng YP, Chen X, Shi J, and He JF. Development of a Frame-Synchronized System for Continuous Acquisition and Analysis of Sonomyography, Surface EMG and Corresponding Joint Angle. The Open Biomedical Engineering Journal 2007; 1: 77-84.

Huang QH, Zheng YP, Lu MH, and Chi ZR. Development of a portable 3D ultrasound imaging system for musculoskeletal tissues. Ultrasonics 2005; 43: 153-63.

Huang QH, Zheng YP, Chen X, He JF, and Shi J. Synchronization between somyography, electromyography and joint angle. Open Biomedical Engineering Journal 2007; 1:77-84.

Ichinose Y, Kawakami Y, Ito M and Fukunaga T. Estimation of active force-length characteristics of human vastus lateralis muscle. Acta anatomica 1997; 159(2-3):78-83.

Ichinose Y, Kawakami Y, Ito M, Kanehisa H, Fukunaga T (2000) *In vivo* estimation of contraction velocity of human vastus lateralis muscle during "isokinetic" action. Journal of Applied Physiology 2000; 88: 851-856.

Ikai M and Fukunaga T. A study on training effect on strength per unit cross-sectional area of muscle by means of ultrasonic measurement. European Journal of Applied Physiology and Occupational Physiology 1970; 28:173-80.

Ishikawa M, Dousset E, Avela J, Kyrolainen H, Kallio J, Linnamo V, Kuitunen S, Nicol C and Komi PV. Changes in the soleus muscle architecture after exhausting stretch-shortening cycle exercise in humans. European Journal of Applied Physiology 2006; 97: 298-306.

Ito M, Kawakami Y, Ichinose Y, Fukashiro S, Fukunaga T. Nonisometric behavior of fascicles during isometric contractions of a human muscle. J Appl Physiol 1998; 85: 1230-1235.

Jaskolska A, Brzenczek W, Kisiel-Sajewicz K, Kawczynski A, Marusiak J, and Jaskolski A. The effect of skinfold on frequency of human muscle mechanomyogram. Journal of Electromyography & Kinesiology 2004; 14: 217-25.

Jaskolska A, Kisiel K, Brzenczek W and Jaskolski A. EMG and MMG of synergists and antagonists during relaxation at three joint angles. European Journal of Applied Physiology 2003; 90:58-68.

Jaskolska A, Kisiel-Sajewicz K, Brzenczek-Owczarzak W, Yue GH and Jaskolski A. EMG and MMG of agonist and antagonist muscles as a function of age and joint angle. Journal of Electromyography and Kinesiology 2006; 16: 89-102.

Jenkyn TR. Ehman RL. An KN. Noninvasive muscle tension measurement using the novel technique of magnetic resonance elastography (MRE). J Biomech 2003:36:1917-1921.

Johnson M A, Polgar J, Weightman D and Appleton D. Data on the distribution of fiber types in thirty-six human muscles. An autopsy study Journal of the neurological sciences 1973; 18: 111-29.

Jones D, Haan A, Round J. Skeletal Muscle From Molecules to Movement. Churchill Livingstone, 2004.

Kanehisa H, Ikegawa S, Tsunoda N and Fukunaga T. Strength and cross-sectional areas of reciprocal muscle groups in the upper arm and thigh during adolescence. International Journal of Sports Medicine 1995; 16: 54-60.

Karamanidis K, Arampatzis A. Mechanical and morphological properties of human quadriceps femoris and triceps surae muscle-tendon unit in relation to aging and running. Journal of Biomechanics 2006; 39(3):406-417.

Karamanidis K, Arampatzis A, and Mademli L. Age-related deficit in dynamic stability control after forward falls is affected by muscle strength and tendon stiffness. Journal of Electromyography and Kinesiology 2008; 18: 980-989.

Karlsson S and Gerdle B. Mean frequency and signal amplitude of the surface EMG of the quadriceps muscles increase with increasing torque- a study using the continuous wavelet transform. Journal of Electromyography and Kinesiology 2001; 11:131-40.

Kawakami Y, Kubo K, Kanehisa H, Fukunaga T. Effect of series elasticity on isokinetic torque-angle relationship in humans. European Journal of Applied Physiology 1999; 87: 381-387.

Kermani MZ, Wheeler BC, Badie K, and Hashemi TM. EMG feature evaluation for movement control of upper extremity prostheses. IEEE Transactions on Rehabiliation Engineering 1995; 3: 324-33.

Kimura T, Fujibayashi M, Tanaka S, Moritani T. Mechanomyographic responses in quadriceps muscles during fatigue by continuous cycle exercise. European Journal of Applied Physiology 2008; 104:651-656.

Klein CS, Rice CL, Marsh GD. Normalized force, activation, and coactivation in the arm muscles of young and elderly men. J. Appl. Physiol. 2001; 91: 1341–1349.

Koike Y, and Kawato M. Estimation of dynamic joint torques and trajectory formation from surface electromyography signals using a neural network model. Biological Cybernetics 1995; 73: 1015–24.

Komi PV, Karlsson J. Skeletal muscle fiber types, enzyme activities and physical performance in young males and females. Acta Physiol Scand 1978; 103:210–218,.

Kouzaki M and Fukunaga T. Frequency features of mechanomyographic signals of human soleus muscle during quiet standing. Journal of neuroscience methods 2008; 173: 241-8.

Kruse SA, Smith JA, Lawrence AJ, Dresner MA, Manduca A, Greenleaf JF and Ehman RL. Tissue characterization using magnetic resonance elastography: preliminary results. Physics in Medicine and Biology 2000;45:1579–90

Kuiken TA Dumanian GA, Lipschutz RD, Miller LA and Stubblefield KA. The use of targeted muscle reinnervation for improved myoelectric prosthesis control in a bilateral shoulder disarticulation amputee. Prosthetics and Orthotics International 2004; 28: 245-53.

Kubo K, Kanehisa H, Fukunaga T. Effects of different duration isometric contractions on tendon elasticity in human quadriceps muscles. Journal of Physiology-London 2001;536(2):649-655.

Kubo K, Ohgo K, Takeishi R, et al. Effects of isometric training at different knee angles on the muscle-tendon complex *in vivo*. Scandinavian Journal of Medicine & Science in Sports 2006;16(3):159-167.

Kubo K, Yata H, Kanehisa H, Fukunaga T. Effects of isometric squat training on the tendon stiffness and jump performance. European Journal of Applied Physiology 2006;96(3):305-314.

Kubo K, Kanehisa H, Fukunaga T. Gender differences in the viscoelastic properties of tendon structures. Eur J Appl Physiol 2003; 88:520–526.

Labarre VA. Assessment of muscle function in pathology with surface electrode EMG. Revue neurologique 2006; 162: 459-65.

Lariviere C, Arsenault AB, Gravel D, Gagnon D and Loisel p. Effect of step and ramp static contractions on the median frequency of electromyograms of back muscles in humans. European Journal of Applied Physiology 2001; 85:552-9.

Larsson L, Sjodin B, Karlsson J. Histochemical and biochemical changes in human skeletal muscle with age in sedentary males, age 22–65 years. Acta Physiol Scand 1978; 103: 31–39.

Larsson L, Li X, Frontera WR. Effects of aging on shortening velocity and myosin isoform composition in single human skeletal muscle cells. Am. J. Physiol. 1997; 272: 638–649.

Leonard CT, Deshner WP, Romo JW, Suoja ES, Fehrer SC, Mikhailenok EL. Myotonometer intra- and interrater reliabilities. Arch Phys Med Rehabil 2003; 84: 928–932.

Levinson SF, Shinagawa M, Sato T. SONOELASTIC DETERMINATION OF HUMAN SKELETAL-MUSCLE ELASTICITY. Journal of Biomechanics 1995; 28(10):1145-1154.

Lieber RL and Friden J. Functional and clinical significance of skeletal muscle architecture. Muscle and Nerve 2000; 23: 1647-66.

Lieber RL. Skeletal Muscle Structure, Function, and Plasticity. 3rd ed. Lippincott Williams & Wilkins, 2009.

Liu MM, Herzog W, and Savelberg HH. Dynamic muscle force predictions from EMG: an artificial neural network approach. Journal of Electromyography and Kinesiology 1999; 9: 391–400.

Lu MH, Zheng YP, and Huang QH. A novel noncontact ultrasound indentation system for measurement of tissue material properties using water jet compression. Ultrasound Med. Biol. 2005; 31: 817–826.

Macaluso A, Nimmo MA, Foster JE, Cockburn M, McMillan NC & De Vito G. Contractile muscle volume and agonist-antagonist coactivation account for differences in torque between young and older women. Muscle Nerve 2002; 25: 858–863.

MacIntosh B, Gardiner p, McComas A. Skeletal Muscle: Form and Function. 2nd ed. Human Kinetics, 2005.

MacIsaac D, Englehart K, Parker p, and Rogers D. Fatigue estimation with a multivariable myoelectric mapping function. IEEE Transactions on Biomedical Engineering 2006; 53:694-700.

Madeleine p, Jorgensen LV, Sogaard K, Nielsen LA and Sjogaard G. Development of muscle fatigue as assessed by electromyography and mechanomyography during continuous and intermittent low-force contractions: effects of the feedback mode. European Journal of Applied Physiology 2002; 87: 28-37.

Madsen EL, Sathoff HJ and Zagzebski JA. Ultrasonic shear wave properties of soft tissues and tissue like materials. Journal of the Acoustical Society of America 1983;74:1346–1355

Mahlfeld K, Franke J, and Awiszus F. Postcontraction changes of muscle architecture in human quadriceps muscle. Muscle and Nerve 2004; 29:597-600.

Mamaghani NK, Shimomura Y, Iwanaga K and Katsuura T. Mechanomyogram and electromyogram responses of upper limb during sustained isometric fatigue with varying shoulder and elbow postures. Journal of physiological anthropology and applied human science 2002; 21: 29-43.

Manduca A, Oliphant TE, Dresner MA, Mahowald JL, Kruse SA, Amromin E, Felmlee JP, Greenleaf JF, and Ehman RL. Magnetic resonance elastography: Non-invasive mapping of tissue elasticity. Medical Image Analysis 2001; 5: 237-254.

Mannion AF, Pulkovski N, Gubler D, Gorelick M, O'Riordan D, Loupas T, Schenk p, Gerber H and Sprott H. Muscle thickness changes during abdominal hollowing: an assessment of between-day measurement error in controls and patients with chronic low back pain. European Spine Journal 2008; 17: 494-501.

Masuda K, Masuda T, Sadoyama T, Inaki M, and Katsuta S. Changes in surface EMG parameters during static and dynamic fatiguing contractions. Journal of Electromyography and Kinesiology 1999; 9: 39-46.

Matsubayashi T, Kubo J, Matsuo A, Kobayashi K and Ishii N. Ultrasonographic measurement of tendon displacement caused by active force generation in the psoas major muscle. The journal of physiological sciences 2008; 58: 323-32.

Maughan RJ, Watson JS, and Weir J. Relationship between muscle strength and muscle cross-sectional area in male sprinters and endurance runners. European Journal of Applied Physiology 1983; 50: 309-18.

McMeeken JM and Beith ID. The relationship between EMG and change in thickness of transversus abdominis. Clinical Biomechanics 2004; 19: 337-342.

Morse CI, Thom JM, Birch KM & Narici MV. Changes in triceps surae muscle architecture with sarcopenia. Acta Physiol Scand 2005; 183: 291–298.

Muller L, Bergstrom T, Hellstrom M, Svensson E, and Jacobsson B. Standardized ultrasound method for assessing detrusor muscle thickness in children. The Journal of urology 2000; 164:134-38.

Murayama M, Nosaka K, Yoneda T, Minamitani K. Changes in hardness of the human elbow flexor muscles after eccentric exercise. Eur J Appl Physiol 2000; 82: 361–367.

Muthupillai R, Lomas DJ, Rossman PJ, Greenleaf JF, Manduca A, Ehman RL. Magnetic-resonance Elastography by Direct Visualization of Propagating Acoustic Strain Waves. Science 1995; 269(5232):1854-1857.

Muthupillai R, Rossman PJ, Lomas DJ, Greenleaf JF, Riederer SJ, Ehman RL. Magnetic resonance imaging of transverse acoustic strain waves. Magnetic Resonance in Medicine 1996; 36(2):266-274.

Nadeau S, Bilodeau M, Delisle A, Chmielewski W, Arsenault AB and Gravel D. The influence of the type of contraction on the masseter muscle EMG power spectrum. Journal of Electromyography and Kinesiology 1993; 3:205-13.

Narici MV, Landoni L and Minetti AE. Assessment of human knee extensor muscles stress from *in vivo* physiological cross-sectional area and strength measurements. European Journal of Applied Physiology and Occupational Physiology 1992; 65:438-444

Narici MV, Binzoni T, Hiltbrand E, Fasel J, Terrier F and Cerretelli p. *In vivo* human gastrocnemius architecture with changing joint angle at rest and during graded isometric contraction. The Journal of Physiology-London 1996; 496:287-97.

Narici MV, Maganaris CN, Reeves ND & Capodaglio P. Effect of aging on human muscle architecture. J Appl Physiol 2003; 95: 2229–2234.

Narici MV, Maganaris CN, and Reeves ND. Myotendinous alterations and effects of resistive load in old age. Scandinavian Journal of Medicine & Science in Sports 2005; 15: 392-401.

Narici MV, Maganaris CN. Adaptability of elderly human muscles and tendons to increased load. Journal of Anatomy 2006; 208: 433-443.

Narici MV, Maffulli N, Maganaris CN. Ageing of human muscles and tendons. Disability and Rehabilitation 2008; 30: 1548-1554.

Nene A, Byrne C, and Hermens H. Is rectus femoris really a part of quadriceps? Assessment of rectus femoris function during gait in able-bodied adults. Gait & Posture 2004; 20: 1-13.

Nogueira W, Gentil p, Mello SNM, Oliveira RJ, Bezerra AJC and Bottaro M. Effects of power training on muscle thickness of older men. International Journal of Sports Medicine 2009; 30:200-4.

Nordez A, Guevel A, Casari p, Catheline S, Cornu C. Assessment of muscle hardness changes induced by a submaximal fatiguing isometric contraction. Journal of Electromyography and Kinesiology 2009;19(3):484-491.

Nordez A, Hug F. Muscle shear elastic modulus measured using supersonic shear imaging is highly related to muscle activity level. Journal of Applied Physiology 2010; 108:1389-1394

O'Brien TD, Reeves ND, Baltzopoulos V, Jones DA, Maganaris CN. Muscle-tendon structure and dimensions in adults and children. Journal of Anatomy 2010; 216:631-642.

Ochala J, Lambertz D, Pousson M, Goubel F, Van Hoecke J. Changes in mechanical properties of human plantar flexor muscles in ageing. Experimental Gerontology 2004; 39: 349-358.

Ochala J, Valour D, Pousson M, Lambertz D, and Van Hoecke J. Gender differences in human muscle and joint mechanical properties during plantar flexion in elderly age. Journals of Gerontology Series a-Biological Sciences and Medical Sciences 2004; 59: 441-448.

Oertel G. Morphometric analysis of normal skeletal muscles in infancy, childhood and adolescence. An autopsy study. J Neurol Sci 1988; 88:303–313.

Oestreicher HL. Field and impedance of an oscillating sphere in a viscoelastic medium with an application to biophysics. Journal of the Acoustical Society of America 1951; 23:707–714

Okita M, Nakano J, Kataoka H, Sakamoto J, Origuchi T and Yoshimura T. effects of therapeutic ultrasound on joint mobility and collagen fibril arrangement in the endomysium of immobilized rat soleus muscle.. Ultrasound in Medicine & Biology 2009; 35: 237-44.

Ophir J, Cespedes I, Ponnekanti H, Yazdi Y, Li X. Elastography - a Quantitative Method for Imaging the Elasticity of Biological Tissues. Ultrasonic Imaging 1991;13(2):111-134.

Orizio C. Muscle sound: bases for the introduction of a mechanomyographic signal in muscle studies. Critical reviews in biomedical engineering 1993; 21:201-43.

Orizio C, Esposito F, Sansone V, Parrinello G, Meola G and Veicsteinas A. Muscle surface mechanical and electrical activities in myotonic dystrophy. Electromyography and clinical neurophysiology 1997; 37:231-9.

Orizio C, Gobbo M, Diemont B, Esposito F, and Veicsteinas A. The surface mechanomyogram as a tool to describe the influence of fatigue on biceps brachii motor unit activation strategy. Historical basis and novel evidence. European Journal of Applied Physiology 2003; 90: 326-36.

Paavolainen L, Nummela A, Rusko H, and Hakkinen K. Neuromuscular characteristics and fatigue during 10 km running. International Journal of Sports Medicine 1999; 20: 516-21.

Padua DA, Carcia CR, Arnold BL, and Granata KP. Gender differences in leg stiffness and stiffness recruitment strategy during two-legged hopping. Journal of Motor Behavior 2005; 37: 111-125.

Papadopoulos C, Kalapotharakos VI, Chimonidis E, Gantiraga E, Grezios A, and Gissis I. Effects of knee angle on lower extremity extension force and activation time characteristics of selected thigh muscles. Isokinetics and Exercise Science 2008; 16:41-46.

Park HS, Wilson NA, and Zhang LQ. Gender differences in passive knee biomechanical properties in tibial rotation. Journal of Orthopaedic Research 2008; 26: 937-944.

Parker KJ, Huang SR, Musulin RA, Lerner RM. TISSUE-RESPONSE TO MECHANICAL VIBRATIONS FOR SONOELASTICITY IMAGING. Ultrasound in Medicine and Biology 1990;16(3):241-246.

Perry SR, Housh TJ, Weir JP, Johnson GO, Bull AJ and Ebersole KT. Mean power frequency and amplitude of the mechanomyographic and electromyographic signals during incremental cycle ergometry. Journal of Electromyography and Kinesiology 2001; 11: 299-305.

Phillips SK, Bruce SA, Newton D, Woledge RC. The weakness of elderly age is not due to failure of muscle activation. J. Gerontol. 1992; 47: 45–49.

Pincivero DM, Gandhi V, Timmons MK, Coelho AJ. Quadriceps femoris electromyogram during concentric, isometric and eccentric phases of fatiguing dynamic knee extensions. Journal of Biomechanics 2006; 39:246-254.

Pousson M, Lepers R, Van Hoecke J. Changes in isokinetic torque and muscular activity of elbow flexors muscles with age. Exp. Gerontol. 2001; 36: 1687–1698.

Ramirez A, and Garzon DA. Sensitivity analysis for the positioning of electrodes in surface electromiography (semg). Revista Facultad De Ingenieria-Universidad De Antioquia 70-79, 2008.

Reeves ND, Maganaris CN, and Narici MV. Ultrasonographic assessment of human skeletal muscle size. European Journal of Applied Physiology 2004; 91:116-8.

Ringleb SI, Chen QS, Lake DS, Manduca A, Ehman RL, An KN. Quantitative shear wave magnetic resonance elastography: Comparison to a dynamic shear material test. Magnetic Resonance in Medicine 2005; 53: 1197-1201

Ringleb SI, Bensamoun SF, Chen QS, Manduca A, An KN, Ehman RL. Applications of magnetic resonance elastography to healthy and pathologic skeletal muscle. Journal of Magnetic Resonance Imaging 2007; 25(2):301-309.

Robinson CJ, Flaherty B, Fehr L, Agarwal GC, Harris GF, Gottlieb GL. Biomechanical and Reflex Responses to Joint Perturbations during Electrical-stimulation of Muscle - Instrumentation and Measurement Techniques. Medical & Biological Engineering & Computing 1994; 32: 261-272.

Rutherford OM, Jones DA. Measurement of Fiber Pennation Using Ultrasound in the Human Quadriceps In Vivo. European Journal of Applied Physiology and Occupational Physiology 1992; 65:433-437.

Ryan ED, Cramer JT, Egan AD, Hartman MJ, and Herda TJ. Time and frequency domain responses of the mechanomyogram and electromyogram during isometric ramp contractions: A comparison of the short-time Fourier and continuous wavelet transforms. Journal of Electromyography and Kinesiology 2008a; 18:54-67.

Ryan ED, Beck TW, Herda TJ, Hartman MJ, Stout JR, Housh TJ, and Cramer JT. Mechanomyographic amplitude and mean power frequency responses during isometric ramp vs. step muscle actions. Journal of neuroscience methods 2008b; 168:293-305.

Sack I, Bernarding J, Braun J. Analysis of wave patterns in MR elastography of skeletal muscle using coupled harmonic oscillator simulations. Magnetic Resonance Imaging 2002; 20(1):95-104.

Sallinen J, Ojanen T, Karavirta L, Ahtiainen JP, and Hakkinen K. Muscle mass and strength, body composition and dietary intake in master strength athletes vs untrained men of different ages. Journal of Sports Medicine and Physical Fitness 2008; 48:190-6.

Sandrin L, Catheline S, Tanter M, Hennequin X, Fink M. Time-resolved pulsed elastography with ultrafast ultrasonic imaging. Ultrasonic Imaging 1999; 21(4):259-272.

Sandrin L, Tanter M, Catheline S, Fink M. Shear modulus imaging with 2-D transient elastography. IEEE Transactions on Ultrasonics Ferroelectrics and Frequency Control 2002; 49(4):426-435.

Sandrin L, Tanter M, Gennisson JL, Catheline S, Fink M. Shear elasticity probe for soft tissues with 1-D transient elastography. IEEE Transactions on Ultrasonics Ferroelectrics and Frequency Control. Apr 2002; 49(4):436-446.

Sanchez JH, Solomonow M, Baratta RV and Dambrosia R. Control Strategies of the Elbow Antagonist Muscle Pair during 2 Types of Increasing Isometric Contractions. Journal of Electromyography and Kinesiology 1993; 3:33-40.

Sepulveda F, Wells DM, and Vaughan CL. A neural network representation of electromyography and joint dynamics in human gait. Journal of Biomechanics 1993; 26: 101–9.

Shi J, Zheng YP, Chen X, and Huang QH. Assessment of muscle fatigue using sonomyography: Muscle thickness change detected from ultrasound images. Medical Engineering & Physics 2007; 29: 472-9.

Shi J, Zheng YP, Chen X, and Huang QH. Assessment of muscle fatigue using sonomyography: Muscle thickness change detected from ultrasound images. Med Eng Phys. 2007; 29(4):472-479.

Shi J, Zheng YP, Huang QH and Chen X. Continuous monitoring of sonomyography, electromyography and torque generated by normal upper arm muscles during isometric contraction: Sonomyography assessment for arm muscles. Biomedical Engineering, IEEE Transactions on Biomedical Engineering 2008; 55: 1191-8.

Shinohara M, Sabra K, Gennisson JL, Fink M, Tanter M. Real-time visualization of muscle stiffness distribution with ultrasound shear wave imaging during muscle contraction. Muscle & Nerve 2010; 42: 438–441.

Shorten MR. Muscle elasticity and human performance. Medicine and Sport Science 1987; 25:1–18.

Sikdar S, Shah JP, Gilliams E, Gebreab T and Gerber LH. Assessment of Myofascial Trigger Points (MTrPs): A New Application of Ultrasound Imaging and Vibration Sonoelastography. In: 30th Annual International Conference of the IEEE-Engineering in Medicine and Biology Society, 2008; pp 5585-5588

Simoneau J-A, Bouchard C. Human variation in skeletal muscle fiber-type proportion and enzyme activities. Am J Physiol 1989; 257:E567–572.

Simoneau J-A, Lortie G, Boulay MR, Thibault M-C, Thériault G, Bouchard C. Skeletal muscle histochemical and biochemical characteristics in sedentary male and female subjects. Can J Physiol Pharmacol 1985; 63:30–35.

Springer BA and Gill NW. Characterization of lateral abdominal muscle thickness in persons with lower extremity amputations. Journal of Orthopaedic & Sports Physical Therapy 2007; 37:635-43.

Staron RS, Hagerman FC, Hikida RS, et al. Fiber type composition of the vastus lateralis muscle of young men and women. Journal of Histochemistry & Cytochemistry 2000; 48:623-629.

Suga M, Matsuda T, Minato K. Measurement of in-vivo local shear modulus by combining multiple phase offsets MR elastography. In Medinfo 2001: Proceedings of the 10th World Congress on Medical Informatics, Pts 1 and 2 (eds Patel VL, Rogers R, Haux R), 2001; 933-937.

Suter E, and Herzog W. Extent of muscle inhibition as a function of knee angle. Journal of Electromyography and Kinesiology 1997; 7: 123-130.

Suzana D, Rodica T, Petrica B and Mircea D. Quantitative analysis of ultrasound data in assessment of muscle layer thickness of quadriceps muscle in young subject pre and post isometric contraction. In: 4th WSEAS International Conference on Cellular and Molecular Biology, Biophysics and Bioengineering/2nd WSEAS International Conference on Computational Chemistry, (Puerto de la Cruz, SPAIN: World Scientific and Engineering Acad and Soc), 2008; pp 33-37.

Talebinejad M, Chan AD, Miri A, and Dansereau RM. Fractal analysis of surface electromyography signals: a novel power spectrum-based method Journal of Electromyography and Kinesiology 2009; 19: 840-50.

Toursel T, Stevens L, Mounier Y. Evolution of contractile and elastic properties of rat soleus muscle fibers under unload conditions. Exp Physiol 1999; 84:93–107.

Uffmann K, Maderwald S, Ajaj W, et al. *In vivo* elasticity measurements of extremity skeletal muscle with MR elastography. Nmr in Biomedicine 2004;17(4):181-190.

Urban MW, Chen SG, and Greenleaf JF. Error in Estimates of Tissue Material Properties from Shear Wave Dispersion Ultrasound Vibrometry. IEEE Transactions on Ultrasonics Ferroelectrics and Frequency Control 2009; 56: 748-758.

Wang CZ, Zheng YP. Comparison between reflection-mode photoplethysmography and arterial diameter change detected by ultrasound at the region of radial artery. Blood Pressure Monitoring 2010; 15: 213-219.

Wang L, and Buchanan T S. Prediction of joint moments using a neural network model of muscle activations from EMG signals. Transactions on Neural Systems and Rehabilitation Engineering 2002; 10: 30–7.

Wang LI. The kinetics and stiffness characteristics of the lower extremity in older adults during vertical jumping. Journal of Sports Science and Medicine 2008; 7: 379-386.

Watanabe K, Akima H. Cross-talk from adjacent muscle has a negligible effect on surface electromyographic activity of vastus intermedius muscle during isometric contraction. J Electromyogr Kinesiol 2008; 19(4):280-289.

Whittaker J, Teyhen D, Elliott J, Cook K, Langevin H, Dahl H, and Stokes M. Rehabilitative Ultrasound Imaging: Understanding the Technology and its Applications. Journal of Orthopaedic & Sports Physical Therapy 2007; 37: 435-49.

Willan PLT, Mahon M, Golland JA. MORPHOLOGICAL VARIATIONS OF THE HUMAN VASTUS LATERALIS MUSCLE. Journal of Anatomy 1990; 168:235-239.

Willan PLT, Ransome JA, Mahon M. Variability in human quadriceps muscles: Quantitative study and review of clinical literature. Clinical Anatomy 2002; 15:116-128.

Wilson GJ, Murphy AJ, Pryor JF. Musculotendinous Stiffness - Its Relationship to Eccentric, Isometric, and Concentric Performance. Journal of Applied Physiology 1994; 76(6):2714-2719.

Withrow TJ, Huston LJ, Wojtys EM, and Ashton-Miller JA. The relationship between quadriceps muscle force, knee flexion, and anterior cruciate ligament strain in an in vitro simulated jump landing. American Journal of Sports Medicine 2006; 34: 269-274.

Wu Z, Hoyt K, Rubens DJ, and Parker KJ. Sonoelastographic imaging of interference patterns for estimation of shear velocity distribution in biomaterials. Journal of the Acoustical Society of America 2006; 120: 535-545.

Wu Z, Taylor LS, Rubens DJ, and Parker KJ. Sonoelastographic imaging of interference patterns for estimation of the shear velocity of homogeneous biomaterials. Physics in Medicine and Biology 2004; 49: 911-922.

Xie HB, Wang ZH, Huang H, and Qin C. Support vector machine in computer aided clinical Electromyography. In: Proceedings of the Second InternatIona1 Conference on Machine Learning and Cybernetics, Xi'an, 2003; pp. 1106–1108.

Xie HB, Zheng YP, Guo JY, Chen X and Shi J. Estimation of wrist angle from sonomyography using support vector machine and artificial neural network models. Medical Engineering & Physics 2009a; 31:384-91.

Xie HB, Zheng YP and Guo JY. Classification of the mechanomyogram signal using a wavelet packet transform and singular value decomposition for multifunction prosthesis control. Physiological Measurement 2009b; 30:441-57.

Yoshitake Y, Ue H, Miyazaki M and Moritani T. Assessment of lower-back muscle fatigue using electromyography, mechanomyography, and near-infrared spectroscopy. European Journal of Applied Physiology 2001; 84:174-9.

Zhang LQ, Zeng KF, Wang GZ, Nuber G, and Ieee I. Dynamic and static properties of the human knee joint in axial rotation. In: Proceedings of the 19th Annual International Conference of the Ieee Engineering in Medicine and Biology Society, Vol 19, Pts 1-6 - Magnificent Milestones and Emerging Opportunities in Medical Engineering 1997, p. 1738-1741.

Zheng YP and Mak AFT. Load-indentation responses of multi-layered soft tissues. 1997 IEEE International Ultrasonics Symposium, Toronto, Sept 1997.

Zheng YP, Chan MMF, Shi J, Chen X and Huang QH. Sonomyography: Monitoring morphological changes of forearm muscles in actions with the feasibility for the control of powered prosthesis. Medical Engineering & Physics 2006; 28:405-15.

Zheng YP, Leung SF, Mak AFT. Assessment of neck tissue fibrosis using an ultrasound palpation system: a feasibility study. Medical & Biological Engineering & Computing 2000; 38(5):497-502.

Zheng YP, Mak AFT, Lue B. Objective assessment of limb tissue elasticity: Development of a manual indentation procedure. Journal of Rehabilitation Research and Development 1999; 36(2):71-85.

Zheng YP, Chan MMF, Shi J, Chen X and Huang QH. Sonomyography: Monitoring morphological changes of forearm muscles in actions with the feasibility for the control of powered prosthesis [J]. Medical Engineering & Physics 2006; 28(5): 405-415.

Zhou YJ and Zheng YP. Revoting Hough Transform (RVHT) and its application for muscle fiber orientation estimation in ultrasound images. Ultrasound in Medicine and Biology 2008; 34: 1474-81.

APPENDIX

I. Information Sheet

Project Title: Ultrasound Measurement of Muscle Elasticity

Principle Investigator: Dr. Yongping Zheng

Department of Health Technology and Informatics, The Hong Kong Polytechnic University

The aim of this project is to develop a new method to evaluate the muscle elasticity using ultrasound, and to study the muscle elasticity under different contraction level, which is expressed as percent of the maximum voluntary contraction (MVC). The MVC is a maximum exertion of force reported as a moment around a joint. This study can provide more information of the muscle mechanical properties and may help to evaluate the muscle functions more extensively.

All the subjects should volunteer to participate for this study. There is no gender and age restriction for the subject selection. They should guarantee to not sustain a recent injury on their knee joints and thigh muscles that might increase the risk of injury in this study and affect the findings. They also should not participate in any strength or flexibility training one day before the measurement. The contraction of quadriceps femoris muscles of subject will be monitored using a commercial ultrasound scanner and the surface electromyography. The isometric moment generated by the knee joint will be measured by a commercial isokinetic dynamometer. An electromagnetic vibrator will be hung over the thigh and touch the skin surface to generate mechanical shear waves. The maximum force is 10 N and maximum displacement is 6 mm, which means

the generated vibrations are very safe to the subject. A linear array ultrasound probe, nine electrodes of electromyography, and three accelerometers will be attached on the skin surface using medical adhesive tape. The clinical used ultrasound gel will be applied between the ultrasound probe and the skin. The subject will feel no pain or uncomfortableness, and the attachment of the devices will have no hurt to the body. During the experiment, the subject will be asked to contract the quadriceps femoris muscles to different percents of MVC and extend the knee joint to different levels. The subject can stop the experiment any time if they do not want to continue.

If you have any complaints about the conduct of this research study, please do not hesitate to contact Ms Kath Lui, Secretary of the Human Subjects Ethics Sub-Committee of The Hong Kong Polytechnic University in person or in writing (Tel: 2766 7933; E-mail: rokath@ ; c/o Research Office of the University).

實驗指引

項目名稱： 用超聲波測量肌肉彈性的研究

項目負責人：鄭永平教授

醫療科技及資訊學系, 香港理工大學

本項目的目標是開發一項新的用超聲波測量肌肉彈性的方法，并以此研究肌肉在不同收縮水平下彈性的變化。肌肉的收縮水平用最大自願收縮（MVC）的百分比來表徵，即圍繞某一關節用力而產生的最大力矩。此項研究有助於提供更多有關肌肉力學屬性的信息，并將有助於從更全面的角度評估肌肉功能。

所有受驗者必須自願參與本研究。對受驗者的性別和年齡沒有限制。受驗者須保證近期並無膝關節或大腿肌肉受傷，以避免實驗中的受傷風險及對實驗結果的可能影響。受驗者亦須保證近期並無進行肌肉力量或柔韌性方面的訓練。一台商用超聲設備和表面肌電設備會被用於測量受驗者股四頭肌的收縮情況。一台商用測力計會被用於測量受驗者膝關節處產生的力矩。一個電磁振盪裝置會被用於在大腿表面產生剪切波。其最大輸出壓力為 10 牛頓，最大移動距離為 6 毫米，以保證對受驗者絕對安全。超聲探頭，肌電電極和加速度傳感器會被醫用膠帶固定於皮膚表面。醫用耦合劑會被置於探頭和皮膚之間。這些設備都不會對受驗者造成任何傷害。受驗者也不會感覺到任何疼痛或不適。實驗過程中，受驗者將被要求收縮其股四頭肌以使膝關節達到不同百分比的 MVC 水平。如果不想繼續，受驗者可以隨時終止實驗。

如果受驗者對於在研究中受到的對待有任何投訴意見，請立即通過電話或電郵聯繫香港理工大學研究辦公室的 Ms Kath Lui 尋求幫助（Tel: 2766 7933; E-mail: rokath@ ; c/o Research Office of the University）。

II. Consent Form

I, _____ (name), hereby consent to participate in as a subject for the research project entitled as "Ultrasound Measurement of Muscle Elasticity".

I understand the effect and details of the experimental procedures which have been explained to me.

I understand that I have the right to discontinue, with no reason given, my participation anytime, even during the experiment. I realize that any findings of the study will only be used for research purpose and will be properties of the Department of Health Technology and Informatics, The Hong Kong Polytechnic University.

Please fill your age, height and weight in the following blanks. This information will be only used in this study and not leaked out.

_____

Name of participant

_____

Signature of participant

_____

Name of researcher

_____

Signature of researcher

_____

Date

_____

同意書

我_____（受試者姓名），在此同意作爲受驗者參加“用超聲波测量肌肉彈性的研究”。我已經清楚該測試的具體步驟以及可能造成的影響。

我已經知道我可以在任何時間，甚至是在測試中而終止測試，無需給予任何理由。我已經知道測試的結果只能用作科學研究，並且屬于香港理工大學，醫療科技及資訊學系。

受試者

姓名 _____

簽名 _____

日期 _____

實驗人

姓名 _____

簽名 _____

日期 _____

請填寫您的年齡，身高和體重。這些信息將僅用于本次研究用途。

年齡：_____

身高：_____

體重：_____